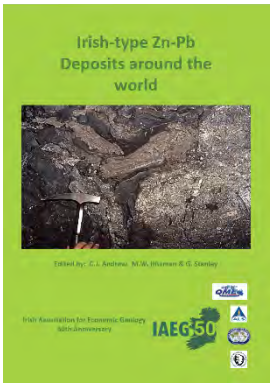

Irish Association for Economic Geology

(founded 1973)

Home Page: https://www.iaeg.ie

Carbonate-hosted "Alpine-type" Zn-Pb deposits in the Eastern and Southern Alps – trace element geochemistry and isotopic data of sulphides

Frank Melcher[1], Viktor Bertrandsson Erlandsson[1], Veronika Gartner[1], Elisabeth Henjes-Kunst[1], Johann Raith[1], Gerd Rantitsch[1], Peter Onuk[1,2], Friedhelm Henjes-Kunst[3], Barbara Potočnik Krajnc[4] & Aleš Šoster[4]

[1]Department of Geosciences and Applied Geophysics, Montanuniversität Leoben, Peter-Tunner-Strasse 5. 8700 Leoben, Austria
[2]Department of Petrology and Geochemistry, University of Graz, 8010 Graz, Austria
[3]Federal Institute of Geosciences and Natural Resources (BGR), Stilleweg 2, 30655 Hannover, Germany
[4]Faculty of Natural Sciences and Engineering, University of Ljubljana, Aškerčeva c. 12, SI-1000 Ljubljana, Slovenia

Corresponding Author: Frank Melcher frank.melcher@unileoben.ac.at

To cite this article: Melcher, F., Berttrandsson-Erlandsson, V., Gartnetr, V., Henjes-Kunst, E., Raith, J., Rantitsch, G., Onuk, P., Henjes-Kunst, F., Potocnik-Kranjnc, B. & Soster, A. (2023) Carbonate-hosted "Alpine-type" Zn-Pb deposits in the Eastern and Southern Alps – trace element geochemistry and isotopic data of sulphides. *In:* Andrew, C.J., Hitzman, M.W. & Stanley, G. '*Irish-type Deposits around the world*', Irish Association for Economic Geology, Dublin. 443-478. DOI: https://doi.org/10.61153/NIWU8065

To link to this article: https://doi.org/10.61153/NIWU8065

Carbonate-hosted "Alpine-type" Zn-Pb deposits in the Eastern and Southern Alps – trace element geochemistry and isotopic data of sulphides

Frank Melcher[1], Viktor Bertrandsson Erlandsson[1], Veronika Gartner[1], Elisabeth Henjes-Kunst[1], Johann Raith[1], Gerd Rantitsch[1], Peter Onuk[1,2], Friedhelm Henjes-Kunst[3], Barbara Potočnik Krajnc[4] & Aleš Šoster[4]

[1]*Department of Geosciences and Applied Geophysics, Montanuniversität Leoben, Peter-Tunner-Strasse 5. 8700 Leoben, Austria*
[2]*Department of Petrology and Geochemistry, University of Graz, 8010 Graz, Austria*
[3]*Federal Institute of Geosciences and Natural Resources (BGR), Stilleweg 2, 30655 Hannover, Germany*
[4]*Faculty of Natural Sciences and Engineering, University of Ljubljana, Aškerčeva c. 12, SI-1000 Ljubljana, Slovenia*

Abstract: More than 500 occurrences of carbonate-hosted Pb-Zn ores are documented in the Eastern and Southern Alps. They are invariably hosted by shallow lagoonal and reef carbonates of Middle and more frequently Upper Triassic (Anisian and Carnian) age and are collectively termed "Alpine-type" deposits. The local palaeogeography and synsedimentary structures influenced ore mineralization. Although they occur in a wide region, they share common features such as a simple mineralogical composition, complex ore textures, light sulphur isotopic compositions, Late Palaeozoic Pb model ages, and similar trace element compositions in sphalerite, galena and pyrite. Sphalerite records a low-temperature (60-140°C) precipitation. It is low in Fe, Mn, Co, Ag and In, but commonly contains elevated Cd, Ge, As, Tl and Pb. Galena is Ag-poor, although both sphalerite and galena tend to higher Ag concentrations towards the northern Districts. Minor Fe sulphides are low in Co and Ni but carry considerable As and Tl. Rb-Sr dating of sphalerite from the type locality Bleiberg reveals an age of ≈229 Ma for ores of the Raibl Group, and ages of ≈207 and ≈201 Ma for trace element-rich breccia ore in the western part of the Bleiberg deposit. The older age corresponds to U-Pb ages obtained on calcite associated with the Pb-Zn mineralization at the Gorno deposit (Southalpine). The younger age suggests fluid flow within the carbonate sequence in an extensional tectonic regime due to fracturing of the carbonate platform during initial rifting of the Penninic Ocean.

Keywords: Alpine-type, geochemistry, isotopic data, ore mineral geochemistry, Upper Triassic

Alpine-type Pb-Zn deposits

Pb-Zn ores are widespread in Triassic carbonates of the Austroalpine and Southalpine units (Fig. 1). The deposits, which have collectively been termed "Alpine-type" ("APT") (Jicha, 1951), have a long mining history starting most likely in Roman times and terminating in the early 1990s when the last operations closed at Bleiberg (Austria), Cave del Predil/Raibl (Italy), and Mežica/Mies (Slovenia) (Schroll, 2008). The Bleiberg deposit was closed in 1993 after more than 700 years of mining. It is regarded as a world-class deposit (Leach *et al*., 2005) and represents the type locality of APT Pb-Zn deposits. The historical total metal production from APT deposits exceeded 6 million tonnes (Mt) Zn and Pb from a resource exceeding 110 Mt (Table 1; Cerny, 1989; Cerny & Schroll, 1995; Leach *et al.,* 2003, 2005; Spangenberg & Herlec, 2006). Renewed interest in base metals, and especially in their by-products such as Ge, Ga, In and Cd, has initiated modern exploration activities in some of the mining Districts. Germanium and Cd have been recovered from ores in the past; about 200tonnes Ge, mostly from Bleiberg and Raibl, were produced from APT deposits (Höll *et al.*, 2007). Elevated Ag concentrations are restricted to deposits in the Northern Calcareous Alps (Lafatsch – "Silberner Hansl"; Nassereith –"Silberleiten") and to certain ore types at Mežica.

The mineralization is spread over a large area in the Eastern and Southern Alps, within Anisian to Norian carbonates in diagenetic to upper greenschist facies metamorphic conditions. Ore bodies are strata-bound, occasionally stratiform, formed at low-temperature (<150°C) and, with notable exceptions, are relatively small and low-grade carrying from 3 to 10% Pb and Zn, present as galena, sphalerite and wurtzite. Common trace elements in sphalerite are Ge, As, Cd, Tl and Pb. Fluorite and barite are present as a gangue mineral in many occurrences.

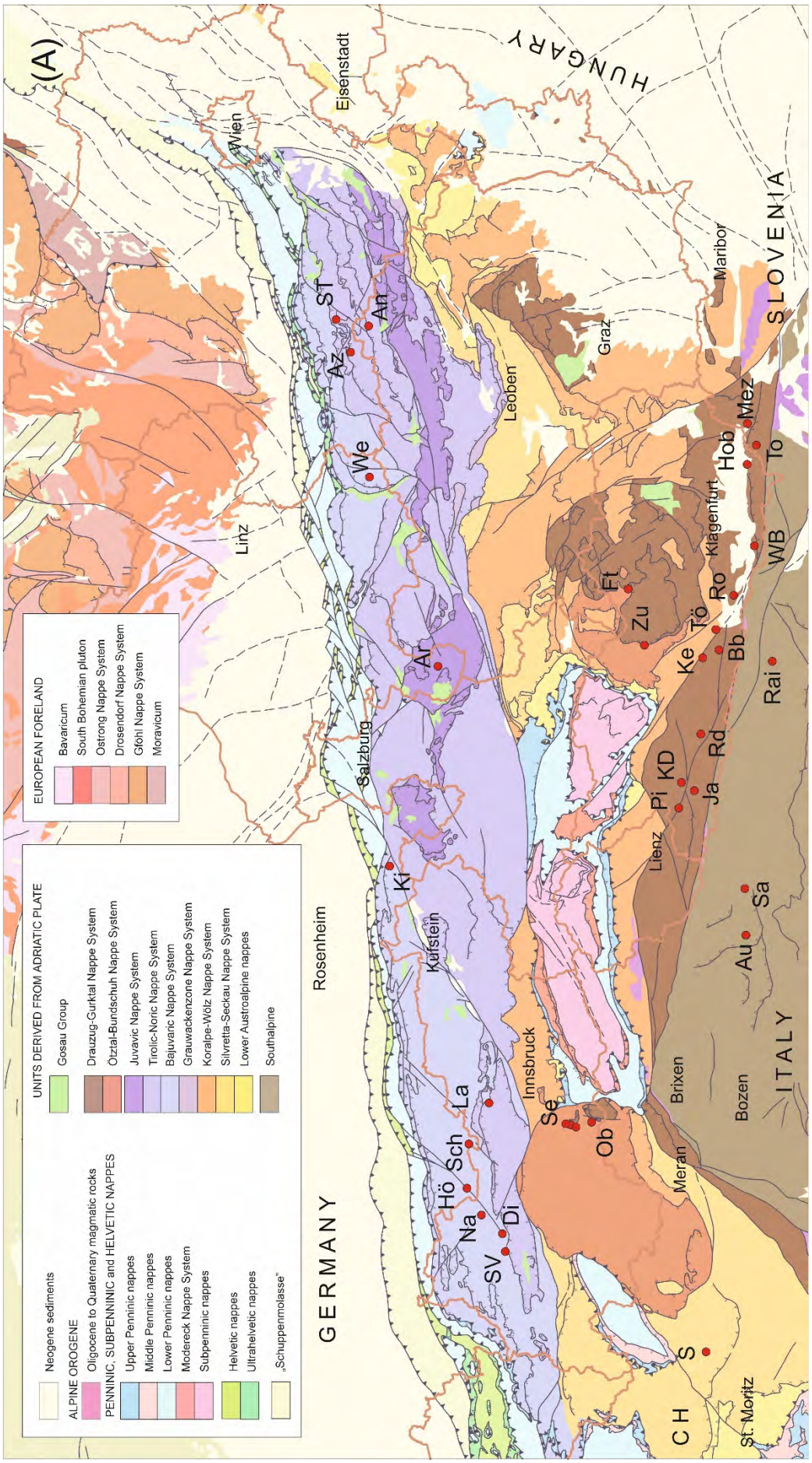

Figure 1A: *Tectonic (A) and geologic map (B) of the Eastern Alps showing Pb-Zn deposits/occurrences mentioned in the text (A) and APT Districts I – XII with localities sampled for geochemical analysis (B). Abbreviations: An, Annaberg; Ar, Arikogel; Au, Auronzo; Az, Arzriedel; Bb, Bleiberg; Di, Dirstentritt; Ft, Flattnitz; Hö, Höllental; Hob, Hochobir/Fladung; Ja, Jauken; KD, Kolm/Dellach; Ke, Kellerberg; Ki, Kienberg-Rauschberg; La, Lafatsch; Mez, Mežica; Na, Nassereith/Silberleiten; Ob, Obernberg; Pi, Pirkach-Hochstadel; Rai, Raibl/Cave del Predil; Rd, Radnig; Ro, Rosegg; S, S-charl; Sa, Salafossa; Sch, Scharnitz; Se, Serles (Brenner Mesozoic); ST, Schwarzenberg/Tirnitz; SV, Sankt Veit; To, Topla; Tö, Töplitsch; WB, Windisch-Bleiberg; We, Weyer; Zu, Zunderwand. Map base: Schmid et al. (2004) and Schuster et al. (2013)*

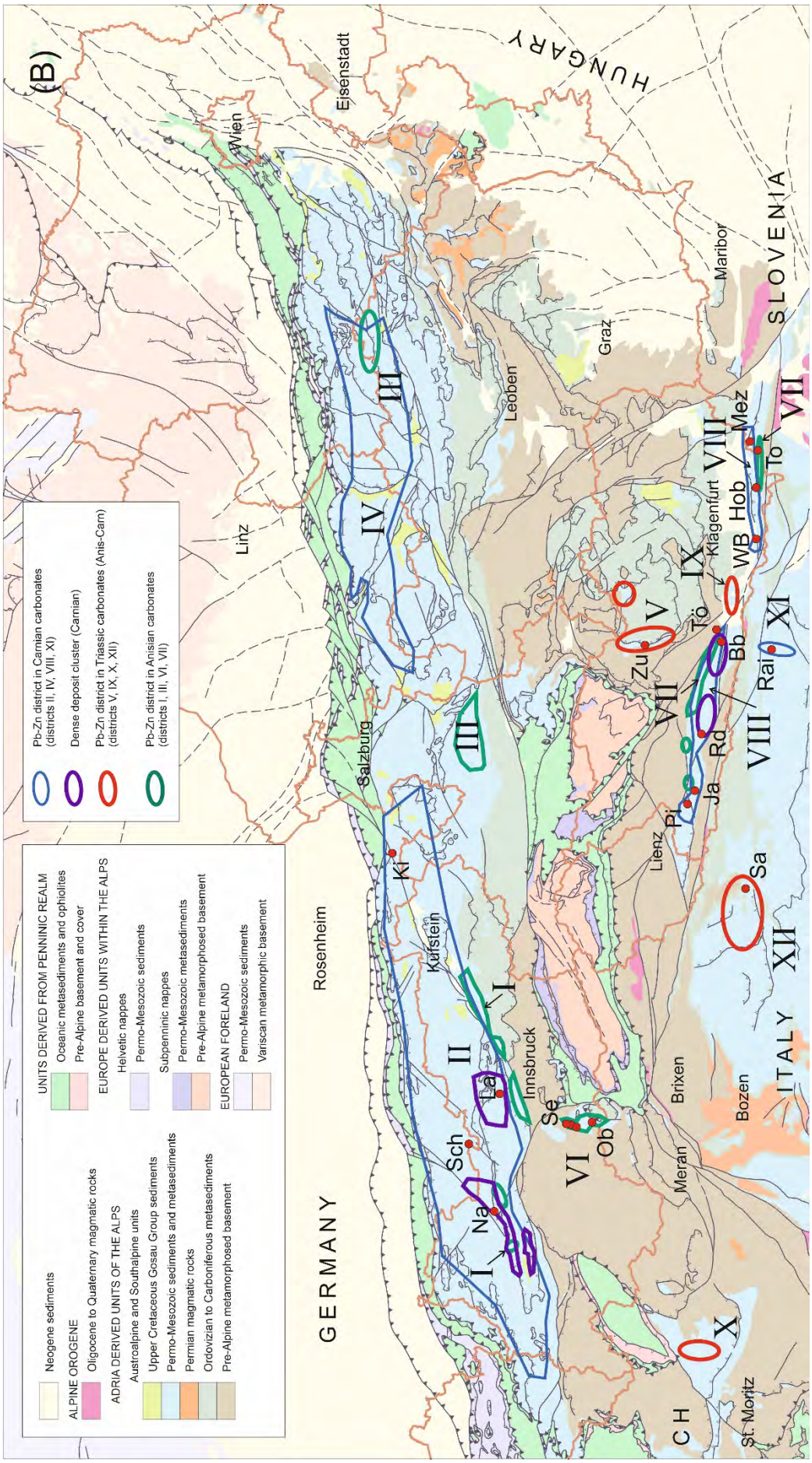

Figure 1B: *Geologic map (B) of the Eastern Alps showing Pb-Zn deposits/occurrences mentioned in the text (A) and APT Districts I – XII with localities sampled for geochemical analysis (B). Abbreviations: An, Annaberg; Ar, Arikogel; Au, Auronzo; Az, Arzriedel; Bb, Bleiberg; Di, Dirstentritt; Ft, Flattnitz; Hö, Höllental; Hob, Hochobir/Fladung; Ja, Jauken; KD, Kolm/Dellach; Ke, Kellerberg; Ki, Kienberg-Rauschberg; La, Lafatsch; Mez, Mežica; Na, Nassereith/Silberleiten; Ob, Obernberg; Pi, Pirkach-Hochstadel; Rai, Raibl/Cave del Predil; Rd, Radnig; Ro, Rosegg; S, S-charl; Sa, Salafossa; Sch, Scharnitz; Se, Serles (Brenner Mesozoic); ST, Schwarzenberg/Türnitz; SV, Sankt Veit; To, Topla; Tö, Töplitsch; WB, Windisch-Bleiberg; We, Weyer; Zu, Zunderwand. Map base: Schmid et al. (2004) and Schuster et al. (2013)*

Deposit	Country	District	Host rock age	Resource (Mt)	Pb %	Zn %	Production (Mt metal)
Lafatsch	Austria	II	Carnian	3.5*	1.6	6.2	0.05*
Bleiberg	Austria	VIII	Carnian	43.0	1.1	5.9	2.20
Mezica	Slovenia	VIII	Carnian	25.0	5.3	2.7	1.50
Topla	Slovenia	VII	Anisian	0.25	3.3	10	0.03*
Cavel del Predil/Raibl	Italy	XI	Carnian	18.2	1.2	6.0	1.50
Salafossa	Italy	XII	Carnian	11.0	0.9	4.9	0.50
Argentiera	Italy	XII	Anisian	1.0	1.0	6.0	0.07*
Gorno	Italy	XIII	Carnian	6.2	2.3	11.5	0.90

District number according to Fig. 1 and Table 1; Mt, million tonnes
Resource and production data using published data (Cerny, 1989; Cerny & Schroll, 1995; Leach *et al.*, 2005; Rečnik *et al.*, 2014); or estimates (*)

***Table 1**. Major APT Pb-Zn deposits in the Alps*

The scientific discussion on the ore genesis dates back to the late 19th century and peaked in the 1960s to 1980s when international cooperation between Austria, Italy, former Yugoslavia, and Germany led to four very productive ISMIDA (International Symposium on Mineral Deposits of the Alps) conferences from 1966 to 1983 (Schneider *et al.*, 1983), and a large number of national and international workshops on carbonate-hosted Pb-Zn deposits (Schroll, 2008). Due to mine closure, scientific investigations declined after the 1990s, with only few publications thereafter that focussed on the Bleiberg, Mežica and Gorno deposits (e.g., Kuhlemann *et al.*, 2001; Spangenberg & Herlec, 2006; Herlec *et al*., 2010). In this contribution, we summarize and partly re-evaluate those data. In addition, we present new results of trace element studies in sulphides, sulphur and lead isotopes, and on Rb-Sr dating of sphalerite from the Bleiberg deposit (Melcher *et al*., 2010a,b; Henjes-Kunst, 2010, 2014; Henjes-Kunst *et al.*, 2017; Onuk, 2018; Potočnik Krajnc, 2021; Gartner, 2023) to devise a more complete model of APT ore genesis.

Similarities and differences between APT and Mississippi Valley-type (MVT) deposits are discussed using textural observations, trace element, isotope data, and Rb-Sr dating results. For the first time, a comprehensive overview covering the major Pb-Zn Districts hosted by Mesozoic carbonates in the Eastern and Southern Alps is provided.

APT Districts in Austroalpine and Southalpine tectonic units

The Austroalpine units hosting APT deposits are subdivided into Lower and Upper Austroalpine Nappe Systems composed of Late Precambrian to Cretaceous sedimentary and magmatic rocks that have experienced a number of orogenic and metamorphic events including the Variscan orogeny (ca. 340-300Ma), the Permian (ca. 280-240Ma) and the Eoalpine (ca. 100-80Ma) tectonothermal events (Schmid *et al.*, 2004). The Southalpine unit south of the Periadriatic Lineament shows a lithostratigraphic succession similar to the Austroalpine units but has not been included into generally NW directed Alpine nappe tectonics. Most of the Austroalpine nappes contain Neoproterozoic to Upper Palaeozoic medium- to high-grade metamorphic rocks locally overlain by Upper Carboniferous to Mesozoic cover sediments (Fig. 1B).

Following Carboniferous terrestrial to mixed terrestrial/marine post-Variscan overstep sequences (e.g., Neubauer *et al*., 2022), the Permo-Mesozoic Tethyan sedimentary cycle usually starts with uppermost Permian to Lower Triassic clastics and shallow-marine carbonate rocks followed by thick carbonate successions in the Middle-Late Triassic, and a deeper marine Jurassic to Lower Cretaceous sedimentary sequence. Extensive carbonate production started around the Lower/Middle Triassic boundary with build-up of carbonate ramps changing from restricted to open-marine conditions in the Anisian (cf. Fig. 2). During the Anisian, horst- and graben structures evolved (e.g., Gawlick & Missoni, 2019). Extension of the passive continental margin was accompanied by locally intense volcanism in the Late Anisian, mainly in the Southalpine (Kukoč *et al.*, 2023). From Late Anisian to Late Ladinian, deep-water siliceous limestone and radiolarite with intercalated volcanic ashes were deposited. The Wetterstein Carbonate Platform represents a phase of intense carbonate production from the early Carnian (Cordevolian) into the Julian, terminating in the Julian Stage by the Mid-Carnian event (Ogg, 2015). It was followed by the cyclic deposition of mudstones, argillites, marls and sandstones with intercalated shallow-water carbonates of the Raibl Group. The Hauptdolomit/Dolomia Principale/Dachstein Carbonate Platform formed in the Norian and Rhaetian (Gawlick & Missoni, 2019). An environmental crisis at the Triassic/Jurassic boundary was accompanied by a sea-level drop, followed by the drowning of the carbonate platform in the Lower Jurassic and the deposition of pelagic limestones (e.g., Ammonitico Rosso) (Gawlick & Missoni, 2019).

Starting from the seminal publication on Austrian ore Districts (Weber, 1997), the Interactive Raw Material Information System (IRIS) provides an open access database (https://iris.geologie.ac.at), maintained by Geosphere Austria (www.geosphere.at). In IRIS, APT deposits in Austria are grouped into 9 ore Districts with 455 individual occurrences (Fig. 1B); for this presentation, four Districts have been added for areas outside

District name (IRIS) with type locality (Roman number according to Fig. 1)		Number of occurrences	Sphalerite (ppm)								Galena (ppm)					Sulphides $d^{34}S$ ‰		Sulphates $d^{34}S$ ‰
			Fe	Mn	Ag	Cd	Ga	Ge	As	Tl	Ag	Cu	As	Sb	Tl	min	max	
I	Pb-Zn (fahlore) district Tirolic-Noric Nappe System Northern Calcareous Alps Anisian (Sankt Veit-Tarrenton)	48 (A)	5000	22	48	2475	59	135	300	13	200	600	4000	400	50	-16.8	4.2	
II	Pb-Zn ore district Tirolic-Noric- and Bajuvaric Nappe System – Northern Tirolian Calcareous Alps Carnian (Lafatsch)	107 (A), 8 (B)	520	4	180	2800	10	144	340	70	50	6	800	620	4	-30	-2.2	16.1
III	Pb-Zn (fahlore) district Tirolic-Noric Nappe System Northern Calcareous Alps (Annaberg)	15 (A)	3500	48	1.8		0.3	6		3	50		100	10		-19.5	30.5	25.7
IV	Pb-Zn ore district Tirolic-Noric- and Bajuvaric Nappe System – eastern Northern Calcareous Alps Carnian (Weyer)	17 (A)	1000	30	10	1000	100	30		3	300		300	100		-20.7	-13.8	
V	Pb-Zn ore district Bundschuh Nappe - Stangalm Mesozoic (Erlacher Bock)	10 (A)	5%	1000	3	3000					50			30	50	-1.4		+18.2 to +22.7
VI	Pb-Zn ore district Ötztal-Bundschuh Nappe System- Stubai-Brenner Mesozoic (Griesbach)	8 (A)	3%	400		3000										-34.6	-29	
	Pb-Zn ore district Ötztal-Bundschuh Nappe System- Stubai-Brenner Mesozoic (Obernberg)	2 (A)	2300	3		6050	17	3.7	10	3	3000			5000		-2.4	-1.3	
VII	Pb-Zn ore district Drau Range-Gurktal Nappe System – Drauzug Mesozoic Anisian (Kellerberg)	28 (A)	4000	79	0.5	908	4.5	14	33	42	30		750	20	30	-13.5	2.6	
	Pb-Zn ore district Drau Range-Gurktal Nappe System – Drauzug Mesozoic Anisian (Topla)	1 (S)	1000	20	3	1000		0.3	3	3	3	3	30	700	30	-29.9	13.7	
VIII	Pb-Zn ore district Drau Range-Gurktal Nappe System – Drauzug Mesozoic Carnian (Bleiberg)	213 (A), 3 (S)	5000	24	8	1745	16.5	174	161	74	1.5	0.25	90	1.7		-39	2.4	+7.0 to 19.3
IX	Polymetallic ore district Permomesozoic Seengebirge Nappe (Rosegg)	7 (A)	5000	500	10	3000		10	300	3	<5		<100	<50	<50	-7.2	-6.8	24.2
X	Pb-Zn-ore district Silvretta-Seckau Nappe System - Engadine Dolomites (S-charl)	11 (CH)				2500					1500							
XI	Pb-Zn-ore district Southalpine Mesozoic Carnian (Raibl)	5 (I), 2 (S)	3000	26		900	10	500	1200	360	<5		3000	300	40	-25.6	-6.4	14
XII	Pb-Zn-ore district Southalpine Mesozoic (Salafossa)	9 (I)	5000	90	1.2	1000	1	480	420	170								
	Pb-Zn-ore district Southalpine Mesozoic (Auronzo)		2310	50	10	1500	10	75	1200	50	300		2000	500	10	-27	-12	
XIII	Pb-Zn-F-ore district Southalpine Mesozoic Carnian (Gorno)	15 (I)	5000	50	60	2000	180	100	20	1.7	500			1000	3	-9.8	+3.8	

Occurrences in Austria (A), Bavaria (B), Italy (I), Slovenia (S) and Switzerland (CH); IRIS for Austria; Schmid & Weinelt (1978) for Bavaria; Brigo & Omenetto (1979) for Italy; https://map.georessourcen.ethz.ch for Switzerland;

Data sources: Cerny & Schroll (1995); Drovenik *et al*. (1988); Fruth & Maucher (1966); Götzinger & Pak (1983); Melcher & Krois (1992); Schroll (1950, 1951, 1954, 1996, 1997); Schroll & Pak (1983); Schroll & Rantitsch (2005); Schroll *et al.* (1994); Štrucl (1984); unpublished data of the authors

***Table 2**: Pb-Zn Districts in Austroalpine and Southalpine units with compositional data of sulphide and sulphate from literature before 2010*

of the Austrian borders. The total number of APT deposits and occurrences is estimated at >500 (Table 2, Fig. 1). Ore Districts summarize deposits of similar type and genesis. The most important APT Districts within the Austroalpine tectonic units of Permo-Mesozoic age are defined within the "Drauzug-Gurktal" and "Tirolic-Noric" Nappe Systems. In addition, smaller Districts with less abundant and smaller deposits are known from the "Silvretta-Seckau", "Ötztal-Bundschuh" and "Bajuvaric" Nappe Systems. In the Southalpine of northern Italy, Anisian, Ladinian and Carnian carbonate rocks also host important APT deposits including Cave del Predil/Raibl, Salafossa and Gorno.

APT Districts within the Tirolic-Noric and Bajuvaric Nappe Systems

The Pb-Zn (-fahlore) ore District in Anisian strata of the North Tirolian Calcareous Alps (label I in Fig. 1B, Table 2) summarizes 48 occurrences. At the type locality at Sankt Veit-Tarrenton, sphalerite rhythmites with estimated 100,000 tonnes of ore have been mined previously (Wetzenstein, 1972; Sidiropoulos, 1983; Cerny & Schroll, 1995). Mineralization in Anisian strata is known on both sides of the Inn valley for a distance of >100km. Compared to the Pb-Zn mineralization hosted by Carnian rocks, the orebodies are less frequent and smaller, and many are polymetallic with locally Cu-Ag-bearing fahlore, pyrargyrite, acanthite and native silver (Paar, 1995). A Devonian dolomite in the footwall of some of the deposits is locally rich in Cu-Ag fahlore and barite. Partly, the mineralization was mobilized from earlier mineralization during younger events. Such processes are particularly evident in a polymetallic mineralization, where vein-type ores occur in Anisian to Norian rocks (Gstrein & Heissel, 1989).

The Pb-Zn ore District II (type locality Lafatsch) comprises 107 locations (Fig. 1B, Table 2). In addition, 8 occurrences are listed in Bavaria (Schmid & Weinelt, 1978). They are hosted by Carnian platform carbonates. The largest Pb-Zn deposit in the Northern Calcareous Alps, Lafatsch-Vomperloch (total resource ca. 3-4 million tonnes @ 1.6% Pb, 6.2% Zn; Cerny & Schroll, 1995; Leach *et al.*, 2005) was previously mined for Pb and Ag. Small mines operated since medieval time up to 1963, and are exposed by around 150 adits (Schulz, 1981). The mineralization occurs within a W-E oriented syncline composed of

Wetterstein limestone, sediments of the Raibl Group and Hauptdolomit. The mineralization is restricted to the uppermost 240m of the Wetterstein limestone forming cloud- and nest-shaped ore bodies, sheared and folded during the Eoalpine orogeny (Schulz, 1981). The mineral paragenesis is dominated by galena, sphalerite, marcasite, calcite and fluorite.

At the village Nassereith, Zn-Pb mineralization hosted by Wetterstein limestone forms a deposit cluster within District II (Fig. 1B, Table 2). Light-grey sphalerite forms a matrix of tectonic breccia and is associated with Ag-rich galena and fine-grained pyrite in calcite gangue (Vohryzka, 1968; Wolkersdorfer, 1989). Mining of the Silberleiten deposit NE of Nassereith dates back to the 15th century and ceased in 1921. The mineralization is mainly controlled by SE-NW trending veins. Isser (1881) identified stratiform primary Pb-Zn sulphides that have later been altered and remobilized into secondary minerals. Lead and calamine ores were mined in Kienberg-Rauschberg (Fig. 1) from the 16th century until 1894, followed by unsuccessful exploration from 1921-1925 (Knauer, 1937; Cerny, 1989; Läntzsch, 2015). The mineralization extends in a steeply inclined zone over 1200m in an E-W direction and 250m vertical extension, up to about 300-400m below the Raibl Group. Sphalerite is often developed as schalenblende, also showing stalactitic textures, and forms cement in a limestone breccia. Lead-zinc ores have also been mined from the 16th century until the late 19th century in the area of Scharnitz and Mittenwald (Fig. 1). Sulphide and calamine ores occur in irregular zones, often following tectonic structures. Ag-rich galena and calamine accumulated preferentially in zones of fault intersections (Jerz & Ulrich, 1966). Wulfenite is a common mineral of the oxidation zone (Weiß, 1982).

The Pb-Zn (-fahlore) ore District III in the eastern part of the Alps (Salzburg, Upper Austria) comprises 15 occurrences (Fig. 1B, Table 2). In addition to major galena and subordinate sphalerite, fahlore and various Cu sulphides occur as minor phases. The mineralization is structurally controlled and interpreted as of epigenetic origin at temperatures between 200-300°C (Götzinger, 1985; Weber, 1997). Revising the age of host rocks at the type locality Arikogel (Fig. 1A) to Upper Carnian/Lower Norian (Lampl *et al.,* 2008), Annaberg in eastern Austria is regarded here as a type locality for the District (Fig. 1A). It is hosted by thick-bedded limestone of the Gutenstein Formation (Hagenguth *et al.,* 1982; Götzinger, 1985). Mining in the 18th century primarily recovered native silver and chlorargyrite from a cementation zone. Oxide Pb-Zn(-Cu) ores (calamine, secondary Zn- and Pb-rich carbonate and silicate ores) that formed from galena-rich sulphide ore were extracted later. Mineralization follows SW to S trending faults.

The Pb-Zn ore District IV (Fig. 1B, Table 2) with its type locality at Weyer comprises 17 entries, indicating a fading out of Pb-Zn deposits towards the east. The mineralization comprises major galena, minor sphalerite and pyrite. It is hosted by Wetterstein limestone and dolomite and occurs along discordant structures and nappe boundaries. Some occurrences are Cu-bearing, and most have experienced extensive supergene alteration into calamine ore.

APT Districts within the Ötztal-Bundschuh Nappe System

Permo-Mesozoic sediments of the Stangalm Mesozoic that have experienced Eoalpine metamorphic temperatures around 500°C (Rantitsch *et al.,* 2020) host the Pb-Zn ore District V, comprising 10 occurrences (Fig. 1B, Table 2). Grey bedded dolomites to dolomite marbles host small but remarkable occurrences of Pb-Zn mineralization in several places. Although the stratigraphic classification of the individual mineralizations is still insufficient, they are likely to be developed in both Anisian and Carnian carbonates. The vein-type silver-bearing Pb-Zn mineralization of Flattnitz (Fig. 1A) are correlated with the top of the Wetterstein dolomite. In contrast, the mineralization further to the west (e.g., Erlacher Bock – Zunderwand) are partly hosted by Anisian strata. The mineralization comprises both vein-type and stratiform impregnations with galena, sphalerite, accompanied by bournonite, tennantite, tetrahedrite, jamesonite, chalcopyrite, pyrite, wulfenite, and barite, fluorite, dolomite and calcite gangue (Götzinger & Leute, 1998; Gröbner, 1998).

Stratiform and strictly strata-bound carbonate-hosted Fe-Zn-Pb sulphides occur in dolomite of the Brenner Mesozoic south of the Stubai Valley, Tirol (Melcher, 1990; Melcher & Krois, 1992). The Brenner Mesozoic rests unconformably on retrogressed amphibolite-facies metasediments and orthogneiss of the Ötztal-Stubai Basement. The pyrite-rich Pb-Zn ores are part of the Pb-Zn ore District VI with 10 occurrences (Fig. 1B, Table 2). They are laterally extensive, forming numerous oxidized limonitic layers within a dark dolomite of presumably Anisian age, overlying clastic sediments of the Lower Triassic "Alpine Verrucano" (Melcher & Krois, 1992). The sulphide layers carry primary (often collomorphous) pyrite, sphalerite, galena and accessory molybdenite. Molybdenum concentrations in oxidized limonitic ore reach up to 860 ppm. The metamorphic temperature at the base of the Brenner Mesozoic in this area exceeds 450°C (Reiser *et al.,* 2019).

The vein-type Obernberg Zn-Cu-(Pb-Ag) deposit (Fig. 1) was intermittently mined from the 14th century until 1923. It is hosted by metamorphosed Hauptdolomit of the Brenner Mesozoic. Major ore minerals are sphalerite, tennantite, galena, with subordinate pyrite, stibnite, bournonite, jamesonite and chalcopyrite.

APT Districts within the Drauzug - Gurktal Nappe System

Most APT occurrences including some medium-size and a few large deposits are known from Mesozoic carbonates within the Drauzug-Gurktal Nappe System. A District in Anisian strata containing 28 occurrences in Austria and a major one in Slovenia (District VII), is separated from the important Pb-Zn District hosted by rocks of Carnian age (District VIII: 213 occurrences in Austria, 3 in Slovenia).

The Pb-Zn ore District VII (Fig. 1B, Table 2) with its type locality at Kellerberg carries stratiform Pb-Zn mineralization in clastic dolomites of Anisian age occurring along the northern margin of the Drau Range (Austria), and at Topla in Slovenia (Fig. 1). In Topla, about 250,000 tonnes of ore grading 10% Zn and 3.3% Pb were mined from 1974 to 1988 from rhythmically

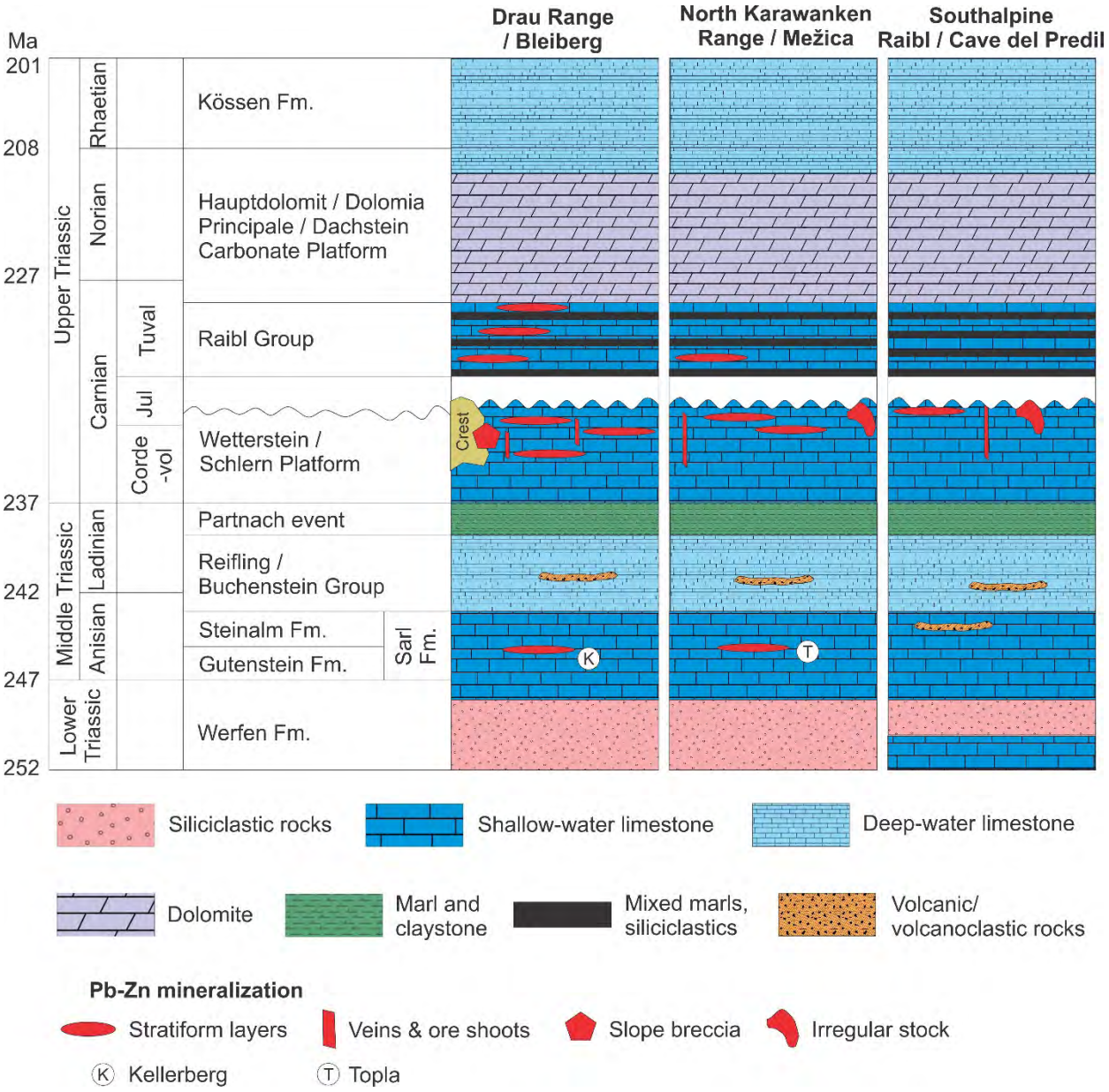

***Figure 2**: Stratigraphic and lithofacies chart of Austroalpine (Drauzug-Gurktal Nappe System) and Southalpine Triassic units. The position and shape of Pb-Zn orebodies in the deposits of Bleiberg, Kellerberg, Mežica, Topla and Raibl/Cave del Predil is indicated.*

laminated sphalerite ores, with Pb-Zn ratios of 1:4 to 1:6 (Drovenik *et al.*, 1988; Spangenberg & Herlec, 2006). The ores are hosted by dolomites of the Koprivna Formation, equivalent to the Gutenstein Formation in the northern Alps (Fig. 2). Most Anisian deposits, though, are small and are commonly unaffected by later processes. Locally, sphalerite and galena are accompanied by molybdenite and fahlore, explaining elevated Mo, Ag, Cu and As contents compared to Pb-Zn mineralization hosted by Carnian rocks (Warch, 1984).

In the Pb-Zn ore District VIII (Fig. 1B, Table 2), ore is hosted by Carnian carbonates of the Drau Range and the North-Karawanken Range. The District extends from Mežica (Slovenia) in the east over 180 km to the west. Most important are the deposits Mežica, Hochobir, Windisch Bleiberg, Bleiberg, Radnig, Jauken and Pirkach-Hochstadel (Fig. 1A), with an estimated initial resource exceeding 60 million tonnes. Bleiberg (Table 1; 43 million tonnes @ 1.1% Pb, 5.9% Zn; Leach *et al.*, 2005) and Mežica (*ca.* 25 million tonnes @ 5.3% Pb, 2.7% Zn; Rečnik *et al.*, 2014) constitute the largest resources. Bleiberg produced approximately 2.2 million tonnes of metals from ores hosted by Carnian carbonate rocks (Schroll, 2008). The mining area was active from 1333 until 1994.

Lead largely dominates the metal content of the complex large-scale deposits hosted by Wetterstein limestone (Bleiberg Pb/Zn

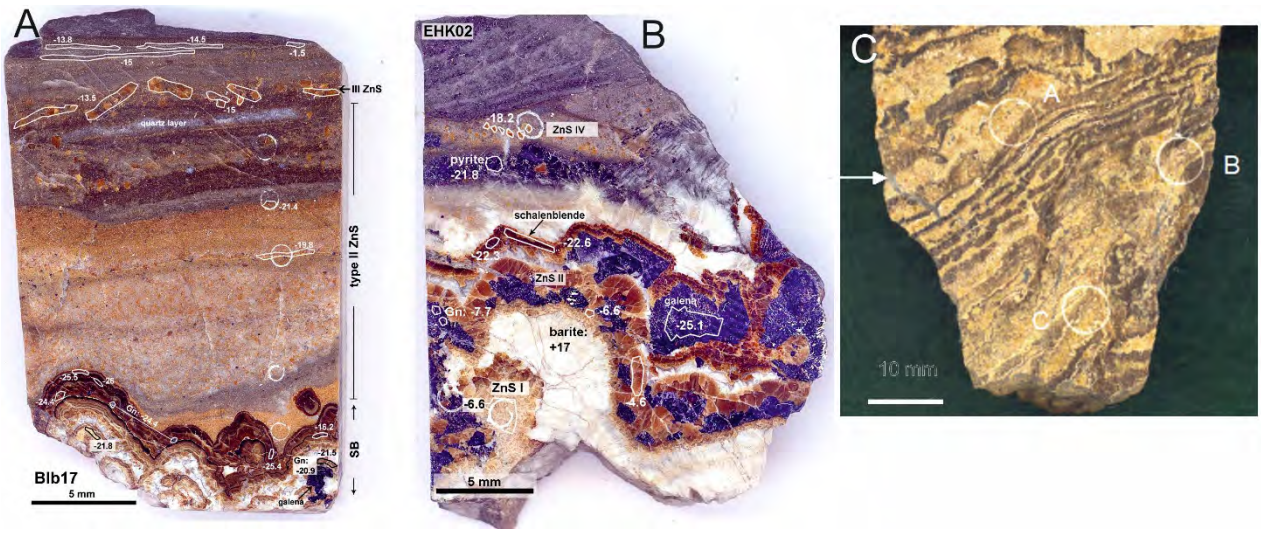

Figure 3: *Ore types from the different ore horizons at Bleiberg. (A) Maxer Bänke (sample Blb 17): fine-grained layered sphalerite ore with schalenblende of different colour at the bottom; the gangue is rich in fluorite and quartz. (B) Erzkalk (sample EHK02): galena and different types of sphalerites (ZnS I to IV); the gangue is barite, fluorite, calcite and dolomite. Values in (A) and (B) are $\delta^{34}S$‰ values of sphalerite (for details see Henjes-Kunst et al., 2017). (C) Massive sphalerite ore, Crest horizon (Schwellenfazies). The dark brown sphalerite bands are interpreted as mineralized microbial mats. Fractures (arrow) are filled with late-stage anhydrite, photo courtesy H. Kucha.*

= 1/1.5, Mežica Pb/Zn = 1). The ore bodies in the Raibl Group are consistently Zn-dominated (Pb/Zn = 1/4 to 1/6). The metal content of most individual deposits is in the order of 10^3 to 10^4 t. The main minerals are galena, sphalerite and subordinate iron sulphides (marcasite, melnikovite, pyrite). Molybdenite is rather rare and bound to bituminous sedimentary rocks. An exception is known from Mežica, where molybdenite has been found in the paragenesis of a fracture mineralization. More than 50 secondary minerals have been described from the oxidation zones, including abundant wulfenite, as well as descloizite and vanadinite. Gangue minerals are quartz, anhydrite, gypsum, fluorite, barite, calcite and dolomite (Schroll, 1953; Kanaki, 1972). Fluorite-bearing mineralization is always rich in Zn and associated with quartz. Fluorite is the predominant gangue in the west of the Bleiberg deposit (Antoni shaft). Barite dominates the eastern part of Bleiberg (Rudolf District), in Windisch Bleiberg and in the Hochobir areas (Fig. 1), but is missing in Mežica, which has a carbonate-dominant gangue.

The bulk of the metals occurs thin the Wetterstein Formation top (Cordevol), where a "special facies" comprises a 60m thick sequence of cyclothems of subtidal to supratidal sediments (Bechstädt, 1975) (Fig. 2). A sequence of green marls, mudstones, breccias, stromatolites and mussel banks formed, interrupted by evaporitic periods. Emergence resulted in karstification, local erosion, resedimentation and extensive cavity formations. The "special facies" ores are characterized by fluorite, anhydrite and quartz. At the top boundary to the Raibl Group, an oolite horizon is mineralized with pyrite, marcasite, melnikovite, and rarely sphalerite, galena and barite (Schulz, 1983).

Ore is present also as tens of meters thick bodies in the footwall of the oolitic horizon and in a rhythmic sequence, where the lowest ore horizon is 200 to 300m (Bleiberg), or even 600m (Mežica) below the base of the overlying Raibl Group (Fig. 2). The Raibl Group sediments are rarely mineralized, but occasionally iron-sulphide-containing geodes occur. The Pb-Zn mineralization is confined to the intermediate dolomite and grauwacke, and to breccia and dolomite in the hangingwall of the uppermost Raibl shale. In the Drau Range, the mineralization within the Raibl Group is common, whereas it is missing in the North-Karawanken Range.

A special ore type is represented by a massive zinc-rich mineralization on the southern edge of the intensely dolomitized lagoonal carbonates (Bleiberg and Mežica). The layered mineralization is consistently Zn-rich, while the vein mineralization is Pb-rich.

At Bleiberg, several strata-bound to stratiform ore horizons are known in carbonate rocks of the upper Wetterstein Formation ("Maxer Bänke", "Erzkalk", "Crest") and in the overlying Raibl Group (Fig. 2). Zn-dominated ores at the Maxer Bänke horizon occur in a dolomitic/marly sequence about 170-190m below the 1st Cardita shale, which was deposited in a sub- to supratidal environment (Hagenguth, 1984). They consist of fine-grained disseminated sphalerite often showing stratiform features and botryoidal sphalerite (schalenblende) with very little galena (Fig. 3A). The gangue is dominated by fluorite, quartz and minor dolomite and calcite (Henjes-Kunst *et al.*, 2017).

The "Erzkalk" mineralization comprises eight concordant ore bodies ("Edle Flächen) in the uppermost 120m of the Wetterstein Formation. The hosting lagoonal carbonates include sub- to intratidal cyclic sequences with stromatolites, breccias, and marls. They were deposited in a topographically elevated zone of the carbonate platform that was periodically emerged and karstified. The stratabound ore bodies within the Erzkalk horizon seem to be connected to these emergent horizons that are traceable over kilometres in the mine (Cerny, 1989). These smaller volume orebodies were the most extensively mined ores at Bleiberg (1.5 million tonnes) containing galena,

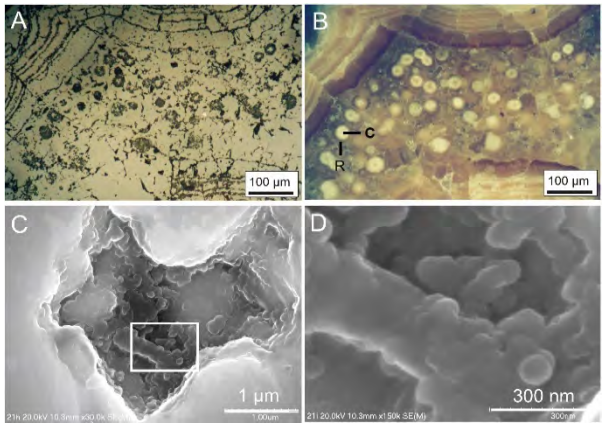

Figure 4: *Microbial textures in sphalerite ores from Bleiberg, Crest horizon ("Kalkscholle").* ***(A, B)*** *Photomicrograph of sphalerite band formed by replacement of former microbial mat. Detail of circle C in Fig. 4C. The band consists of circular biogenic (?) globules with core and rim (C, R). (A) Reflected light, (B) with crossed polars.* ***(C)*** *FE-SEM image of etched cavity within micro-globular sphalerite showing nano-globules of sphalerite.* ***(D)*** *FE-SEM image showing details of (C) with ZnS nano-globules and part of a mineralized bacterial filament. Photos H. Kucha.*

sphalerite (Pb/Zn = 1 to 1/4), and minor Fe sulphides. The gangue typically contains barite in addition to calcite, dolomite, fluorite and quartz and ore specimens commonly record sequential crystallisation (Fig. 3B; Henjes-Kunst *et al.* 2017).

The "Crest Horizon" is an irregular, breccia-dominated high-grade Zn-rich (ca. 7% Zn) ore body in dolomitized limestone of the upper Wetterstein Formation. It is highly mineralized with a low Pb/Zn ratio of 1/10 and low Ge contents in sphalerite (Cerny, 1989). Diagenetic mobilization processes are responsible for Mn enrichment and Sr depletion. Partly, banded ore textures are preserved (Fig. 3C). Individual layers consist of globular micro-structures which are partially replaced by sphalerite. These bands, which are intercalated between schalenblende were interpreted as mineralized microbial mats (Fig. 4A, 4B; Kucha *et al.*, 2005; Kucha *et al.*, 2010). Elongate filaments and nano-globules of ZnS were made visible by FE-SEM imaging of etched micro-voids in these globular sphalerites (Fig. 4C, 4D). In combination with the light sulphur isotope values these textures were interpreted as microbial features and products of microbial metabolism (Kucha *et al.*, 2010).

Breccia ores formed by large-scale slumps of Crest and Cardita material into a basin. Such breccia bodies are in places highly mineralized, such as in "Revier Erlach" in the westernmost part of the Bleiberg mine area where massive ore components are embedded in a shale matrix. Such ores are interpreted as resedimented breccia that formed in the Carnian during deposition of the third Cardita shale horizon (Cerny, 1989).

Three additional ore horizons (Cardita horizons) are developed in the carbonate rocks intercalated between the three shale horizons of the Carnian Raibl Group.

Detailed studies from Bleiberg documented a multitude of discordant ore features (for details see Schroll, 2008). These include irregular stockwork-like breccia ore bodies, discordant veins as well as tubular ore bodies and mineralized cavities. The economically most important ones were limestone-dolomite breccia ore bodies of the Crest horizon ("Kalkscholle" etc., Schulz, 1985). The formation of irregular cavities has been linked to karstification due to emergence of the carbonate platform (Bechstädt, 1975). Ore rhythmites with geopetal structures within these up to metre-sized cavities were interpreted as sedimentary ores formed in cavity depressions (Siegl, 1956). Higher grade ore zones were often developed at the intersection of bedding parallel and discordant fault structures. Schulz (1968) assumed that some of the discordant veins formed syn-diagenetically, providing pathways for the mineralizing fluids.

To the west of the Bleiberg deposit, small and medium-size APT deposits are known (Fig. 1). The Radnig Pb-Zn-(F-Ba) deposit (0.25 Mt remaining reserve; Cerny, 1989) is hosted by shallow-water sediments similar to the "special facies" of the Bleiberg deposit, overlain by barren sediments of the Raibl Group. Sphalerite occurs as dark honey-coloured crystals up to 1mm in size hosted by coarse dolomite, as rhythmic layers ("zebra ore") of calcite, barite and yellow hypidiomorphic sphalerite, and as brecciated ore (Onuk, 2018). The Jauken deposit was mined for Pb-Zn- (calamine) ores for several centuries. Later, also Pb-Zn sulphides were mined. Ores consisting of sphalerite, galena, some pyrite and chalcopyrite are restricted to the uppermost Wetterstein Formation and the Raibl Group. Sphalerite is high in Ge (Cerny & Schroll, 1995).

The Pb-Zn occurrence of Pirkach-Hochstadel (Fig. 1) is hosted by the topmost members of the Raibl Group. The mineralization is strictly stratiform and occurs as a consistent layer of 1m thickness about 20m in the hangingwall of the third Raibl shale (Cerny, 1989). Ore samples are rich in pyrite but locally carry coarse sphalerite crystals that are high in Cd, Ga and Ge, but poor in Tl (Schroll, 1954).

The deposit cluster at Hochobir with the Fladung deposit in the Northern-Karawanken Range (Fig. 1) is bound to the Upper Wetterstein Formation, 20-30m below the first Raibl shale. Ores are present as layered sphalerite-galena rhythmites with common colloform textures (Onuk, 2018).

The Mežica deposit occupies a 10km^2 area below Peca (Petzen) mountain between Črna na Koroškem and Mežica (in Slovenia) (Fig. 1). This Pb-Zn district includes more than 350 orebodies with a total production of 19 million tonnes of ore and estimated remaining reserves of 6 million tonnes (Rečnik *et al.*, 2014). After 350 years of mining activity, production at Mežica stopped in 1994, and the mine closed in 2004. The mineralization is hosted in the upper 600m of the Wetterstein formation of the Northern-Karawanken Range, in the carbonate sequence between the 1st and 2nd Raibl Group shales and in the Hauptdolomit (Štrucl, 1960; 1984) (Fig. 2). The mineralization occurs as (i) reef-bound, (ii) concordant, (iii) discordant and (iv) breccia ore bodies (Cerny, 1989; Potočnik Krajnc, 2021). Economically important are discordant and breccia-type mineralizations (Fig. 5A-D). Discordant ore bodies occur as

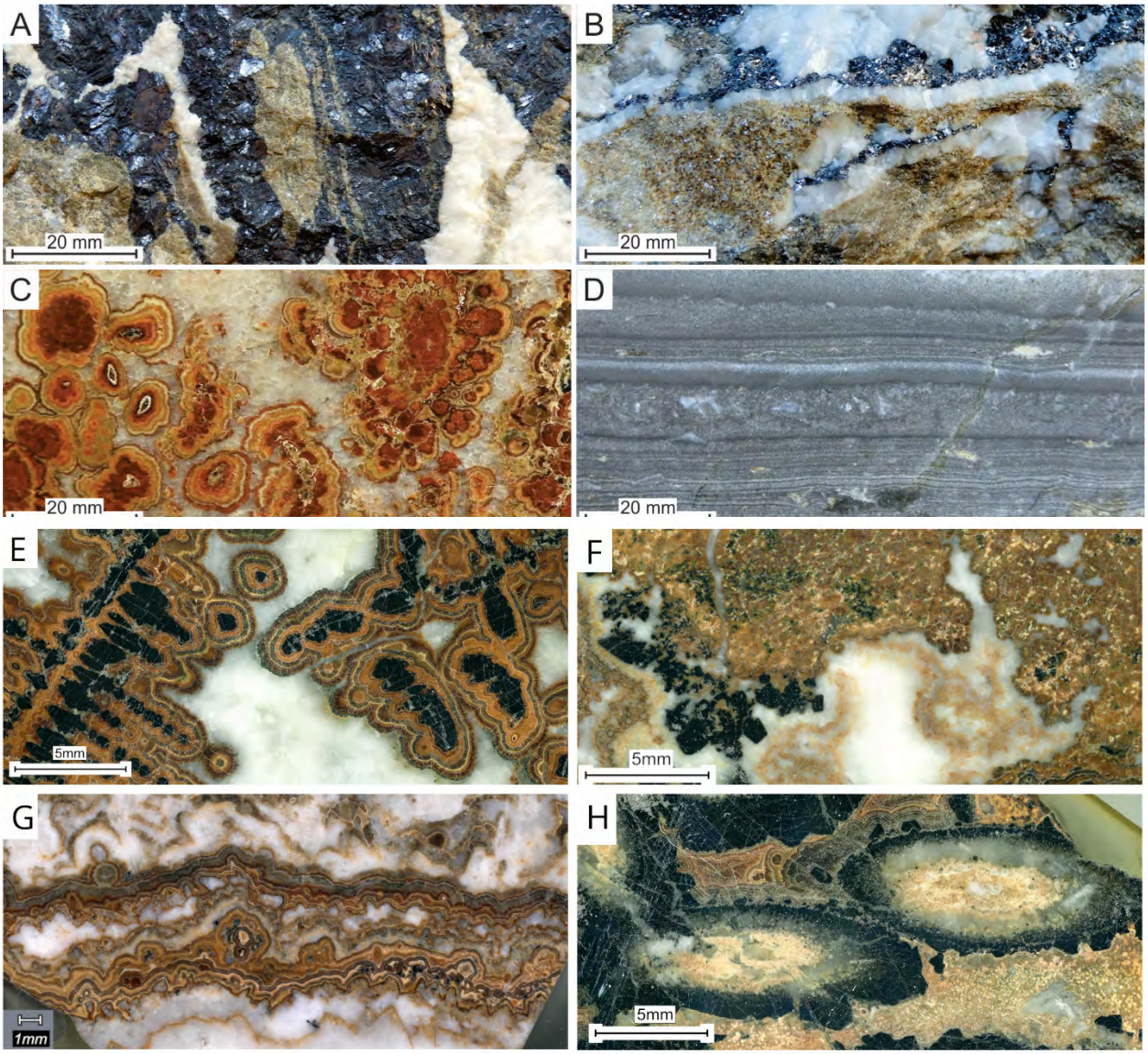

Figure 5: *Textures of Pb-Zn ore from the Mežica and Raibl deposits.* ***(A-D)*** *Macroscopic images of the main ore textures of the Mežica deposit.* ***(A, B)*** *Breccia- and vein-type mineralization showing impregnation and replacement of host rock clast by sphalerite (brown). Sphalerite is overgrown by bands of galena and late hydrothermal calcite.* ***(C)*** *Irregularly shaped, concentric, alternating banding of colloform sphalerite in cockade breccia.* ***(D)*** *Concordant mineralization in the form of ore rhythmite – alteration and replacement of initial laminated host-rock by sphalerite, minor galena and dolomite.* ***(E-H)*** *Macroscopic images of important ore textures of the Raibl deposit.* ***(E)*** *Dendritic ore, composed of colloform grey sphalerite overgrown by galena and a second generation of sphalerite with brown to yellow colours. Pyrite forms an outer rim of the dendritic texture (sample R63a).* ***(F)*** *Agglomerated sphalerite consisting of rounded individual sphalerite grains overgrown by galena in a gangue of dolomite and barite, next to bands of brown sphalerite (sample R45).* ***(G)*** *Sphalerite bands showing varying shades of brown, intergrown with barite (sample R59).* ***(H)*** *Tubular ore composed of galena tubes filled by light brown sphalerite, dolomite and barite. Tubes are cemented by a second generation of dark brown sphalerite (sample R67).*

steeply dipping fracture-controlled structures, that extend vertically for more than 60m. Such ore bodies represent post-Triassic faults, which were probably conduits for upward migrating ore-forming fluids (Herlec et al., 2010). Typical textures associated with discordant orebodies are cockade breccias (Fig. 5C), veins, breccias, ore-impregnations and replacements of host-rock clasts (Štrucl, 1984). Breccia-type mineralizations occur as irregular and columnar ore unrelated to the stratigraphic and tectonic position. Breccias were likely formed as the result of tectonism, collapse of karst caves, and the selective dissolution of the host-rock by hydrothermal fluids (Herlec *et al.*, 2010). Alternatively, these breccias have been interpreted as karstified and brecciated palaeotopographical highs that were later mineralized by Pb-Zn sulphides (Bechstädt, 1975; Cerny, 1989).

The small polymetallic ore District IX (Fig. 1B, Table 2) with 7 occurrences is confined to the Middle Triassic dolomite overlying metamorphic basement rocks. This mineralization is historically important with mining activities in the 18th century

and probably in pre-Roman times (Enzfelder, 1972), but do not have any economic potential. The vein-type deposits consist mainly of Hg-rich tetrahedrite and galena, with chalcopyrite, sphalerite and barite plus quartz as gangue minerals (Pichler, 2003). Oxidized ore samples carry cerussite, hemimorphite, wulfenite, greenockite, anglesite, azurite and malachite.

APT deposits in the Silvretta-Seckau Nappe System

Triassic sedimentary cover sequences in the Lower Austroalpine and structurally lowest Upper Austroalpine nappes locally host insignificant sulphide mineralization. The Pb-Zn ore District X in the Engadine Dolomites of Switzerland (Fig. 1B, Table 2) is hosted by Triassic sediments overlying the basement rocks of the Silvretta-Seckau Nappe System. The small deposits around Scharl have been intermittently mined from the 4th century until 1828. They occur in the Anisian limestone and the lower part of the Wetterstein dolomite. Reddish brown and grey sphalerite, Ag-rich galena, pyrite, chalcopyrite and fahlore mineralization is found in fracture and breccia zones associated with barite, quartz, Fe carbonate, wulfenite and calamine ore (Escher, 1935; Kellerhals, 1962; Büttner & Saager, 1983). Based on textural relations, the timing of Pb-Zn mineralization predates nappe thrusting.

Further to the west, in the areas of Arosa, Davos and Sertig, Pb-Zn mineralization occurs in a similar stratigraphic position, with major sphalerite and minor galena, pyrite, jamesonite and secondary minerals (Escher, 1935).

APT deposits in the Southalpine

The Southalpine unit hosts Pb-Zn Districts within Anisian to Norian limestone, dolomite and shale. A total of 46 occurrences of "stratiform Pb, Zn, fluorite, barite ores" are reported in the Dolomites, the Julian Alps and the Orobic Alps (Brigo & Omenetto, 1979).

The Pb-Zn-ore District XI at Cave del Predil/Raibl (Fig. 1B, Table 2) is hosted by the *ca.* 1000m thick Schlern Dolomite (Fig. 2). Minor mineralization occurs at the contact of the Schlern Dolomite to the Raibl Group, but the deposit does not extend into the Raibl Group itself (Brigo & Omenetto, 1978). About three ore horizons are known and have been mined from the Middle Ages until 1988. The original resource was 34 million tonnes. 15 to 20 million tonnes @ 5% Zn and 1% Pb have been produced with a metal output of 1.5 million tonnes Pb + Zn (Cerny, 1989). Leach *et al.* (2005) reported 18.2 million tonnes @ 1.2% Pb and 6.0% Zn (Table 1). Sphalerite and galena are the ore minerals, Fe sulphides are rare, fluorite is absent, and barite is locally abundant. The mineralization is bound to fault systems but may deviate slightly from the main mineralizing faults (Jicha, 1951). The mineralization itself has been described as vein-like or as veinlets (Cerny, 1989), but also as columnar stocks (Omenetto, 1980). Stratiform ores at the contact of Schlern Dolomite and Raibl Group are subordinate (Brigo *et al.,* 1977).

The deposit of Raibl shows a variety of massive to disseminated ores. Various breccias have been described (e.g., Pošepny, 1873). Colloform sphalerite (schalenblende) is the most common ore texture (Jicha, 1951; Pošepny, 1873) (Fig. 5E and 5G). The bands of colloform sphalerite sometimes enclose dendritic galena grains (knitted galena; Fig. 5E) (Gartner, 2023). Galena also occurs as cubes or octahedrons, hexahedrons with blunt corners, crusts and vein fillings and as bands (Cotta, 1863; Pošepny, 1873; Göbl, 1903; Jicha, 1951). Granular and disseminated sphalerite (Göbl, 1903; Gartner, 2023) shows similar colour zoning as colloform textures (Fig. 5F). This ore type, described in Bleiberg as well (Schulz, 1959), is transitional between disseminated and colloform textures (Gartner, 2023).

Tubular ore consists of galena tubes surrounded by bands of sphalerite and pyrite (Fig. 5H). The tubes may sometimes be hollow but are more often filled by either weathered material or a mixture of gangue and sphalerite (Posepny, 1887; Pošepny, 1873; Gartner, 2023). Sphalerite-stalactites ("Röhrenerz") have also been described (Kraus, 1913).

The Pb-Zn ore District XII (Fig. 1B, Table 2) in northern Italy contains several small, and two medium size APT deposits. The Pb-Zn mineralisation of Salafossa is mainly hosted by the South Alpine Cassian Formation (Ladinian to Carnian) and is located close to a thrust plane with Permian evaporites and sandstones in the footwall. The stock-like orebody some 700 x 50m to 200 x 50m size (Leach *et al.,* 2003) was mined from 1957 until depletion in 1986 and yielded 10 million tonnes of ore @ 4.9% Zn, 0.95% Pb (Cerny, 1989). The ore was mined from a breccia that graded into massive dolomite and featured a Pb-Zn ratio of 1/5. Deeper parts were rich in pyrite, marcasite and barite, whereas the higher parts consisted of colloform sulphides and saddle dolomite.

In the Auronzo area (Fig. 1A), several Pb-Zn occurrences are known, among them, the stock-like Argentiera deposit that was been in production until 1971, producing 1 million tonnes of oxide ore @ 6% Zn, 1% Pb (Cerny, 1989). Breccia ores are mostly hosted by the Anisian Upper Sarl Dolomite, and are exclusively structure-controlled (Assereto *et al.,* 1976).

The Pb-Zn-F ore District XIII at Gorno in the Bergamo province (northern Italy; Table 2), hosts Pb-Zn-Ag and fluorite-barite orebodies within the Carnian lagoonal Calcare Metallifero, followed by deeper-water marly limestones of the Gorno Formation, correlated to the Raibl Group (Mondillo *et al*., 2020). The stratabound deposits mainly carry sphalerite, galena, fluorite and barite, with minor Ag-bearing tetrahedrite-tennantite (Mondillo *et al.,* 2018, 2020). Mining was active until the 1980s, and exploration restarted in 2015. A production target of 6.0 million tonnes at a cut-off grade of 3.5% Zn was estimated (Altamin, 2023). Leach *et al.* (2005) list a resource of 6.2 million tonnes @ 2.3% Pb and 11.5% Zn (Table 1).

Trace element and isotopic geochemistry of ore-related minerals

Analytical methods

Samples for this study were collected from mine workings, dumps and mineral collections at the Federal Institute for Geosciences and Natural Resources (BGR), Montanuniversität Leoben and University of Ljubljana. The samples used for the trace element study by Henjes-Kunst (2010) and for radiometric dating were collected underground in the western and deepest accessible parts of the then-active Bleiberg mine in

1990 by O. Schulz, F. Vavtar and F. Melcher (University of Innsbruck).

Sulphide minerals were analysed using electron microprobe (EPMA) and laser ablation-inductively coupled plasma mass spectrometry (LA-ICP-MS) techniques. EPMA was carried out using the JEOL JXA 8200 superprobe at the Chair of Resource Mineralogy, Montanuniversität Leoben (Austria) and a CAMECA SX 100 probe at the Federal Institute for Geosciences and Natural Resources (BGR) in Hannover (Germany) (for analytical conditions see Henjes-Kunst, 2014). This research focussed on samples from the Bleiberg deposit, with additional samples included from Jauken, Radnig, Mežica, Topla, Windisch-Bleiberg, Zunderwand, Raibl and Lafatsch (Fig. 1B, Table2).

LA-ICP-MS was used for minor and trace elements in sphalerite and pyrite, employing a New Wave Research Nd:YAG 213 nm nano second laser ablation system coupled to an Agilent 8800 triple quadrupole ICP-MS. The laser beam was focussed to a spot size of 50µm at 10Hz and 2-3J/cm². Helium (750ml/min), mixed with argon (900ml/min) was used as carrier gas. The following isotopes were measured using acquisition times between 0.02 and 0.05seconds: ^{34}S, ^{51}V, ^{52}Cr, ^{55}Mn, ^{57}Fe, ^{59}Co, ^{60}Ni, ^{63}Cu, ^{66}Zn, ^{71}Ga, ^{74}Ge, ^{75}As, ^{82}Se, ^{95}Mo, ^{107}Ag, ^{111}Cd, ^{115}In, ^{118}Sn, ^{121}Sn, ^{197}Au, ^{210}Hg, ^{205}Tl, ^{208}Pb and ^{209}Bi

For quantification of the element content, the matrix-matched sintered pressed powder pellet reference material (MUL-ZnS 1; Onuk *et al.*, 2017) and for quality control, the USGS powder pressed polysulfide reference material MASS-1 (Wilson *et al.*, 2002) were used. The software package Iolite V3.1 (Paton *at al*., 2011) was used for data reduction.

For diagrams and tables (Table 4), median, interquartile range (IQR) and total ranges are used. Spider diagrams for sphalerite from different APT deposits are normalized to an average APT composition calculated from the median of 13 deposit medians derived from the LA-ICP-MS data (Table 4). These are (in ppm): Mn 3.2, Fe 2267, Cu 136, Ga 1.9, Ge 194, As 56, Ag 1.0, Cd 2422, Sn 0.12, Sb 0.52, Tl 9, Pb 323.

In-situ sulphur isotope analysis using the same analytical instruments was performed as outlined by Onuk (2018) using two in-house reference materials with known δ^{34}S. A precision of better than 1‰ was achieved. All sulphur isotope analyses are given in standard δ^{34}S notation (^{34}S/^{32}S) in per mil (‰) relative to the Vienna-Canyon Diablo Troilite (VCDT) defined by the assignment of δ^{34}S of -0.30‰ to the IAEA S-1 reference material. Sulphur isotope analyses were also performed at the Scottish Universities Environmental Research Centre (SUERC) in East Kilbride (UK) at the Stable Isotope Laboratory in cooperation with Adrian Boyce. Analytical details are provided in Henjes-Kunst (2014) and Henjes-Kunst *et al.* (2017).

Rb-Sr isotope analysis of sphalerite and associated gangue carbonate and fluorite was performed at the Technical University Bergakademie Freiberg (Germany; TUBA), at the Federal Institute for Geosciences and Natural Resources in Hannover (Germany; BGR) and at the Department of Lithospheric Research, University of Vienna (Austria). Additionally, lead isotope analysis of galena and sphalerite was carried out at the BGR. Details of sample processing including chemical digestion, element separation and mass-spectrometric isotope analysis can be found in Schneider *et al.* (2007a) and Henjes-Kunst (2014) for analytical work performed at TUBA and BGR, respectively. Rb-Sr isochron calculation and graphical presentation has been performed making use of IsoplotR version 5.2 (Vermeesch, 2018) considering the maximum likelihood model and an ^{87}Rb decay constant of 1.397 x 10^{-11} yr^{-1} (Rotenberg *et al.*, 2012). The goodness of fit of the sample data along the calculated isochron is given by the mean square of weighted deviates (MSWD). Errors were calculated by propagation of analytical uncertainties associated with the sample data and with the decay constant and reported at the 95% confidence level for isochron calculations with an MSWD close to unity. Isochron errors for datasets yielding MSWD values >>1 are given as scatter-enhanced 2δ errors.

Trace element composition of sulphides

The chemical composition of sulphide minerals provides important constraints on physico-chemical parameters of ore formation, and likely on the metal sources (e.g., Möller *et al.*, 1983). Trace element data of sulphide minerals in APT deposits have been collected for over 70 years, starting with Schroll (1950, 1951, 1953a,b, 1954, 1955). The development of analytical methods from semiquantitative spectrometric determination of a few trace elements on single ore samples (e.g., Hegemann, 1960; Fruth & Maucher, 1966; Kuhlemann & Zeeh, 1995) over in-situ electron and ion probe microanalysis (since the 1980's; e.g., Pimminger *et al.*, 1985; Henjes-Kunst, 2010, 2014; Henjes-Kunst *et al.*, 2017) to laser ablation-ICP-MS analysis of complete trace element inventories (Onuk, 2018; Melcher & Onuk 2019) has resulted in an extensive dataset on a significant number of APT deposits. In the following, results of EPMA studies (Henjes-Kunst, 2010, 2014) and of several extensive LA-ICP-MS studies on sphalerite are summarized, including Mežica (Potočnik-Krajnc, 2021), Raibl (Gartner, 2023) and a number of other deposits in Austria (Onuk, 2018) and Bavaria. Trace element data of pyrite/marcasite are available from only a few deposits. For galena, the data obtained by Schroll (1951, 1953a, 1954, 1997) and Schroll *et al.* (1994) are still the only ones available.

Literature data for sphalerite and galena compositions from deposits hosted by Anisian and Carnian carbonate rocks are compiled in Table 2. Sphalerite compositions determined by EPMA from ten APT deposits in Districts II, V, VII, VIII and XI are summarized in Table 3 (Henjes-Kunst, 2014). Statistical parameters for trace elements measured by LA-ICP-MS are shown in Table 4.

Sphalerite in APT deposits is, with only a few exceptions, poor in Fe (median 0.01-0.5%), Mn, V, Cr, Co, Ni, In, Sn and Sb. It often carries elevated to high Ge (median commonly 50-300ppm), As, Tl, Pb, and variable Cu, Ag, Ga (Onuk, 2018; Melcher & Onuk, 2019) (Fig. 6). Ores hosted by Anisian strata carry higher Ga, Sn, Sb, and lower Ag than those in Carnian rocks (Table 2). The different trace element composition is attributed to the proximity to, often fahlore-bearing, Palaeozoic carbonate-hosted ores in the footwall. Germanium concentrations are elevated in both, Anisian and Carnian strata, but are generally lower in the Northern Calcareous Alps compared to stratigraphically and mineralogically similar ores of the Drau

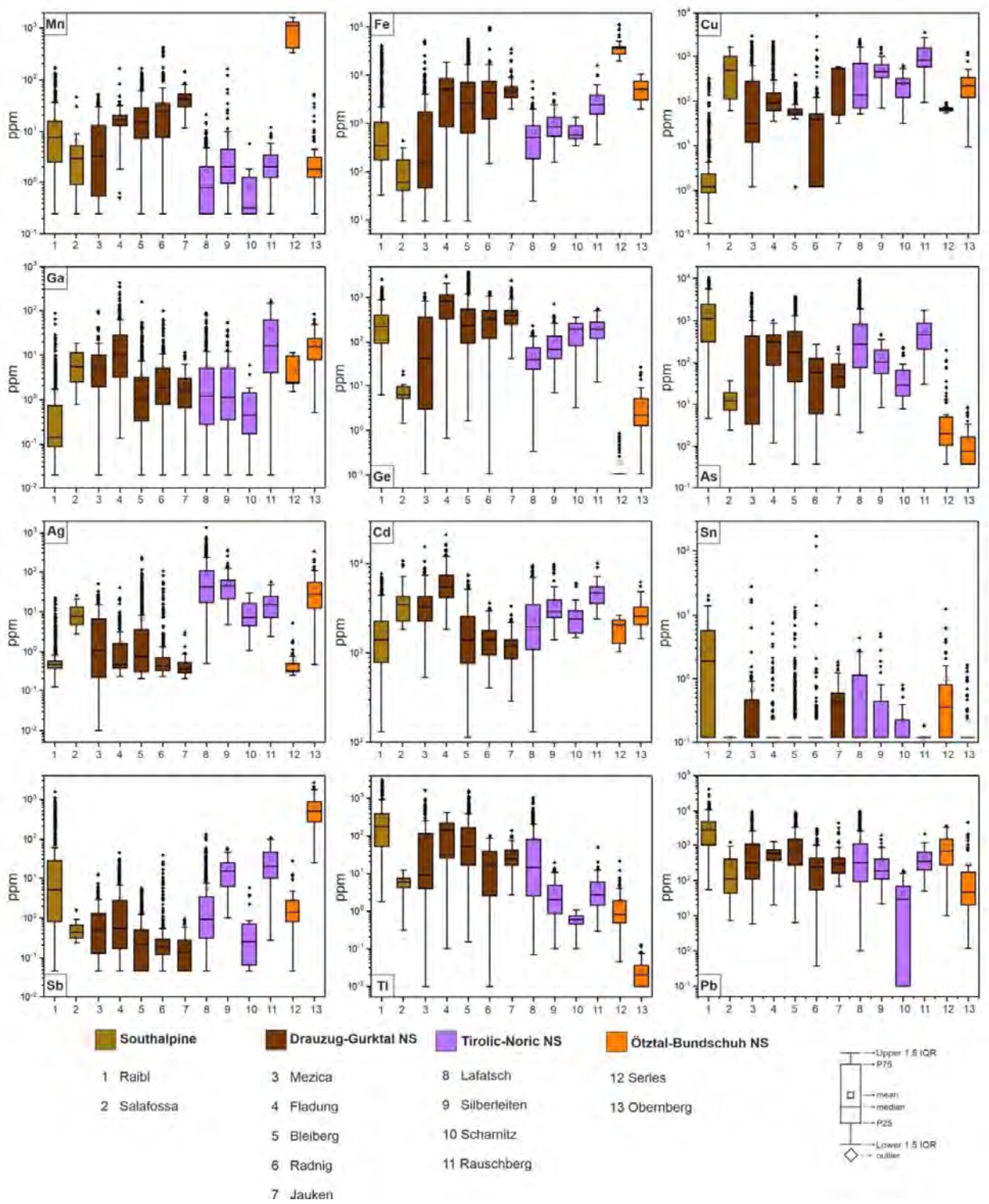

Figure 6: *Trace element variations in sphalerite from different APT deposits of Southalpine and Austroalpine units*

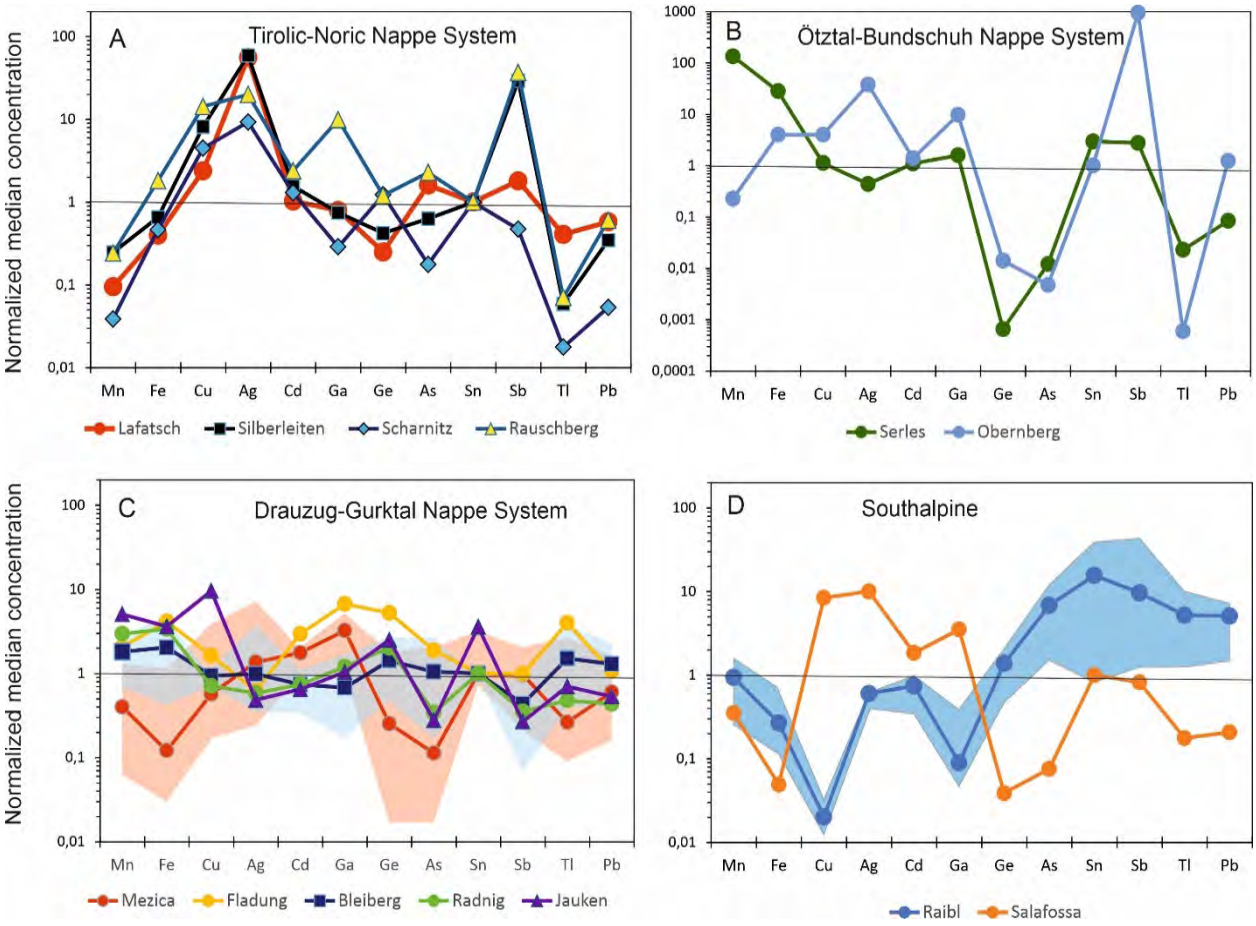

Figure 7: *Median trace element composition of sphalerite in APT deposits measured by LA-ICP-MS from four tectonic units. (A) Tirolic-Noric Nappe System (Northern Calcareous Alps); (B) Ötztal-Bundschuh Nappe System (Brenner Mesozoic); (C) Drauzug-Gurktal Nappe System (Drau Range, North-Karawanken Range); (D) South Alpine. Coloured fields indicate inter-quartile range (Q1, Q3) for Bleiberg (blue colour in (C)), Mežica (brown colour in (C)) and Raibl (in D).*

For normalizing values see section on trace element and isotopic geochemistry of ore minerals

Range, Northern-Karawanken Range and the Southalpine. Silver concentrations in all stratigraphic units of the Northern Calcareous Alps are well above those in the Drau Range and Southalpine. Galena is Ag- and Sb-bearing (30-300ppm Ag, and 50-500ppm Sb at Lafatsch; Schroll, 1951, 1953a).

Trace element distribution patterns in sphalerite both display similarities and significant differences (Fig. 6, Fig. 7). Similarities are well expressed within the tectonic units. If normalized to an average sphalerite composition for APT deposits, median compositions of sphalerite from the Drauzug-Gurktal Nappe System display positive Mn/Fe ratios, low Ag and Sb, and elevated Tl (Fig. 7C). In contrast, sphalerite from the Northern Calcareous Alps (Tirolic-Noric Nappe System) is characterized by lower Mn/Fe ratios, distinctly elevated Cu, Ag and Sb, and lower Ge (Fig. 7A). Sphalerite from the Raibl deposit in the Southalpine tectonic realm exhibits a high Mn/Fe ratio, very low Cu and Ge, and high As, Sn, Sb, Tl and Pb (Fig. 7D).

The Obernberg deposit in the Brenner Mesozoic is characterized by low Mn/Fe, high Ag and exceptionally high Sb, with low Ge, As and Tl values. Metamorphosed sphalerites from the Anisian dolomite in the Brenner Mesozoic are rich in Mn and Fe, and low in Ge, As, Tl and Pb (Fig. 6, Fig. 7B).

Within geographically and tectonically well-defined groups, a Random Forest analysis (Breimann, 2001) identifies deposit discriminating elements and validates them by a randomized cross-stratification approach. The results provide evidence with high confidence of the importance of local trace element signatures as geochemical fingerprints and extract geochemical relationships within the ore district (Fig. 8).

In particular, Ag discriminates the Lafatsch deposit, Mn the Jauken deposit and Ge the Fladung deposit. The Raibl deposit is unique by a very low Cu concentration, showing a relation also to the Radnig and Mežica deposits, possibly explained by a palaeogeographic proximity at the time of mineralization.

Application of the GGIMF geothermometer (Ge-Ga-In-Mn-Fe in sphalerite reveals temperatures of between 60°C and 140°C (Table 4) (Frenzel *et al.*, 2016). These values are consistent with temperature models for the Drau Range (Rantitsch, 1995, 2001, 2003), but in conflict with temperatures calculated from

		Elements (ppm)																				
		V	Cr	Mn	Fe	Co	Ni	Cu	Ga	Ge	As	Se	Mo	Ag	Cd	In	Sn	Sb	Hg	Tl	Pb	Bi	GGIMFis T°C
Southalpine																							
Raibl	Median	< BDL	< BDL	7.70	336	< BDL	< BDL	< BDL	< BDL	222	1122	< BDL	< BDL	0.452	1391	< BDL	< BDL	5.07	12.5	179	2860	< BDL	97
S = 25	P75	0.0398	0.630	15.9	1061	0.112	0.600	2.27	0.729	410	2416	6.14	0.518	0.553	2249	0.0326	5.71	27.8	16.5	399	4900	0.0101	
N = 581	P25	< BDL	< BDL	2.55	174	< BDL	< BDL	< BDL	< BDL	91.7	304	< BDL	< BDL	< BDL	782	< BDL	< BDL	0.800	8.50	53.0	1053	< BDL	
	% BDL	88	92	0	0	84	93	72	55	0	0	92	95	13	0	98	53	0	0	0	0	99	
Salafossa	Median	0.610	2.88	61.7	0.0710	< BDL	479	5.43	6.24	12.4	12.4	0.142	7.52	3445	< BDL	< BDL	0.432	*na*	6.07	116	< BDL	56	
S = 1	P75	0.124	0.726	4.88	153	0.102	0.266	898	10.8	9.37	18.9	13.0	0.413	12.8	4140	0.0211	< BDL	0.664		7.47	362	< BDL	
N = 20	P25	< BDL	0.559	0.968	45.4	< BDL	< BDL	117	2.57	5.17	7.40	11.7	< BDL	4.96	2293	< BDL	< BDL	0.307		4.09	45.6	< BDL	
	% BDL	55	10	20	10	25	75	0	0	0	0	0	30	0	0	60	100	0		0	0	95	
Drauzug-Gurktal Nappe System																							
Mezica	Median	< BDL	< BDL	3.28	152	0.0657	< BDL	32.4	4.99	40.7	18.5	16.0	< BDL	1.02	3291	< BDL	< BDL	0.509	7.60	9.01	335	< BDL	66
S = 22	P75	< BDL	< BDL	12.8	1737	0.106	< BDL	270	9.82	347	409	18.4	< BDL	6.49	4331	0.0200	0.464	1.31	9.38	111	1121	< BDL	
N = 191	P25	< BDL	< BDL	0.622	46.3	< BDL	< BDL	11.7	1.89	3.31	3.53	13.2	< BDL	0.22	2243	< BDL	< BDL	0.133	6.07	3.75	110	< BDL	
	% BDL	88	87	24	14	48	82	2	0	1	5	5	82	5	0	70	52	18	0	1	0	82	
Fladung	Median	< BDL	0.627	16.9	5196	0.105	< BDL	92.9	10.3	846	310	11.3	< BDL	0.467	5515	0.0510	< BDL	0.522	*na*	137	594	< BDL	93
S = 13	P75	< BDL	0.903	20.4	8318	0.164	0.500	158	27.8	1127	445	12.3	< BDL	1.58	7323	0.0782	< BDL	2.86		219	770	< BDL	
N = 282	P25	< BDL	0.508	12.7	865	0.0616	< BDL	63.5	3.15	356	86.3	< BDL	< BDL	0.371	4099	0.0331	< BDL	0.172		25.4	396	< BDL	
	% BDL	85	23	0	1	24	72	0	0	0	39	88	0	0	5	90	7			0	0	94	
Bleiberg	Median	< BDL	0.627	14.8	2551	0.0750	< BDL	53.5	1.05	229	172	11.6	< BDL	0.742	1379	< BDL	< BDL	0.229	*na*	51.8	724	< BDL	117
S = 41	P75	< BDL	0.780	28.1	7160	0.192	< BDL	63.8	3.18	530	554	12.6	< BDL	3.52	2538	0.0185	< BDL	0.506		162	1531	< BDL	
N = 795	P25	< BDL	0.539	7.00	643	< BDL	< BDL	48.5	0.328	93.9	34.4	10.7	< BDL	0.317	769	< BDL	< BDL	< BDL		16.8	271	< BDL	
	% BDL	80	17	0	0	37	80	9	4	0	0	12	84	0	0	74	85	26		0	0	98	
Radnig	Median	< BDL	0.54	24.3	4229	0.0820	< BDL	40.6	1.86	325	56.1	< BDL	< BDL	0.438	1383	< BDL	< BDL	0.187	*na*	16.4	243	< BDL	118
S = 17	P75	< BDL	0.660	34.6	7573	0.103	< BDL	50.2	4.98	523	129	10.9	< BDL	0.719	1794	< BDL	< BDL	0.290		38.1	436	< BDL	
N = 318	P25	< BDL	< BDL	7.41	1277	< BDL	< BDL	< BDL	0.798	121	6.15	< BDL	< BDL	0.328	955	< BDL	< BDL	0.118		2.49	56.8	< BDL	
	% BDL	88	44	8	0	35	92	30	0	7	11	53	92	0	0	81	86	14		4	0	88	
Jauken	Median	< BDL	0.630	41.5	4530	0.157	< BDL	546	1.60	404	45.4	< BDL	< BDL	0.363	1212	0.049	0.43	0.141	*na*	24.0	298	0.114	135
S = 5	P75	0.167	0.790	51.5	5680	0.216	< BDL	567	2.92	524	91.9	11	0.072	0.517	1403	0.088	0.61	0.272		42.9	459	0.183	
N = 93	P25	< BDL	0.540	30.1	3520	0.117	< BDL	47.2	0.633	247	25.7	< BDL	< BDL	0.288	870	< BDL	< BDL	< BDL		16.1	168	< BDL	
	% BDL	69	18	0	0	0	90	0	6	0	0	60	72	0	0	43	39	31		0	0	42	
Tirolic-Noric Nappe System																							
Lafatsch	Median	< BDL	0.644	0.777	498	< BDL	< BDL	136	1.22	40.2	264	10.7	< BDL	41.8	1927	0.023	< BDL	0.950	*na*	14.0	323	< BDL	75
S = 18	P75	< BDL	1.32	2.05	911	< BDL	< BDL	721	5.13	71.4	811	11.6	< BDL	107	3421	0.065	1.16	3.30		79.6	1087	0.0162	
N = 430	P25	< BDL	0.53	< BDL	189	< BDL	< BDL	68.8	0.275	24.8	73.5	< BDL	< BDL	17.2	1107	< BDL	< BDL	0.312		2.46	93.2	< BDL	
	% BDL	78	20	39	0	86	95	0	5	0	0	35	93	0	0	41	60	6		0	0	71	
Silberleiten	Median	< BDL	< BDL	2.01	821	< BDL	< BDL	465	1.15	67.8	104	< BDL	< BDL	44.4	2904	< BDL	< BDL	15.3	16.2	2.02	194	< BDL	92
S = 1	P75	< BDL	< BDL	4.47	1322	0.0626	< BDL	666	5.03	132	195	< BDL	< BDL	65.2	3886	0.0347	0.440	25.3	40.4	4.82	413	< BDL	
N = 82	P25	< BDL	< BDL	0.949	538	< BDL	< BDL	339	0.355	40.8	55.7	< BDL	< BDL	21.4	2471	< BDL	< BDL	6.44	9.84	0.851	115	< BDL	
	% BDL	76	90	20	0	73	89	1	2	0	0	99	80	0	0	60	66	0	0	0	0	100	
Scharnitz	Median	< BDL	< BDL	< BDL	582	0.410	< BDL	255	0.443	197	29.1	17.6	< BDL	6.95	2423	< BDL	< BDL	0.248	7.76	0.608	29.9	< BDL	67
S = 1	P75	< BDL	< BDL	1.23	868	0.645	< BDL	313	1.35	260	60.0	19.1	< BDL	14.5	3001	< BDL	0.225	0.673	8.66	0.740	67.0	< BDL	
N = 28	P25	< BDL	< BDL	< BDL	495	0.336	< BDL	122	0.174	83.4	16.8	16.1	< BDL	4.33	1702	< BDL	< BDL	< BDL	6.91	0.440	< BDL	< BDL	
	% BDL	100	89	50	0	0	100	0	7	0	0	4	96	0	0	100	57	25	0	0	29	86	
Rauschberg	Median	< BDL	< BDL	1.97	2267	0.315	< BDL	813	15.2	194	374	16.5	< BDL	14.9	4462	< BDL	< BDL	19.3	13.5	2.41	337	< BDL	65
S = 2	P75	0.0447	< BDL	3.16	3738	0.358	< BDL	1576	47.7	270	873	19.3	< BDL	23.5	5280	< BDL	< BDL	44.8	15.1	5.38	628	0.0120	
N = 52	P25	< BDL	< BDL	1.20	1428	0.258	< BDL	549	3.54	116	171	15.5	< BDL	7.06	3422	< BDL	< BDL	9.60	11.8	1.10	190	< BDL	
	% BDL	69	77	2	0	2	98	0	2	0	0	2	92	0	0	98	98	0	0	0	0	65	
Ötzal-Bundschuh Nappe System																							
Serles	Median	< BDL	< BDL	1102	35300	< BDL	< BDL	63.92	2.44	< BDL	1.98	12.2	0.26	0.329	2055	0.0669	0.355	1.45	*na*	0.783	47	< BDL	387
S = 4	P75	0.209	0.560	1282	37400	< BDL	< BDL	67.95	9.44	< BDL	4.50	13.3	1.08	0.448	2321	0.169	0.791	2.66		1.60	166	< BDL	
N = 59	P25	< BDL	< BDL	420	29920	< BDL	< BDL	61.22	2.26	< BDL	1.06	11.0	< BDL	0.309	1320	0.0419	< BDL	0.849		0.495	20.4	< BDL	
	% BDL	58	64	0	0	90	86	0	0	76	24	5	27	0	0	0	34	3		0	0	80	
Obernberg	Median	< BDL	< BDL	1.86	4993	2.61	< BDL	228	15.0	2.28	0.779	< BDL	< BDL	28.4	2595	< BDL	< BDL	498	3486	0.0204	687	< BDL	137
S = 2	P75	0.36	< BDL	2.97	7448	3.21	< BDL	345	23.9	5.18	1.62	< BDL	< BDL	53.7	3228	0.0505	< BDL	862	5074	0.0363	1506	< BDL	
N = 92	P25	< BDL	< BDL	1.27	3018	1.86	< BDL	123	7.86	1.34	< BDL	< BDL	< BDL	12.4	2112	< BDL	< BDL	275	2017	< BDL	291	< BDL	
	% BDL	57	86	8	0	0	87	0	0	4	48	98	93	0	0	52	83	0	0	49	0	93	

BDL, below detection limit; na, not analyzed

Table 3: *Trace element concentrations in sphalerite from carbonate-hosted Pb-Zn deposits determined by LA-ICP-MS. S, number of samples studied; N = number of analytical spots.*
(GGIMF = Ge – Ga – In – Mn – Fe)

	Raibl (7)	**Mezica (2)**	**Jauken (19)**	**Pirkach (30)**	**Serles (15)**
District	XI	VIII	VIII	VIII	VI
Mn	132 (75-219)	94-156	14 (22-241)	33 (18-115)	33 (8-617)
Cu	bdl (bdl – 1.2)	6.6-12.6	bdl (bdl – 118)	0.3 (bdl – 1500)	2.5 (bdl – 10)
Zn	bdl (bdl – 295)	168-183	bdl (bdl – 10)	18 (1-1000)	236 (2-1190)
Ge	bdl	2.0-3.6	0.05 (bdl – 0.8)	1.4 (bdl – 9.8)	0.05 (bdl – 0.14)
As	9590 (7378-16079)	17-358	403 (106-1003)	75 (3-4510)	1066 (196-7700)
Sb	24 (20-56)	bdl	2.0 (0.8-9.9)	bdl (bdl – 1.5)	0.6 (bdl – 1.8)
Tl	393 (191-1027)	274-515	10 (1.6-56)	421 (10-1134)	18 (bdl – 132)
Pb	10091 (3230-12082)	7121-10258	bdl (bdl – 187)	557 (17-1693)	318 (3-730)

Table 4: *Summary of pyrite/marcasite composition (in ppm) determined by LA-ICP-MS. Median and range (in brackets) of N analyses (in brackets after locality) (bdl – below detection limiut)*

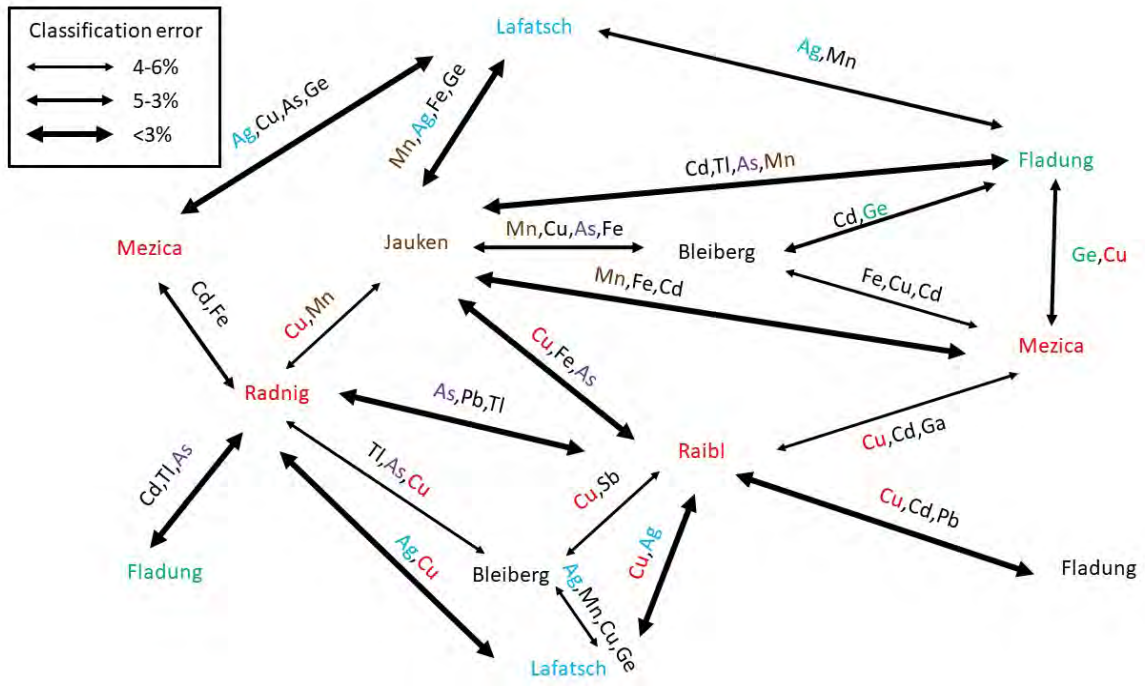

Figure 8: *Trace elements discriminating APT deposits. The graph is a result of a binary Random Forest analysis among the shown deposits and evidence that the labelled elements discriminate the deposits with a confidence of >95%. Low classification errors (bright arrows) indicate strong differences between the trace element composition of the deposits. The colours indicate elements, discriminating characteristically a deposit or a deposit group (same colour).*

fluid inclusion microthermometry (Zeeh et al., 1998). Based on the sedimentary cover, maximum temperatures at the Triassic/Jurassic boundary did not significantly exceed 100°C for the Raibl Group. The east-west trend to higher temperatures estimated by Rantitsch (2001) is mirrored by sphalerite data, with Mežica (<70°C) revealing the lowest and Jauken (135°C) the highest temperatures within the Drau Range-North-Karawanken unit. APT deposits in the Northern Calcareous Alps record 60-100°C, similar to Southalpine deposits. Obernberg (137°C) and Serles (>300°C) have experienced higher metamorphic temperatures.

In APT deposits, galena is commonly poor in trace elements. A detailed LA-ICP-MS study of galena is still missing, and the available data are based on bulk spectroscopic methods. For the Bleiberg deposit, Schroll *et al*. (1994) provided compositional values for 57 galena analyses, yielding median contents of 1.5ppm Ag, 90ppm As, 11ppm Cd, 0.25ppm Cu, 35ppm Sb, 1.7ppm Tl and below 0.5ppm of each Ge, In, Mn, Mo, Sn and V. In other deposits (e.g., in Districts I-IV, VI, XII and XIII), semiquantitative analyses reveal higher Ag and locally considerable As, Sb and Tl (Schroll, 1951, 1953a, 1954, 1955) (Table 2).

In a small number of deposits, Fe sulphides were analysed by LA-ICP-MS: they invariably display an As-Tl-Pb signature (Table 5). Pyrite from the Anisian basal dolomite in the Brenner Mesozoic is poor in trace elements except for As (median 1066 ppm, maximum up to 1%) and in cases Tl (some analyses exceed 100 ppm). The Co/Ni ratio varies around a median of 0.05. Concentrations of Ge, Ga and In are below 1 ppm. The concentrations of Mo reach up to 35 ppm in some analytical spots that are also high in Zn and Pb, thus representing mixed data. The median value of 3 ppm Mo, however, indicates that some Mo is hosted in pyrite.

Pyrite-rich ore collected along a contact of bituminous dolomite with schist and sandstone of the Raibl Group in the Waldloch adit on the north slope of Jauken (Canaval, 1931) is slightly enriched in As, with some Tl present. In a pyrite-rich Zn ore from the adit “Mühlenstollen” at the Pirkner Graben (Pirkach, Fig. 1), pyrite is poor in trace elements except for As, Hg (1-100ppm) and Tl that occasionally reach high levels. Germanium concentrations (maximum 10ppm) are among the highest measured in Fe sulphides.

Pyrite analyses from the Southalpine Raibl deposit reveal high As, Tl and Pb (Table 5). Two analyses of marcasite from the Mežica deposit also reveal high Tl and Pb, but lower As.

Hegemann (1949) and Schroll (1953a) analysed pyrite and marcasite from the Bleiberg and Mežica deposits. Iron sulphides carry 50-100ppm Tl and 10ppm to 1% As. Cobalt (20-100ppm) and Ni (175-300ppm) are only concentrated in pyrite from the Cardita shale (Schroll, 1953a). Concentrations of Mo and V were below the detection limits of 50ppm.

Sulphur and lead isotope data

Sulphur isotope data

Large datasets available for sulphur isotopes in both ore sulphides and associated sulphates have been summarized in ma

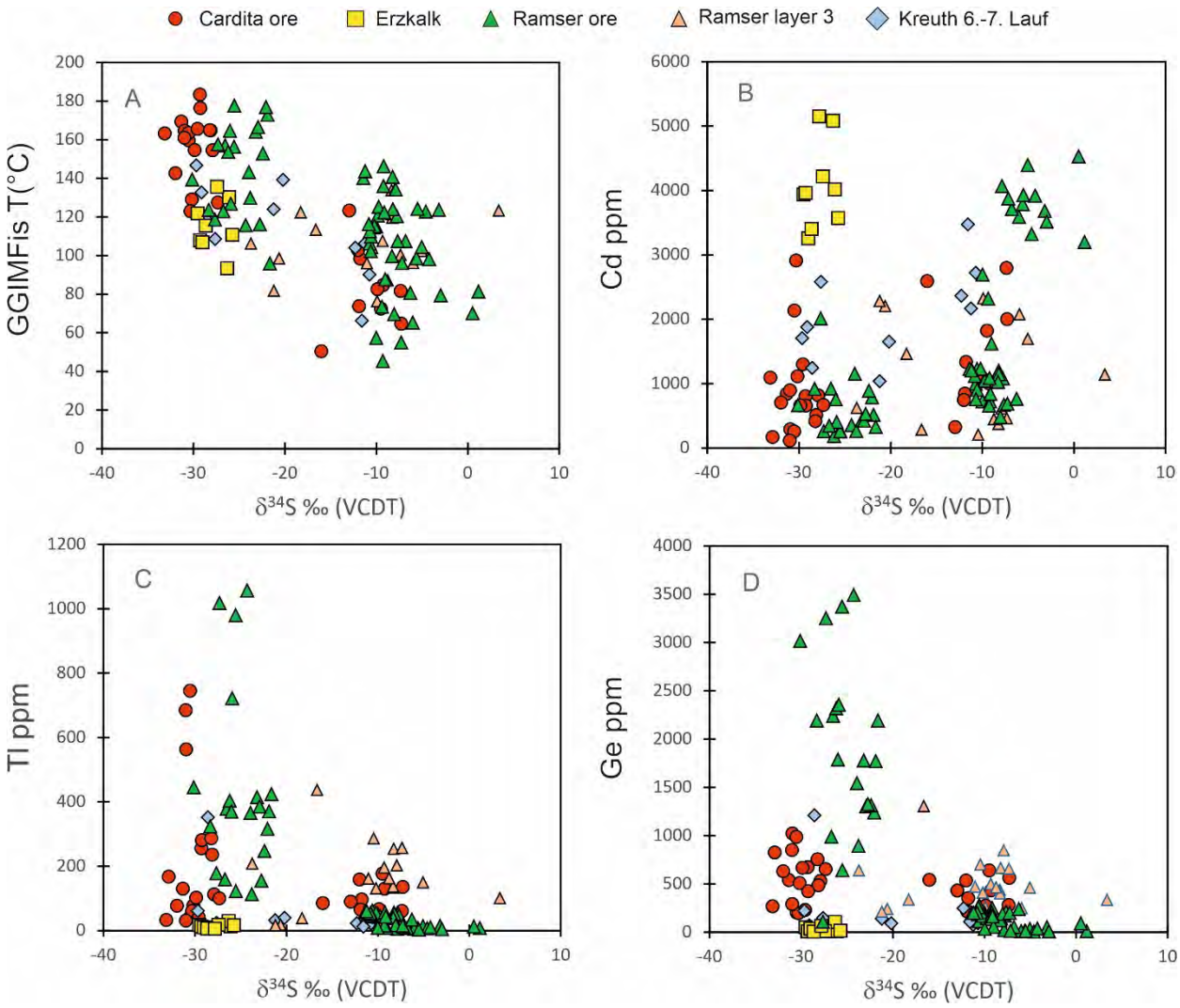

Figure 9: *LA-ICP-MS data of $\delta^{34}S$ (‰, VCDT) versus sphalerite GGIMFis temperature (A), trace elements Cd (B), Tl (C) and Ge (D) for single ablation spots in different ore types from the Bleiberg deposit.*

many publications (e.g., Schroll & Wedepohl, 1972; Schroll *et al.*, 1983; Schroll & Pak, 1983; Schroll, 1996, 1997; Kuhlemann *et al.*, 2001; Schroll & Rantitsch, 2005; Herlec *et al.*, 2010). The most important findings are summarized below.

The sulphur isotope composition of sulphides in APT deposits varies over a wide range and is often bimodally distributed, attaining a maximum at highly negative values ($\delta^{34}S \leq -20‰$) explained by bacteriogenic sulphate reduction, and a second maximum at $\delta^{34}S$ = -10 to 0‰ explained by thermogenic sulphate reduction from a second source (Kuhlemann *et al.*, 2001; Henjes-Kunst *et al.*, 2017). Schroll & Rantitsch (2005), in their compilation of data from the Bleiberg deposit, distinguished three populations, (1) one yielding very light sulphur (-25 to -29‰), (2) one yielding heavier sulphur (-6 to -8‰), and (3) a group in between. No isotopic equilibrium between coexisting pyrite, sphalerite and galena has been reached. Sulphates commonly reflect the composition of contemporaneous seawater, e.g., +22 to +25‰ in Anisian, and +13 to +16‰ in Carnian strata (Schroll, 1996). According to a compilation by Brigo *et al.* (1977), $\delta^{34}S$ values in sulphides in the largest APT deposits hosted by Carnian rocks range from -30.4 to -4.4‰ in Bleiberg, -25.6 to -6.4‰ in Raibl, and -29.0 to -1.4‰ (Herlec *et al.*, 2010) in Mežica.

Sulphur isotope data of pyrite from the Anisian basal dolomite in the Brenner Mesozoic (Serles) reveal a bacteriogenic origin ($\delta^{34}S$ = -29 to -34‰; Schroll, 1997). In contrast, sphalerite from the vein-type Obernberg deposit has $\delta^{34}S$ of -2.4 to -1.3‰ (Schroll, 1997). Data compiled for ores hosted by Anisian rocks in the Northern Calcareous Alps (Districts I and III), the Drau Range-North Karawanken District (District VII) and the Southalpine deposit Auronzo (District XII) show a large variation from -30 to +30‰ (Schroll, 1996; Kuhlemann *et al.*, 2001). The heavier values are found in ores deposited in late-tectonic veinlets, and the most extreme values are interpreted by fluids derived from oil-field brines. In the Topla deposit (District VII), $\delta^{34}S$ ranges from -29.8 to +14.9‰ (Drovenik *et al.*, 1988; Schroll, 1996). An in-situ study of samples from Topla found values ranging from -20.6 to -23.1‰ in one

sample, whereas a second sample yielded values of -9.8 and -12.9‰ (Henjes-Kunst, 2014). Marcasite aggregates range from -23.9 to -16.0‰.

In a study of sphalerite from four ore horizons in the Gorno District (District XIII), Fruth & Maucher (1966) pointed to a local dependence of trace element and sulphur isotope compositions. Samples from the deeper basin have lower Ge/Ga and more negative (lighter) $\delta^{34}S$ values than those from a transition to the lagoon, where shallow-water, quiet sedimentation conditions prevailed and $\delta^{34}S$ values are all positive (average +2.4‰), while Ge/Ga values are higher. However, $\delta^{34}S$ values at Gorno are within a narrower range (-9.8 to +3.8‰) compared to the sulphides from Bleiberg, Mežica, Raibl and Lafatsch, and the influence of bacteriogenic sulphate reduction is likely smaller.

Henjes-Kunst *et al.* (2017) documented a large sulphur isotope variation within single ore samples using in-situ techniques (Fig. 3A, 3B). In a sample from the Erzkalk horizon at Bleiberg, four sphalerite generations revealed a variation from -18.2 to -4.6‰ and galena from -25.1 to -7.7 ‰. In contrast, schalenblende from Erzkalk is light at -22.3 to -22.6‰, similar to pyrite with -21.8‰; barite yielded $\delta^{34}S$ +17‰. In a sample from the Maxer Bänke horizon, $\delta^{34}S$ in schalenblende is more variable, ranging from -16.2 to -26.0‰, overlapping with galena (-20.9 to -24. ‰) and type II and III sphalerite (-13.5 to -21.4‰). Only one analysis yielded a heavier $\delta^{34}S$ value of -1.5‰.

In an in-situ LA-ICP-MS study, Onuk (2018) documented a bimodal distribution both in sphalerite from Bleiberg from the Cardita horizon (n = 26; maxima at -30 and -8‰) as well as the Erzkalk horizon (n=89; maxima at -26 and -8‰). Similar ranges are reported for the Radnig (-28 to -21‰) and the Fladung deposits in the Drau Range (-26 to -10 ‰; Onuk, 2018). The Jauken deposit is an exception, yielding positive $\delta^{34}S$ of +1 to +6 ‰ (Onuk, 2018).

In the Bleiberg deposit, light $\delta^{34}S$ is related to higher Fe, Mn, Ge, As and Tl concentrations (Fig. 9C, 9D), whereas light $\delta^{34}S$ is related to elevated Cd in some Bleiberg sphalerite (Fig. 9B). Consequently, lighter sulphur isotope ratios are associated with compositions that reveal slightly higher GGIMFis temperatures, e.g. 80-180°C for the population at $\delta^{34}S$ = -20 to -35‰, versus 50-150°C for the population at -5 to -15‰ (Fig. 9A).

At Bleiberg the population showing the very light $\delta^{34}S$ values is associated with sphalerite microtextures (globular ZnS, nanospheres, mineralized filaments) indicating direct involvement of microbes in the formation of low-temperature sphalerite (Kucha *et al.*, 2005, 2010) and thus, supporting the importance of BSR for providing the sulphur for ore formation.

APT deposits hosted by Carnian carbonates in the western Northern Calcareous Alps (District II) yield ranges comparable to the Drau Range – Northern-Karawanken Range. In sphalerite from the Lafatsch deposit, $\delta^{34}S$ ranges from -30 to -13.2 ‰ (n = 52; average -18.6 ‰; Schulz, 1981; Schroll, 1997). In-situ LA-ICP-MS measurements of sphalerite reveal a similar range from -35 to -10‰ with a median at -21‰ (Onuk, 2018). For sphalerite from Silberleiten, a $\delta^{34}S$ value of -14.8 ‰ was previously reported (Schroll, 1997)

Zeeh *et al.* (1998) and Kuhlemann *et al.* (2001) provided evidence for a trend of $\delta^{34}S$ to lighter values with decreasing age, i.e., sphalerite that precipitated in a first ore phase together with CSD (clear saddle dolomite) is less negative than sphalerite of the second ore phase co-existing with blocky calcite or cloudy saddle dolomite. Paragenetically later, botryoidal sphalerite carries higher trace element contents (Fe, Ge, As, Tl) at lower $\delta^{34}S$ than earlier, granular sphalerite.

Kuhlemann *et al.* (2001) furthermore proposed an evolution towards heavier $\delta^{34}S$ with time together with a major TSR reservoir. At Mežica, Herlec et al. (2010) observed increasing $\delta^{34}S$ from earlier to late-stage sphalerite, and a decrease from more stratiform to discordant orebodies. However, Schroll & Rantitsch (2005) and Herlec *et al.* (2010) argue against a major TSR derived sulphur reservoir due to the predominance of very negative $\delta^{34}S$ in sulphides from most of the APT deposits.

Lead isotope data

The origin of Pb in Austroalpine APT Pb-Zn deposits was repeatedly discussed in the past (Köppel, 1983, 1997; Köppel & Schroll, 1978, 1985, 1988; Schroll *et al.*, 2006; Henjes-Kunst, 2014). A compilation of Pb isotope data for galena and sphalerite from various deposits within Ladinian and Carnian strata of the Austroalpine units (Köppel & Schroll, 1985; Köppel, 1997) supplemented by new Pb isotope data for deposits in the Drau Range (Henjes-Kunst, 2014) indicates very homogeneous common lead values on the scale of individual deposits (e.g., Bleiberg) but a scatter in the Pb isotopic signature on the regional scale (e.g., Drau Range, Northern Calcareous Alps) (Fig. 10A, 10B).

The Pb isotopic systematics of the Bleiberg District has been investigated in detail. Comparative studies on mineralized and unmineralized host rock samples and on selected Triassic and older sedimentary and crystalline rocks (Köppel & Schroll, 1985, 1988; Schroll *et al.*, 2006) reveal the following findings:

1) Selected mineralized whole-rock samples of the Bleiberg District yield a Pb-Pb isochron model age of 180 ± 48 Ma. The isochron passes through the Pb data points of ore (Schroll *et al.*, 2006).

2) The common lead isotopic signature of unmineralized Wetterstein limestone differs from that of Bleiberg ore (galena, sphalerite) and mineralized whole-rock samples by less radiogenic $^{207}Pb/^{204}Pb$ and $^{208}Pb/^{204}Pb$ values (Fig. 10A, 10B).

3) The lead isotopic signature of unmineralized host rocks is also identified in mineralized samples. Leaching experiments reveal an isotopic signature for barite similar to unmineralized Wetterstein limestone while galena overgrowth on barite is enriched in ^{207}Pb and ^{208}Pb.

4) According to the growth model for crustal lead of Stacey & Kramers (1975), the Bleiberg ore lead has a Late Paleozoic model age. However, the ^{207}Pb and ^{208}Pb enriched lead compositions of the Bleiberg ore require higher μ (e.g., $^{238}U/^{204}Pb$) and k (e.g., $^{232}Th/^{238}U$) values compared to the respective model parameters of Stacey & Kramers (1975) (Fig. 10 A, 10B).

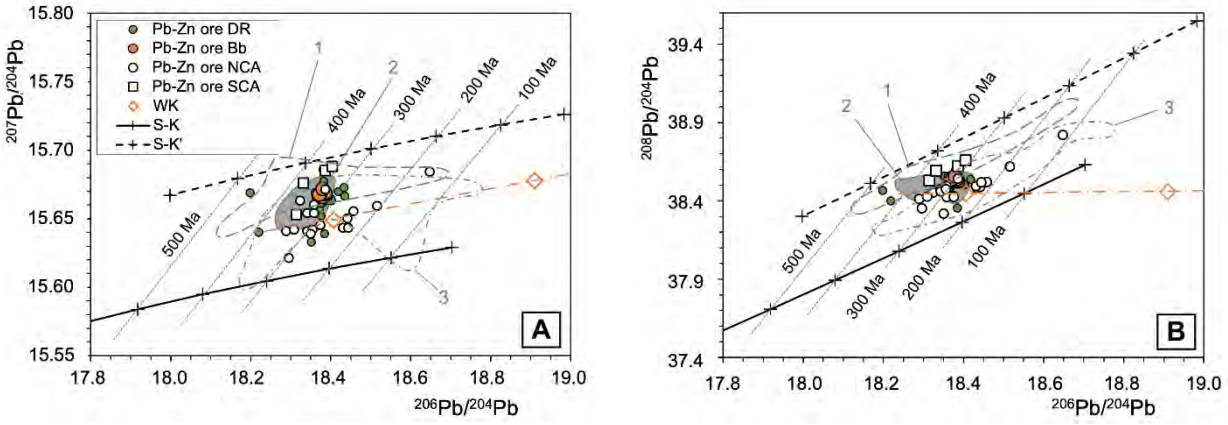

Figure 10: *Pb-Pb isotope diagrams for Pb-Zn ores of APT deposits in the Eastern and Southern Alps and of selected unmineralized Wetterstein limestone samples from the Drau Range.* ***(A)*** *$^{206}Pb/^{204}Pb$ – $^{207}Pb/^{204}Pb$ diagram,* ***(B)*** *$^{208}Pb/^{204}Pb$ – $^{206}Pb/^{204}Pb$ diagram. The solid line (labelled S-K) represents the Pb isotopic growth curve according to the original model parameters by Stacey & Kramers (1975) (e.g., μ = 9.74 and κ = 3.78) while the dashed line (S-K') shows the Pb evolution curve based on model parameters (e.g., μ = 10.1 and κ = 4.1). Ticks along the growth curves mark Pb model ages of 0 – 500 Ma, tie lines between ticks of identical ages on the two curves represent Pb-Pb isochrons of corresponding model ages. The fields labelled "1" (vein-type mineralization; enclosed by grey dashed line) and "2" (galena of Gröden Sandstone; grey field) indicate that the Pb isotope compositions of galena in the Southern Alps is not related to the APT deposits while "3" (enclosed by dashed-dotted line) denotes the common Pb isotopic composition of feldspar of late Palaeozoic to early Mesozoic igneous and sedimentary rocks of the southeastern Alps. The dashed-dotted line (in brown) is the best-fit line for data points for unmineralized Wetterstein limestone samples (only two data points are depicted). Note that Pb isotope data for feldspar are not age corrected. DR: Drau Range; Bb: Bleiberg; NCA: Northern Calcareous Alps; SCA: Southern Calcareous Alps; WK: Wetterstein limestone. See text for details and references.*

APT ores of the Eastern Alps in general show lead isotopic compositions plotting above the crustal lead growth curves of Stacey & Kramers (1975) (Fig. 10 A, 10B). The enrichment in ^{207}Pb and ^{208}Pb distinguishes APT ore from Pb deposits in the Penninic realm (Western Alps) or Pb-Zn sedimentary deposits of the Iberian Peninsula. The latter are characterized by less radiogenic common lead compositions compatible with the Stacey & Kramers (1975) model lead growth curve (Köppel, 1997; Milot et al., 2021). The variable enrichment in ^{207}Pb and ^{208}Pb of APT ore samples has been explained by an origin of lead from an isotopically enriched continental source (Köppel, 1997). Early Palaeozoic metasedimentary rocks in the southeastern Alps fulfill this requirement as they are characterized by a relatively high amount of Proterozoic and older detrital materials high in U and Th (e.g., zircon, monazite) (Köppel, 1997). Overlapping common lead values for APT ore on the one hand and for feldspar and galena of Late Paleozoic to Mesozoic igneous and sedimentary rocks of the Eastern and Southern Alps on the other hand are compatible with a model that the APT ore lead is largely sourced from older rocks of the southeastern Alpine realm (Fig. 10 A, 10B). Especially, galena from the Permian Gröden Sandstone (Köppel & Schroll, 1985) shows a Pb isotopic match with the majority of the APT data points. The relatively large scatter in the lead model ages (ca. 450 Ma to <200 Ma) of APT deposits indicates that the ore-forming fluids were not well mixed on a regional scale. It can thus be assumed that local differences in the bedrock geology and/or its variable common Pb composition (*c.f.* fields labelled 1 and 3 in Fig. 10A, 10B) are responsible for the variability in the Pb isotopic compositions of the individual APT deposits.

Ore mineral geochemistry in APT Districts

District I: Pb-Zn (fahlore) District in Anisian rocks of the Tirolic-Noric Nappe System of the Northern Calcareous Alps (type locality: Sankt Veit-Tarrenton)

Sulphide mineralogy and compositions are variable and heterogeneous, with some Ag and Cu present in fahlore. While Ge and Tl in sphalerite are lower than in Carnian-hosted APT, As and Ga appear to be elevated (Table 2). However, no in-situ investigations of trace elements have been carried out to date. A sphalerite concentrate from the Sankt Veit deposit revealed 135ppm Ge, 59ppm Ga, 301ppm As, 13ppm Tl and 48ppm Ag (Table 2; Cerny & Schroll, 1995). Sulphur isotopic compositions are more typical of TSR (-6.8 to +4.2; Schroll, 1997), with the exception of the type locality at Sankt Veit (-12.5 to -3.2‰).

District II: Pb-Zn ore District in Carnian rocks of the Tirolic-Noric and Bajuvaric Nappe System of the North Tirolian Calcareous Alps (type locality: Lafatsch)

Cerny & Schroll (1995) reported 150ppm Ge, 15ppm Ga, 2300ppm Cd, 45ppm Tl and 120ppm Ag in a sphalerite concentrate from the type locality Lafatsch, similar to the dataset published by Schroll (1996; Table 2). Recent LA-ICP-MS work revealed median values of 40ppm Ge, 1.2ppm Ga, 1927ppm Cd, 14ppm Tl and 42ppm Ag hosted in sphalerite (Table 4; Onuk, 2018). LA-ICP-MS measurements of sphalerite from the Nassereith/Silberleiten deposit show an overall similar composition compared to Lafatsch, especially concerning the median Ag content of >40ppm (Table 4, Fig. 6, Fig. 7).

Copper, Cd and Sb are higher at Silberleiten, whereas Lafatsch has higher Tl, As and Se. Maximum concentrations are 713ppm Ge, 54ppm Ga, 0.5ppm In and 1038ppm Ag. Silver, As and Sb in galena vary over a wide range, with highest concentrations reported for Dirstentritt and Lafatsch, and low values for ores in Bavaria, e.g., Höllental, Mittenwald and Kienberg-Rauschberg (Schroll, 1954).

LA-ICP-MS data from the Kienberg-Rauschberg deposit reveal a highly variable trace element composition in sphalerite, with elevated Ge, As, Cu, Sb, Ga, Ag and Cd. Compared to Bleiberg, sphalerite is higher in Cu, Ga, Sb, Ag, but lower in Tl; Ge and Fe concentrations are at about the same levels (Table 4, Fig. 6, Fig. 7). A sample from the Franz-Adolf mine (Scharnitz/Mittenwald; Fig. 1) revealed low Fe, Mn, Ga, In, Sn, Sb, Pb and Tl concentrations in sphalerite, but elevated Ge (median 197ppm), Cu (255ppm) and Ag (7ppm) (Table 4, Fig. 6, Fig. 7). Sulphur isotope compositions (-30 to -2.2‰) indicate a major bacteriogenic sulphur source in most of the District II deposits, as summarized by Schroll (1997), similar to deposits in Carnian rocks of the Drau Range – North Karawanken Range (District VIII).

District III: Pb-Zn (fahlore) District in Anisian rocks of the Tirolic-Noric Nappe System of the Northern Calcareous Alps (type locality: Annaberg)

Trace element information for sulphides in this District is scant. The data available (Schroll, 1954) point to low trace element concentrations in sphalerite except for Mn (500-1000 ppm; Table 2). Galena from Annaberg yields 100 ppm Ag and some As and Sb. Sulphur isotopes are extremely variable, including rare light sulphur values in galena (-17.7‰, Schroll, 1997). However, most values range from 0 to 13‰, e.g. in sphalerite from Annaberg with +10.7‰. Isotopically extremely heavy sulphur from the Arzriedel deposit (Fig. 1A; +27.7 to +30.5‰) is interpreted as related to oil-field brines (Götzinger & Pak, 1983; Schroll, 1996).

District IV: Pb-Zn ore District in Carnian rocks of the Tirolic-Noric and Bajuvaric Nappe System of the eastern Northern Calcareous Alps (type locality: Weyer)

The small database indicates low trace element concentrations in sphalerite, and 1-300ppm Ag, 300ppm As and 10-50ppm Sb in galena (Table 2; Schroll, 1954). Sulphur isotope ratios of galena and sphalerite from three occurrences range from -20.8 to -13.8‰ (Schroll & Pak, 1983). Isotopically light sulphur in galena (-20.7‰) from a vein mineralization hosted by Wetterstein limestone in the Schwarzenberg/Türnitz deposit (Fig. 1A) most likely formed from mobilizing sulphur from adjacent Anisian stratiform ores (-12.4‰, Götzinger & Pak, 1983).

District V: Pb-Zn ore District in Triassic rocks of the Bundschuh Nappe – Stangalm Mesozoic (type locality: Erlacher Bock)

In stratiform dolomite-hosted Pb-Zn mineralization, sphalerite is Fe-rich (4-6%), whereas Zn-F-(Pb-Cu) vein mineralization in grey dolomite of Anisian to Carnian age carries low-Fe sphalerite (<0.1% Fe; Götzinger & Leute, 1998). This corresponds to electron probe microanalyses carried out on sphalerite occurring as a minor component at Zunderwand (Fig. 1), which proved to be low in trace elements, i.e. 0.03-0.3% Fe, maximum 0.01% Cd and no Ge, Cu, Pb detectable by microprobe (Table 3; Henjes-Kunst, 2014). The Fe-rich sphalerite in the stratiform ore corresponds to pyrite-sphalerite-galena ores at the base of the Brenner Mesozoic. Trace elements in galena in one sample yielded 50ppm Ag, 30ppm As and 50ppm Tl, along with some Sn (Table 2; Schroll, 1954). One sulphur isotope ratio determination of sphalerite from Erlacher Bock shows a hydrothermal value (-1.4‰); barite from these deposits yields +18.2 to +22.7‰ (Schroll, 1997).

District VI: Pb-Zn ore District in Triassic rocks of the Ötztal-Bundschuh-Nappe System – Stubai-Brenner Mesozoic (type locality: Griesbach, Serles)

Sphalerite in stratiform ore within the Anisian basal dolomite (Serles, Fig. 1) is significantly enriched in Fe (3-5%) and Mn (>1000ppm) compared to all other APT deposits, but generally low in those trace elements typical for APT-type deposits (e.g. Ge, As, Tl; Fig. 6, Fig. 7); very light sulphur isotopic compositions of ore samples indicate the involvement of bacteriogenic processes.

Sphalerite in the Hauptdolomit-hosted Obernberg deposit is much lower in Fe (0.5%), but significantly higher in Cu, Ga, Ge, Ag, Sb and Hg (Fig. 6, Fig. 7), and has $\delta^{34}S$ slightly lower than 0‰, pointing to hydrothermal fluids. In the samples studied, this sphalerite is intergrown with abundant barite and fluorite, and has inclusions of bournonite, boulangerite, galena and pyrite, with valentinite occurring as frequent oxidation phase in cracks; this points to a pure epithermal genesis postdating the Alpine orogeny in this area.

District VII: Pb-Zn ore District in Anisian rocks of the Drauzug-Gurktal Nappe System – Drau Range Mesozoic (type locality: Kellerberg)

Analytical data for Pb-Zn ores hosted by Anisian carbonates in the Drau Range are only found in Schroll (1954) and Cerny & Schroll (1995). A Zn sulphide concentrate from the ancient mining operation at Kolm/Dellach (Fig. 1A) revealed low trace element contents, with 14ppm Ge, 4.5ppm Ga, 908ppm Cd, 0.4% Fe, 79ppm Mn and low Tl, As, Ag and In. However, 88ppm Sb has been measured in this concentrate. The semi-quantitative data of Schroll (1954) reveal up to 50ppm Ge and several locations in the northern Drau Range. Galena is high in Mn (up to 5000ppm), low in Fe and Ag; sphalerite compositions are more variable, ranging from 1-300ppm Ag and 100-10000ppm As. Sulphur isotope compositions range from -10.3 to +5.8‰ (Schroll, 1997).

For the Topla deposit in Slovenia, an EMPA study of two sphalerite samples revealed low Fe (median 0.07 and 0.05%), Cd (0.10 and 0.19%), As (0.02%) and Pb (0.11 and 0.14%), and no detectable Ge (Table 3; Henjes-Kunst, 2014). An average of 3 analyses published by Schroll (1996) yielded 0.3ppm Ge, 3ppm Tl, 10ppm Sb, 3ppm Ag, 20ppm Mn and 0.1% Fe. Sulphur isotope ratios cover a wide range from -29.8 to +14.9‰ (Drovenik *et al.,* 1988; Schroll, 1996).

District VIII: Pb-Zn ore District in Carnian rocks of the Drauzug-Gurktal Nappe System – Drau Range Mesozoic (type locality: Bleiberg)

	Cerny & Schroll, 1995	Schroll (1997)	Onuk, 2018 (this work)	Henjes-Kunst, 2014
Method	Zn concentrates, bulk analysis	Hand specimen, bulk analysis	In-situ LA-ICP-MS	In-situ EPMA
N	62	146	795	1805
Mn	24	24	15	
Fe	5000	4240	2551	1800
Ga	16.5	11	1.0	
Ge	174	200	229	380
As	161	174	172	470
Ag	8	10	0.74	
Cd	1745	1860	1379	1900
In	0.1	0.1	0.01	
Tl	74	59	52	
Pb	1885		724	1700

Table 6: *Median trace element concentrations in ppm in sphalerite from Bleiberg according to different studies and methods; N = number of analyses*

Drau Range

The vast trace element dataset available for the Bleiberg deposit facilitates geochemical discrimination between different ore types and horizons (Cerny & Schroll, 1995; Schroll, 1950, 1951, 1953a,b, 1954, 1996, 1997, 2008; Schroll *et al*., 1994). EPMA also revealed differences between different regions in ores of the Crest facies and the large breccia bodies in the western part of the deposit (Henjes-Kunst, 2010, 2014). LA-ICP-MS analyses of almost 800 sphalerite grains from different areas of the Bleiberg deposit provide detailed characterisation of trace element patterns (Onuk, 2018) (Table 4, Fig. 6, Fig. 7). The data reveal higher concentrations of Ge, Tl, As, Fe and Mn in stratiform ores of the Cardita orebody (Raibl Group), but also in breccia and discordant ores of the "special facies", especially for the "Riedhartscholle". The "Maxer Bänke" mineralization, which comprises the stratigraphically lowest ore horizon at Bleiberg, has on average the highest contents of Ge (550ppm) and Tl, but the lowest Cd (1450ppm; Schroll, 1996). In addition, stratiform ores in the Erzkalk may also contain high concentrations of Ge (e.g., 900-1200ppm at "Germaniumgugel": Cerny & Schroll, 1995). Due to the variations between ore types and stratigraphic position, calculation of a robust median concentration is problematic. However, the values calculated for a large number of Zn concentrates collected from accessible orebodies, and of singe grain analyses provided by Cerny & Schroll (1995) and Schroll (1996) are not in conflict with the new in-situ data for most race elements (Table 6). The bulk analytical data obviously are too high for Fe, Ag and Ga compared to in-situ data. This is explained by fine intergrowth with Fe sulphides for Fe, and analytical problems for Ga and Ag.

Sphalerite from the former Pb-Zn mine Töplitsch northeast of Bleiberg (Fig. 1) carries low trace elements, e.g., Fe <0.09%, Cd <0.08%, Pb, with no Ge detectable (Table 3). The medium-size Radnig deposit west of Bleiberg (Fig. 1) is characterized by intermediate Ge and As, but low Cd and Tl concentrations. Values of 320ppm Ge, 35ppm Ga, 8ppm Tl, 47ppm As, 11ppm Ag and 1634ppm Cd were reported from a Zn sulphide concentrate (Cerny & Schroll, 1995). Electron microprobe analyses of sphalerite from Radnig by Henjes-Kunst (2014) gave median contents of 420ppm Ge, 1200ppm Cd, 0.2% Fe, 100ppm As and 0.059% Pb (Table 3). LA-ICP-MS analysis yields higher Fe, Mn and Ge (325ppm) than at Bleiberg, but lower Cd, As, Tl and Pb (Table 4, Fig. 6, Fig. 7). $\delta^{34}S$ values range from -26.9 to -21.8‰ (Schroll, 1997).

The Pb-Zn deposit Jauken in the western part of the Drau Range (Fig. 1) is known for extreme Ge concentrations in sphalerite. A Zn sulphide concentrate yielded 1500ppm Ge, 36ppm Ga, 70ppm Tl, 20ppm As, 1318ppm Cd, 0.4% Fe and 30ppm Mn (Cerny & Schroll, 1995). The EPMA study of Henjes-Kunst (2014) confirmed these data with high Ge (median 1400ppm), but low Cd (630ppm) (Table 3). The LA-ICP-MS study of sphalerite from the dumps on the southern slope of Jauken revealed on average 0.5 wt% Fe, elevated Cu and Ge (median 404ppm), some As and Tl, and low Ag (Table 4, Fig. 6, Fig. 7). Sulphur isotope compositions are unusual for APT deposits, ranging from -4.0 to +2.4‰ in Pb-Zn sulphides from the Wetterstein limestone mineralization, with one value of -24.1‰ for galena from mineralization in the Raibl Group (Schroll & Pak, 1983; Schroll, 1997). The in-situ LA-ICP-MS study of sphalerite yielded $\delta^{34}S$ values of +1 to +6 ‰ (Onuk, 2018).

North-Karawanken Range

LA-ICP-MS analysis of sphalerite from Hochobir/Fladung (Fig. 1) yields high Fe, Ge, As, Cd and Tl; the median Ge concentration of 846ppm is the highest measured in an APT deposit in this study. Sphalerite from Hochobir is also slightly enriched in Ga than other APT-type ores (median 10ppm vs 1-5ppm) (Table 4, Fig. 6, Fig. 7). A Zn sulphide concentrate from Hochobir reported by Cerny & Schroll (1995) yielded 900ppm

Ge, 66ppm Ga, 190ppm Tl, 89ppm As and 3828ppm Cd, low Fe (0.3%) and Mn (24ppm). $\delta^{34}S$ ranges from -21.0 to -7.7‰ (Schroll, 1997). EPMA of sphalerite from Windisch-Bleiberg (Fig. 1) in the western part of the North-Karawanken Range revealed lower median Cd (850ppm) and Ge concentrations (230ppm), but also a high Ge maximum of 890ppm (Table 3). Galena in both the Hochobir and Windisch-Bleiberg areas is very low in trace elements except for As (Schroll, 1954).

Several studies of sphalerite compositions from the Mežica deposit (Fig. 1) reach quite different conclusions, with significant deviations especially in the concentrations of Ge, Ga and Tl. In three sphalerite concentrate samples from the Graben Revier, Fe ranges from 0.01 to 1%, Cd 1311-3482ppm, Ge 76-1100ppm, Ga 30-78ppm, and Ag 1.6-14ppm; As (17-800ppm), Tl (4-208ppm) and Pb (0.05-0.38%) vary over a wide range (Cerny & Schroll, 1995). An average of 44 sphalerite analyses carried out by Strucl (1974, 1984) returned 190ppm Ge, 15ppm Ga, 3300ppm Cd and 660ppm As. An electron microprobe study revealed an average of 290ppm Ge, 3500ppm Cd, 0.018% Fe, 870ppm Cu, 580ppm As and 0.14% Pb (Henjes-Kunst, 2014; Table 3). A detailed LA-ICP-MS study of 21 samples yielded the following median values (and interquartile deviations, in ppm): Mn 2 (0.4-11); Fe 136 (40-1555); Ga 4 (1-10); Ge 37 (5-293); As 9 (2-406); Ag 1 (0.3-5); Cd 3028 (2139-4363); Hg 9 (7-12); Tl 7 (3-102); Pb 227 (75-968) (Potočnik Krajnc, 2021). Compared to Bleiberg, Mežica sphalerites are, on average, lower in Fe, Mn, Cu, Ge, As, Tl and Pb, but higher in Ga, Ag, Cd and Sb (Table 4, Fig. 6, Fig. 7). Among the six textural sphalerite types distinguished by Potočnik Krajnc (2021), dark brown colloform sphalerites show the highest concentrations of Ge, As and Tl, whereas brown sphalerites are more Fe-rich. The highest trace element values were determined in brown polycrystalline sphalerite (type 5a) with on average 1333ppm Fe, 441ppm Ge, 3125ppm As and 513ppm Tl, thus matching similar sphalerite types found in Raibl.

On a regional scale, sphalerite compositions within the Drau Range and Karawanken deposits show trends in trace element and sulphur isotope chemistry: as sulphur isotope ratios increase from Mežica towards the west from highly negative values to values around 0‰, Mn, Fe, Cu, Ge and Sn in sphalerite also increase from east to west (Fig. 7; Schroll, 1979, 1983; Schroll *et al.*, 1994).

District IX: Polymetallic ore District in Triassic rocks of the Seengebirge Nappe (type locality: Rosegg)

According to limited data available, mineralization in District IX is structure-controlled within the "Alpine Muschelkalk" (i.e., Anisian), with fahlore and galena as major minerals. Accessory sphalerite carries Fe and Mn concentrations higher than typical APT type sphalerite and low Ge and Tl, especially when compared to Bleiberg (District VIII) which is located only 5 km to the NW. Galena from the deposit Rudnik has very low Ag concentrations, but occurrences further to the east carry elevated Ag (1000 pm) and As, Sb, Tl and Sn (Schroll, 1954). Two sulphur isotope analyses of Zn-Pb ore reveal $\delta^{34}S$ of -7.2 and -6.8‰ (Schroll, 1997). Barite from a vein mineralization gave $\delta^{34}S$ = +26.2‰, pointing to the influence of Triassic formation water.

District X: Pb-Zn-ore District in Triassic rocks of the Silvretta-Seckau Nappe System – Engadine Dolomites (type locality: S-charl)

Production data published at (https://map.geores-sourcen.ethz.ch, access March 1, 2023) show that from 1824 to 1828, 7930 tonnes ore were produced from the deposits in the Engadine Dolomites around the village of S-charl, recovering 91tonnes Pb and 199kg Ag, corresponding to 1.1% Pb and 25ppm Ag. Galena carries 0.1-0.2% Ag, and sphalerite 0.2-0.3% Cd. Small deposits hosted by Mesozoic carbonates of the Silvretta-Seckau Nappe System further to the west at Arosa, Davos and Sertig carry galena with low Ag contents (0.02%).

District XI: Pb-Zn-ore District in Carnian rocks of the Southalpine (type locality: Cave del Predil/Raibl)

Compositions of Pb-Zn ores from the Raibl deposit have been investigated by numerous authors. Brigo & Cerrato (1994) published data from 111 ore samples from all accessible parts of the mine. The following median (minimum and maximum) contents were reported: Zn 34% (5-56%); Pb 5.9% (0.1-47%); Fe 1.0% (0.06-29%); Cd 815ppm (50-4367ppm); Ge 677ppm (56-2912ppm); Ga 26ppm (12-249ppm); Tl 333ppm (31-2895ppm); Sb 20ppm (1-757ppm); As 634ppm (64-3505ppm). These data are not easily comparable to in-situ data, such as the EPMA dataset of Henjes-Kunst (2014; Table 3) and the LA-ICP-MS studies of Onuk (2018) and Gartner (2023; Table 4, Fig. 6, Fig. 7). In these latter datasets, sphalerite from Raibl proves to be highly variable in composition, but generally low in Fe and Cd, and high in As, Tl and Pb. The median Ge and Ga contents of the LA-ICP-MS study are 222ppm and 0.14ppm, respectively, much lower than the values reported by Brigo & Cerrato (1994). Schroll (1996) reports 500ppm Ge, 10ppm Ga, 360ppm Tl and 1200ppm As as an average of 27 analyses (Table 2). The few galena datasets available show low Ag (<5ppm), but high As and Sb (Schroll, 1954). Sulphur isotope ratios of Raibl ores range from -25.6 to -6.4‰ (Brigo et al., 1977), very similar to those at Bleiberg and Mežica. Stalactitic schalenblende and galena from Raibl yield extremely light sulphur (-31‰; Schroll, 1996).

District XII: Pb-Zn-ore District in Triassic rocks of the Southalpine (type localities: Salafossa and Auronzo)

According to Cerny (1989), ores in the Dolomites are free of Ag, Cu and Sb. Nevertheless, average trace element data published by Schroll (1996) indicate that sphalerite hosted by Anisian rocks at Auronzo has lower Fe, Mn, Ge and Tl, but higher Ag, Cd, As and Ga compared to the Salafossa deposit hosted by rocks of Carnian age (Table 2). A small dataset of LA-ICP-MS data indicates low concentrations of Fe, Ge, As, Tl and Pb, but elevated Cu, Ga, Cd and Ag at Salafossa (Onuk, 2018; Table 4). Single sphalerite crystals from a number of small deposits in the Anisian carbonates range from 0.1-0.5% Fe, 5-1000ppm Mn, 5-300ppm Ge, and 3-30ppm As. Galena shows elevated Ag (100-500ppm), As and Sb (500-3000ppm each) and low Tl and Sn (Schroll, 1954). Sulphur isotope data have only been published for Auronzo, ranging from -18 to -12‰ (Schroll, 1996). Pb isotope data of mineralization in the

Auronzo area are largely similar to stratiform Zn-Pb-Ba-F mineralization in Devonian host rocks of the Carnic Alps (Brigo *et al.*, 1988).

District XIII: Pb-Zn-F-ore District in Carnian rocks of the Southalpine (type locality: Gorno)

Trace element concentrations in sphalerite reported by Schroll (1996; Table 2) are in line with previous spectrochemical analyses of Fruth & Maucher (1966): the median of 10 averages of a total of 105 samples representing four distinct ore horizons is 3200ppm Fe, 110ppm Mn, 30ppm Ag, 1450ppm Cd, 210ppm Ga (average of all data: 230ppm), 85ppm Ge (average 130ppm), 310ppm Sb and 60ppm Hg. Maximum contents reported are 370ppm Ge and 800ppm Ga. According to a semi-quantitative analysis published by Schroll (1954), galena is rich in Ag (500ppm) and Sb (500ppm). Although trace element compositions of sphalerite are similar overall to those from other Southalpine and Austroalpine deposits hosted by Carnian carbonates, high Ag and Sb contents in galena, high Ga, Sb and Ag and low Tl in sphalerite along with the presence of Ag sulphosalts and intermediate sulphur isotope compositions (-9.8 to +3.8‰) indicate different conditions of ore formation. According to Mondillo *et al.* (2020), ore formation took place at 100-150°C in a deep burial setting post-dating the growth of Fe-Mn-bearing saddle dolomite, and during Mesozoic extension. In contrast, Giorno *et al.* (2022) propose a Carnian age of mineralization based on calcite dating.

Rb-Sr isotopic dating

Timing of ore formation in carbonate-hosted deposits generally is a contentious issue, and APT is no exception. Textural and sedimentological evidence of an early, probably syngenetic ore formation (e.g. Schulz, 1985, 2006) has been questioned by many, postulating epigenetic Late Triassic, Jurassic or post-Jurassic timing (Zeeh & Bechstädt, 1994; Kuhlemann, 1995; Kuhlemann & Zeeh, 1995; Leach *et al.*, 2003; Muchez *et al.*, 2005). Arguments available until about 2005 have been summarized by Schroll (2008). Geochronological data from ore and associated gangue minerals were first made available by Schroll *et al.* (2006). Rb-Sr isotope analyses of mineralized whole rock samples of the Crest facies in the Bleiberg deposit resulted in an errorchron model age of 210 ± 30Ma. A 180 ± 40Ma errorchron age was calculated from Pb isotopes of galena. These ages are not precise enough to decide in favour of MVT vs. SedEx-type models discussed for Bleiberg but led Schroll *et al*. (2006) to exclude ore formation during the deep burial. Maximum burial of the Carnian Wetterstein Formation to *ca.* 3km was not before the Late Cretaceous-Palaeogene (Rantitsch, 2001).

Since about 1990, Rb-Sr isotopic analysis of sphalerite has been shown to be a feasible method for successful dating of carbonate-hosted deposits. The results of the Rb-Sr sphalerite dating approach have decisively advanced the genetic understanding of this type of mineralisation (Nakai *et al.*, 1990, 1993; Brannon *et al.*, 1992; Christensen *et al.*, 1995a, 1995b, 1996; Schneider *et al.*, 1999, 2007a,b; Oberthür *et al*., 2009; Ostendorf et al., 2015, 2017, 2019; Wang *et al.*, 2023). Melcher *et al.* (2010a,b) and Henjes-Kunst (2010, 2014) reported the following findings of Rb-Sr isotopic analysis of sphalerite and associated gangue minerals from the Bleiberg deposit:

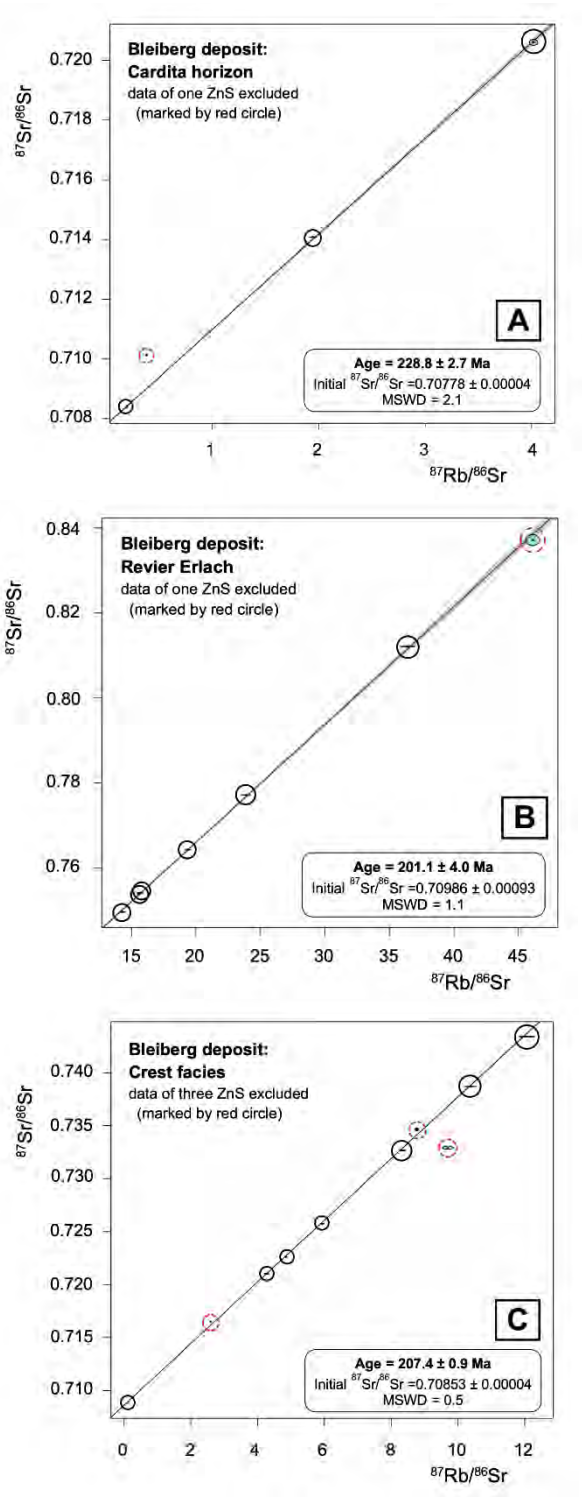

Figure 11: *Rb-Sr isochron diagrams for sphalerite of three structurally different ore Districts of the Bleiberg APT deposits: (A) Cardita horizon, (B) Erlach Revier, (C) Crest facies. Note that the Cardita isochron includes one pyrite data point. Data points marked by a solid black circle are considered for isochron model calculation whereas data points marked by dashed red circle are not considered. Data-point ellipses indicate 2σ errors of the respective isotopic ratios. See text for further details.*

(1) An Rb-Sr 3-point isochron on sphalerite and pyrite from the Cardita horizon yielded a model age of 225.2 ± 2. Ma with an initial Sr isotopic ratio of 0.70778 (MSWD = 2.1)

(2) Rb-Sr isotope data of 17 sphalerite separates of samples from various locations within the Crest facies and from the Erlach Revier define an errorchron (201.3 ± 3.9Ma; initial $^{87}Sr/^{86}Sr = 0.70909 \pm 0.00092$; MSWD =38). The goodness of isochron fit was significantly improved by rejection of 5 outliers resulting in an isochron age of 201.2 ± 1.6Ma and an initial $^{87}Sr/^{86}Sr$ of 0.70892 ± 0.00022 (MSWD =2.2).

(3) Rb-Sr isochron age determination on sphalerite and coexisting gangue carbonate of individual samples ("internal isochron") yielded model ages of 229.9 ± 1.9 and 205.8 ± 1.7Ma (Crest facies; one sample excluded) and 207.6 ± 1.4 Ma and 202.9 ± 1. Ma (Revier Erlach).

(4) The initial Sr isotopic ratio of gangue carbonate (n=19), barite (n=1) and fluorite (n=11) from ore samples of various locations varies between $^{87}Sr/^{86}Sr_{(t=200\ Ma)} = 0.70774$ - 0.70957.

As the Rb-Sr isochron calculations were performed using an old ^{87}Rb decay constant (*c.f.,* Nebel *et al.,* 2011; Rotenberg *et al*., 2012), a recalculation of the isochron parameters is required. In this context, we also re-evaluated earlier isochron model calculations, which leads to the following findings:

(1) The Rb-Sr 3-point isochron on sphalerite and pyrite from the Cardita horizon now gives a model age of 228.8 ± 2.7Ma with an initial Sr isotopic ratio of 0.70778 ± 0.00004 (MSWD = 2.1) (Fig. 11A). The elevated $^{87}Sr/^{86}Sr$ values of gangue carbonate and fluorite of Cardita samples (0.70793 – 0.70957) suggests that they are not strictly cogenetic with the Rb-Sr dated sphalerites.

(2) Seven sphalerites of the Revier Erlach, which forms a special orebody of Ge-rich sphalerite within the Bleiberg deposit, yield a well-defined Rb-Sr isochron providing an age of 198.2 ± 3.0 Ma and an initial $^{87}Sr/^{86}Sr$ of 0.71051 ± 0.00070 (MSWD = 1.9). Rejection of one sample, which gave a poorly defined $^{87}Sr/^{86}Sr$, further improves the goodness-of-fit of the isochron calculation to a MSWD value of 1.1 (t = 201.1 ± 4.0Ma; 0.70986 ± 0.00093) (Fig. 11B). The model ages and initial Sr ratios are within error identical thus demonstrating the geological significance of the isochron calculation for the Erlach Revier samples. The initial $^{87}Sr/^{86}Sr$ values of gangue carbonate of Erlach Revier samples (0.70774 – 0.70836) is significantly less radiogenic compared to the respective sphalerite isochron value.

(3) An isochron calculation on sphalerite of the Crest samples from Josefi-, Riedhard- and Kalkscholle (n = 10) provides evidence for excess scatter (MSWD = 64). The model age is 208.1 ± 6.7 Ma. Omitting 3 data points, which plot significantly off the reference line, results in a well-defined isochron (n = 7; MSWD = 0.5) with a model age of 207.4 ± 0.9 Ma and an initial Sr isotopic value of 0.70853 ± 0.00004 (Fig. 11C). Gangue carbonates of Crest samples show initial $^{87}Sr/^{86}Sr$ values of 0.70797 – 0.70863.

(4) Earlier isochron calculations pooling Rb-Sr isotope data of sphalerite from the Crest facies and the Erlach Revier are not considered here as this approach includes samples from structurally different ore bodies. In addition, a well-defined isochron can only be obtained by omitting of a relatively large amount of sample data (5 from a total of 17).

The Rb-Sr model age of 228.8 ± 2.7Ma for Cardita sphalerite suggests ore formation in the Carnian stage (≈237 to ≈227Ma) according to the International Chronostratigraphic Chart v 2023/04 (Cohen et al., 2013; updated). The isochron age thus fits to the Middle to Upper Carnian age of the host rocks. In addition, the initial $^{87}Sr/^{86}Sr$ isochron value of 0.70778 ± 0.00004 is very close to the Sr isotopic composition of seawater at this time (ca. 0.7077; Korte *et al*., 2003). Therefore, we tentatively interpret the Rb-Sr dating results for the Cardita sphalerite to indicate ore formation very soon after deposition of its host rock and with a Sr isotopic signature close to seawater of Carnian age. However, the geological significance of the Cardita isochron has to be considered with caution as the isochron is only defined by 3 data points.

In contrast to the Cardita isochron, the Rb-Sr isochron age of 201.1 ± 4.0 Ma for sphalerite of the Erlach Revier is well-defined, both on the sample basis (n = 6; 1 data set rejected) and the statistics (MSWD = 1.1). Therefore, we assign a high geological significance to this isochron calculation and interpret the model age to date formation of the Erlach Revier ore at the Triassic-Jurassic boundary (≈201Ma). Compared to an $^{87}Sr/^{86}Sr_{(t\sim 200\ Ma)}$ value of seawater of ≈ 0.70765 (Korte *et al*., 2003; Halverson *et al*., 2014), the initial $^{87}Sr/^{86}Sr$ value of the Revier Erlach isochron (≈0.710) is significantly enriched in radiogenic Sr. This indicates that Sr was predominantly sourced from older crustal rocks during ore formation.

The Rb-Sr isochron age of 207.4 ± 0.9Ma on sphalerite of the Crest facies is also well-defined, although it takes into account a reduced amount of Crest sample data. It is within-error to the errorchron model age obtained for all Crest samples (208.1 ± 6.7Ma) and thus is assumed to be geologically significant. The model age indicates a Rhaetian (≈209 to 201Ma) formation age for ore bodies of the Crest facies. Similar to the Revier Erlach dataset, the initial $^{87}Sr/^{86}Sr$ value of ≈0.7085 for the Crest model isochron is more radiogenic compared to seawater Sr of that age (≈0.7082 – 0.7076) thus indicating the contribution of Sr from an older crustal component. According to Schroll et al. (2006), the range in Sr isotopic composition of whole-rock samples of the Crest facies can in part be modelled by mixing of marine Sr with ^{87}Sr-enriched Sr derived from basement rocks. They obtained a best-fit mixing line for the age-corrected $^{87}Sr/^{86}Sr$ sample values assuming a model age of 21 Ma (with an assigned uncertainty of ±30Ma).

Geochronological data for ore and gangue minerals from other important APT deposits (Mežica, Raibl, Salafossa, Lafatsch) are lacking. However, recent in-situ U-Pb dating of hydrothermal carbonates in ore samples of the APT Gorno Pb-Zn mining District (Southalpine) yielded within-error identical ages of ≈230Ma (Giorno *et al*., 2022). Error-weighted mean ages of 229 ± 9Ma for dolomite predating sulphide formation (n = 2) and 229 ± 3Ma for calcite postdating mineralization (n = 4) indicate an Upper Carnian age of mineralization. As this age is

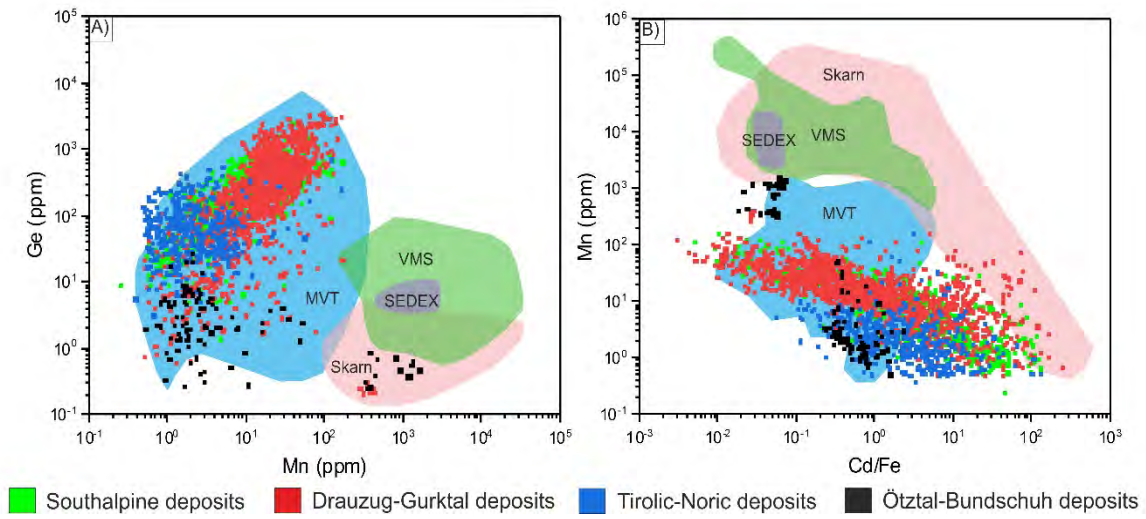

Figure 12: *Binary diagrams of Mn vs. Ge (A) and Cd/Fe vs. Mn (B) for LA-ICP-MS analytical data from APT deposits in four tectonic units. Deposit type fields were constructed using data from Cook et al. (2009), Ye et al. (2016), Li et al. (2020), Wei et al. (2021), Yang et al. (2022) and Liang et al. (2023).*

very close to the depositional age of the host rocks, mineralization likely formed at shallow depths.

Discussion

The Bleiberg and related deposits were described by Jicha (1951), Cerny (1989), Schroll & Rantitsch (2005) and Schroll (2008) as "Alpine-type" deposits. Further investigations by Kucha *et al.* (2005, 2010) showed that the Pb-Zn ores originate, at least partly, in context with microbial activity of sulphate-reducing bacteria. The stratigraphic package of all APT deposits comprises Lower Triassic red beds, Anisian shallow water carbonates that host small Pb-Zn orebodies in all tectonic units studied, Ladinian deep water carbonates, and the Carnian reef facies of the Wetterstein Formation hosting the bulk of the metal endowment. After a hiatus in the Julian, these are overlain by clastic sediments of the Raibl Group (Cardita Shales) and intercalated shallow water carbonates that may host stratiform APT orebodies, between the lagoonal dolomites of the Norian Hauptdolomit Formation that are barren, with very few exceptions (Fig. 2; Cerny, 1989). This sedimentary pile reflects a shelf on a passive continental margin of the Neotethys. The Pb-Zn mineralization at the Bleiberg deposit formed in two stages at 229 and about 205Ma (Fig. 11A-C).

The tectonic regime in which mineralization took place, the source of the metals and heat, the process of mobilization and the reason for the strictly stratiform nature of the ores hosted by only two stratigraphic levels in a carbonate sequence of several 1000m thickness is still not fully understood. In the discussion, we briefly summarize the new data and begin to develop a metallogenic model. We then discuss the APT/MVT dilemma and conclude with the most important findings of this, and previous studies.

Sources of metals and sulphur, and conditions of ore formation

Minor and trace element diagrams for sphalerite are widely used to discriminate deposit types. Sphalerites from APT plot into a "MVT" field constructed from published sphalerite analyses, mainly from deposits in China (Fig. 12). This field differs from high-temperature deposit types such as skarn, VMS (volcanogenic massive sulphides) and SEDEX (sedimentary-exhalative sulphides) by generally lower Mn contents, higher Ge, and a positive correlation of Mn and Ge. Based on the large APT sphalerite dataset, a negative correlation of Cd/Fe versus Mn is noteworthy. Cd/Fe ratios >1 at low Mn contents enlarge the MVT field proposed by Liu *et al.* (2022) and Liang *et al.* (2023) (Fig. 12).

Although sphalerite and galena compositions in APT-type deposits share common features, the data presented also reveal considerable differences within deposits and within ore Districts (Fig. 12). In deposits within the Drauzug-Gurktal Nappe System, sphalerites are higher in Ge and Mn than in other tectonic units. The deviant position of the data from the Brenner Mesozoic (Ötztal-Bundschuh Nappe System) within the "skarn" field (Fig. 12A) is most likely due to the high metamorphic temperature exceeding 450°C (Melcher & Krois, 1992; Reiser *et al*., 2019). At those temperatures, sphalerite exchanges trace elements with host rocks (e.g., Mn-bearing carbonate) and thus changes its original composition (Frenzel *et al.*, 2016). All other sphalerite datasets, however, still indicate the primary sphalerite composition formed at low temperatures.

Trace element concentrations in sphalerite vary over a wide range within individual deposits. Variations often correlate with sphalerite colour and texture. Zeeh & Bechstädt (1994), Kuhlemann (1995), Kuhlemann & Zeeh (1995), Zeeh *et al.*

(1998) and Kuhlemann *et al.* (2001) provided evidence for different sphalerite generations co-crystallizing with carbonate cement types possibly attributed to diagenetic processes. However, within-deposit variations and also variations among textural types show that a consistent model of sphalerite generations and their trace element inventory cannot be provided at this stage. Even within one deposit such as Bleiberg, a correlation is impossible, not to mention the correlation among different ore deposits within a District.

Certain correlations of trace elements with sulphur isotope geochemistry are attributed to enhanced input of bacteriogenic sulphur at slightly elevated temperatures from reservoirs rich in trace elements (Fig. 9). The variation of trace element data within and among ore Districts is also enormous and shows that all deposits investigated have their own trace element signatures (Fig. 8). Differences are most likely due to chemical variations in source rocks, given that other parameters such as fluid composition, fluid temperature and sulphur reservoir are similar. The Pb isotope data point to feldspar from crystalline basement rocks of Palaeozoic age as lead (Ba and Tl) sources; however regional variations exist that also point to a heterogeneous basement composition (Fig. 10). Nevertheless, there is no generally accepted explanation for the sources of the common trace metals Ge, As, Tl and Cd. As some of these metals are redox-sensitive, a source from organic-rich material may be envisaged. Kuhlemann *et al.* (2001) proposed iron-rich Partnach basin sediments and Permo-Triassic red beds and evaporites as potential sources of metal and of thermally reduced sulphur respectively. They also envisaged hydrothermal convection cells progressively moving to greater depth with time and thus tapping progressively deeper and hotter basement rocks. Rantitsch *et al.* (1999) found condensate-like hydrocarbon in sphalerite and galena at Bleiberg, demonstrating that late Cretaceous to Palaeogene fluid migration influenced ore formation.

The sulphur isotope composition of sphalerite, galena and pyrite varies over a wide range and is often bimodally distributed, that can be explained by two sulphur sources: one with highly negative values ($\delta^{34}S \leq -20‰$) reflecting bacteriogenic sulphate reduction, and a second weaker maximum at $\delta^{34}S = -10$ to 0‰ explained by thermogenic sulphate reduction from a second (hydrothermal?) source (Henjes-Kunst *et al.,* 2017). The sulphur reservoir for BSR derived from seawater sulphate. Dissolved sulphate in pore water and/or evaporites could have been the ultimate source derived from the lagoonal "special facies".

Galena and sphalerite of the APT deposits mostly show late Palaeozoic to early Mesozoic common Pb model ages. Their Pb isotopic composition is compatible with a metal source from Palaeozoic basement rocks and Triassic sedimentary strata.

Application of the GGIMFis thermometer reveals temperatures between 60 and 140°C, consistent with thermal models for subsidence of the Drau Range (Rantitsch, 1995, 2001, 2003). These temperatures are in accordance with fluid inclusion data available for some of the deposits, e.g. Bleiberg and Mežica (Zeeh & Bechstädt, 1994; Zeeh *et al.,* 1998; Kuhlemann *et al.,* 2001). Fluids analyzed in fluorite, carbonate and sphalerite from the Triassic/Jurassic mineralization phase indicate formation temperatures from 122° to 159° (for early sphalerite and clear saddle dolomite) to >200°C in fluorite (Zeeh *et al*., 1998). Fluids evolved from relatively low salinities for sphalerite-forming fluids (8-12 wt.% NaCl eq.) to higher salinities during the fluorite precipitation (18-25 wt.% NaCl eq.). Late-stage Alpine mineralization is characterized by more variable fluid temperatures (120-250°C) and salinities (7-25 wt.% NaCl eq.; Zeeh *et al.,* 1998).

Alkali metals and halogens were analysed by ion chromatography on crush-leach fractions from ores and host rocks of the Bleiberg deposit (Schroll & Prochaska, 2004; Schroll, 2006). Molar Na/Br (100-300) and Cl/Br ratios (158-576) of ore samples and mineralized rocks plot on the seawater evaporation trend. The data exclude mixing with meteoric water and the dissolution of marine evaporitic salt by meteoric water. Since evaporitic salts were deposited in the lagoonal sabkha facies, the origin of the halides cannot be traced back exclusively to the ore solutions (Schroll, 2008).

Palaeogeography and metallogeny

According to the data available, the formation of APT deposits took place over an extended period of time, probably starting in the Anisian, with major pulses in the Carnian (Julian) and in the Rhaetian to lowermost Jurassic. Although mineralization in the Anisian has not been confirmed by radiometric data, textures and sulphur isotopes in the stratiform Topla deposit (District VII) indicate early diagenetic emplacement (Spangenberg & Herlec, 2006). Mineralizing fluids are interpreted as basinal brines derived from buried and evaporated seawater that migrated into Palaeozoic and early Mesozoic basement rocks along extensional structures. Both the timing and fluid composition indicate a connection to hydrothermal fluids producing metasomatic magnesite and siderite deposits in the Upper Austroalpine tectonic units mainly during Upper Triassic times (Prochaska & Henjes-Kunst, 2009; Henjes-Kunst *et al.,* 2014).

The metallogenic evolution in the southern and eastern Alps is most likely related to the breakup of Pangaea starting in the Permian, deposition of deep-water pelagic sediments in basins within the Triassic carbonate platform and opening of the Penninic ocean (Alpine Tethys) in the Early Jurassic. Thick Triassic carbonate platforms developed on an extensive, but rapidly subsiding shallow shelf at the westernmost embayment of the Neotethys ocean. Lithospheric extension in the Permian and Early to Middle Triassic (290-240Ma) resulted in high-temperature, low-pressure metamorphism with local migmatization and pegmatite formation in the Austroalpine basement unit (Knoll et al., 2023). In tectonically higher and probably more external positions within the Austroalpine, saline and hot hydrothermal fluids (ca. 200-350°C) locally transformed Palaeozoic carbonates into magnesite and siderite (Prochaska & Henjes-Kunst, 2009; Henjes-Kunst *et al.,* 2014). Magnesite formation in the Breitenau deposit (Graz Palaeozic Nappe Complex within the Drauzug-Gurktal Nappe System; Fig.1A) is dated to an upper Carnian age (≈229Ma; Henjes-Kunst *et al.,* 2014). Ar-Ar dating of polyhalite in salt deposits of the Northern Calcareous Alps points to a massive fluid event at about 235 Ma (Leitner *et al.,* 2013, 2022), although the interpretation is tenuous (See Figure 13).

The fluids responsible for metasomatic magnesite and siderite formation were likely sourced from thick Mesozoic carbonate platforms overlying locally extensive evaporite beds (Prochaska & Henjes-Kunst, 2009). By analogy, we assume that the APT metals were leached from Palaeozoic basement rocks due to enhanced hydrothermal activity, whereby metal-bearing fluids were released that moved along zones of higher permeability to higher stratigraphic levels. According to Pb isotopic evidence, Triassic sedimentary rocks may also have contributed to the metal content of the APT deposits. Textural and isotopic evidence indicates an early sulphide precipitation during the Carnian, whereas most Pb-Zn sulphides in the Bleiberg deposit were likely formed epigenetically in the Rhaetian. Multiphase brecciation and redistribution processes are texturally documented, indicating remobilization of earlier mineralization.

Textural and geochemical variations indicate the polyphase development of APT deposits. Three phases are distinguished.

Phase 1: Based on textural and geochemical arguments, early diagenetic subseafloor mineralization of Fe and Zn-Pb sulphides occurred in the Anisian (Sankt Veit, Topla, Serles; Fig. 1A). The Topla deposit is interpreted as a low-temperature MVT deposit formed in an anoxic supratidal to hypersaline environment (Spangenberg & Herlec, 2006). A relation of ore formation to magmatic activity in the Anisian is possible, especially in the Southalpine, but not yet proven. Magmatic processes associated with the precursor Periadriatic Fault System (PAF) have been dated at 224 to 245 Ma by U-Pb in zircon (Huang *et al*., 2022) and are attributed to the opening of the Meliata oceanic back-arc basin. A Rb-Sr isochron age of 228.8 ± 2.7 Ma for stratiform Pb-Zn ore in the Cardita orebody at Bleiberg gives a late Carnian mineralizing event. At Bleiberg, and at other deposits in the Drau Range and the Tirolic-Noric Nappe System (e.g., Lafatsch), stratiform Pb-Zn ore with preserved biogenic textures are related to the Carnian special sedimentary facies ("Bleiberg special facies"; Cerny, 1989). The Gorno deposit in the Southalpine is also late Carnian age.

Phase 2: An Upper Triassic/Lower Jurassic age of mineralization was postulated by Zeeh & Bechstädt (1994), Kuhlemann (1995), Kuhlemann & Zeeh (1995) and Zeeh *et al.* (1998) based on carbonate cement stratigraphy, fluid inclusion and stable isotope data. They assumed metal transport by gravity-driven fluid flow from the Bohemian Massif in the north. Epigenetic mineralization in the uppermost Triassic (Rhaetian) to lowermost Jurassic is now supported by Rb-Sr isochron ages of 207 ± 1 Ma and 201 ± 4Ma for trace element-rich sphalerite from Bleiberg. This process is probably related to ongoing tectonic instability following deposition of the Upper Hauptdolomit with formation of deep basins (e.g., Seefeld basin), where hydrocarbon source rocks were deposited on a regional scale, and subsequent deposition of the Kössen Formation (Fig. 2).

On paleogeographic maps of the Alpine realm in the Lower Triassic and Late Jurassic compiled by Haas *et al.* (2020), the Southalpine is positioned opposite the Transdanubian Range and the basement of the Noric Nappe, separated by the Mesozoic precursor of the Periadriatic Fault System (PAF). In the Jurassic, this system evolved into a left-lateral transform fault cutting the ridge axis of the Penninic Ocean (Alpine Tethys) that was located further to the NW, at a right angle. Following this paleogeographic model, the PAF precursor structure may have served as potential fluid conduit over an extensive period of time during the Mesozoic. The Pb-Zn ores thus were emplaced in structures related to a continental-scale strike-slip system. The large APT deposits such as Raibl (District XI), Salafossa (District XII), Mežica, Bleiberg (District VIII), and those from District II (Lafatsch) were located close to the PAF precursor throughout the Triassic and thus were supplied with fluids of varying composition. During this phase, sulphur from additional sources (e.g., basin sediments) was added, along with metals, to form typically dark and often massive schalenblende textures. A relation to magmatic events at ≈205Ma is not likely as evidenced by differences in common lead isotopic signatures (Köppel & Schroll, 1985).

Phase 3: Epigenetic remobilization at higher temperatures during or postdating the Upper Cretaceous Eoalpine phase is evidenced by crosscutting mineralization reaching into stratigraphically and tectonically higher units, e.g., into the Norian Hauptdolomit. Such mineralization appears to be more abundant in the Northern Calcareous Alps, especially towards the east, where mineralized young Alpine fault systems predominate (e.g., Annaberg, Hagenguth *et al*., 1982). Spatial relations and chemical signatures in some cases point to metal mobilization from underlying Permo-Triassic sediments by saline fluids. In rare cases (Arzriedel; Fig. 1A), heavy sulphur isotopes in ore sulphides point towards a contribution from oil-field brines associated with hydrocarbon migration, probably during the Cenozoic (see also Rantitsch *et al*., 1995). The Gorno mineralization was probably influenced by magmatic processes (Fruth & Maucher, 1966), as evidenced by crosscutting Oligocene magmatic dikes related to the Periadriatic magmatic province (Mondillo *et al*., 2020). Hydrothermal post-tectonic deposits occur in the greenschist-facies metamorphosed Ötztal-Bundschuh nappe system of the central Alps. (e.g., Obernberg). Trace element data from the syn- to early diagenetic Serles mineralization show that metamorphic temperatures higher than ca. 350°C (Frenzel *et al.*, 2016) shifted the trace element composition of sphalerite to higher Fe and Mn concentrations. Pyrite, however, largely retained its original chemical composition.

*I*n the wider context of central and southern Europe, mineralizing processes during the Mesozoic have been explained as a response to the breakup of Pangaea (Burisch *et al*., 2022). The oldest hydrothermal processes in the circum-Mediterranean are related to the initial rift axes. Mineralization spans an age range from 230 to 160Ma with a maximum at 230-200Ma. The data presented here fit into this pattern. On the continental scale, Burisch *et al.* (2022) interpret the formation of fluorite-barite-Pb-Zn, native metal-arsenide and strata-bound Pb-Zn deposits as a consequence of episodic mixing of basement-derived fluids with seawater-derived brine.

APT – a subtype of MVT?

Pohl (2020) uses the term "diagenetic-hydrothermal carbonate-hosted Pb-Zn (F-Ba) deposits" for Pb-Zn ores hosted by marine carbonate rocks that display end member and mixed characteristics of syngenetic (e.g., SedEx) and epigenetic hy-

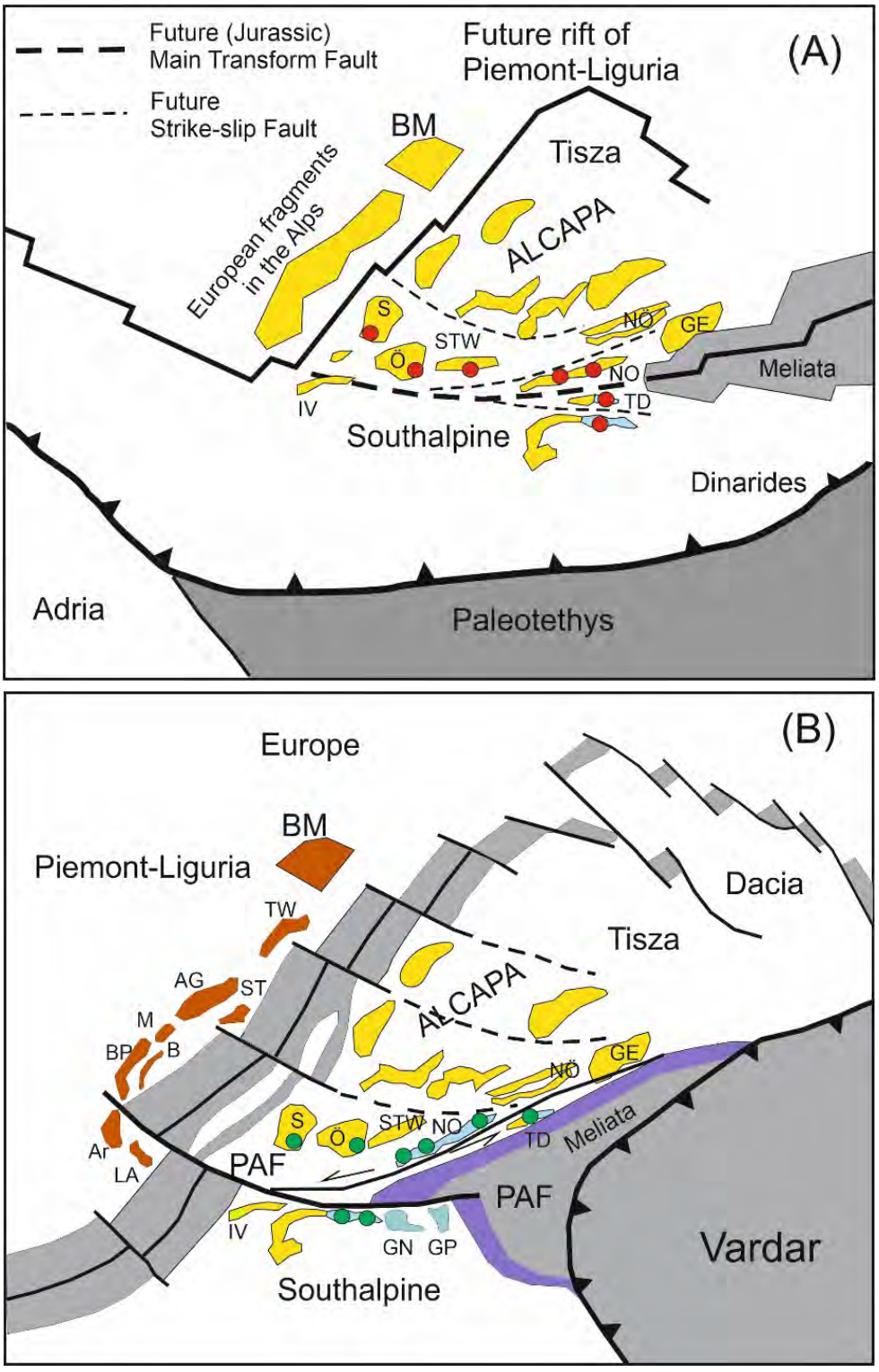

Figure 13: *Late Permian/Lower Triassic (A) and Late Jurassic (B) paleogeography of crustal blocks and continental mega-units; modified after Haas et al. (2020). A, Argentera Massif; AG, Aar-Gotthard Massif; ALCAPA, Alps-Carpathian-Pannonian; Briançonnais; BM, Bohemian Massif; BP, Belledonne-Pelvoux Massif; GE, Gemericum; IV, Ivrea Zoe; M, Montblanc Massif; NO, Noric basement; NÖ, Nötsch (Drau Range); Ö, Ötztal; S, Silvretta; STW, south of Tauern Window; TD, Transdanubian Range and Drau Range; PAF, precursor of Periadriatic Fault. (A) Colours: grey, oceanic crust; yellow, continental clastics; blue, sabkha and shallow marine carbonates. Red circles indicate position of Middle Triassic (Anisian) APT occurrences overlying Lower Triassic clastic rocks. (B) Dark orange, continental and evaporitic facies; yellow, shallow marine Hauptdolomit Facies; light blue, Dachsteinkalk facies; dark blue, pelagic Hallstatt facies. Green circles indicate position of Upper Triassic (Carnian) APT occurrences in rocks of the Wetterstein Platform and the Raibl Group.*

drothermal ore formation. Among the epigenetic type, subtypes have been defined, such as Alpine ('APT'), Irish ('IRT'), Mississippi Valley ('MVT') and Upper Silesian-Cracow ('USCT') subtypes. In contrast, other authors classified all carbonate-hosted Pb-Zn deposits collectively as MVT deposits (Leach *et al.*, 2005). A long discussion has therefore centred on the question whether APT Pb-Zn deposits are to be assigned to the MVT group or represent a separate class of ore deposit. Discussions were summarized by e.g., Fontboté & Boni (1994), Zeeh & Bechstädt (1994), Leach *et al.* (2003, 2005, 2010), and Schroll (1996, 2008). Features that are common to both, APT and MVT, include the following:

(1) Both occur in clusters of deposits, typically hosted in shallow marine carbonate sequences of predominantly Phanerozoic age. Commonly they are found at the margins of basins or above basement highs. Metamorphic basement rocks and clastic sedimentary rocks underlie the carbonate sequence and evaporites are often present in the stratigraphic column. Karst structures, breccia horizons and synsedimentary faults indicate emergence and tectonic instability providing pathways for fluid migration.

(2) The ores show similar elemental composition (Zn-Pb-Ba-F) and similar simple mineralogy (sphalerite/wurtzite, galena, barite, fluorite).

(3) A low temperature (<100 up to 200°C) of ore formation is indicated, and the ore fluids were reduced, acidic NaCl-dominated brines of moderate to high (10-30%) salinity.

Differences between APT and MVT Pb-Zn deposits include:

(1) APT ores form at shallow depth, often close to the surface, whereas MVT typically form at deeper levels.

(2) Ore textures commonly include colloform schalenblende in APT, and finely laminated textures (rhythmites) that occasionally preserve evidence of bacteriogenic sphalerite formation.

(3) APT fluids follow a seawater evaporation trend in Cl/Br and Na/Br ratios, whereas MVT deposits are often formed by mixing of formation water with meteoric water.

(4) APT deposits are dominated by isotopically light sulphur with a wide range of $\delta^{34}S$ ranging from -40 to about 0‰ (Schroll & Rantitsch, 2005). This indicates a predominance of BSR in an open system, with local input from TSR. MVT deposits, in contrast, are dominated by TSR, and no fractionation between ore sulphur and seawater sulphate can be established.

(5) APT deposits yield Pb model ages older than the formation age of the host rocks (so-called "B(leiberg)-type signature"; Köppel & Schroll, 1985; Köppel, 1997; Henjes-Kunst, 2014). In contrast, classic MVT deposits show younger Pb model ages when compared to their host rocks ("J(oplin)-type signature"; Leach *et al*. 2005).

(6) Muchez *et al.* (2005) demonstrated that extensional tectonics played a major role in the formation of sediment-hosted base metal deposits in Europe, including APT deposits. Although MVT deposits in extensional settings have been described (e.g., Ostendorf *et al.*, 2015), this is one important argument to separate APT from MVT as the latter are typically formed in compressional tectonic settings. This also implies elementary differences in the driving forces of large-scale basinal fluid flow: higher crustal heat flow in the platform caused by extensional tectonics due to continental break-up vs. tectonic-driven gravitational fluid flow during compressional tectonics.

(7) Isotopic ages indicate a polyphase history of APT, with syn- to early diagenetic ore formation followed by a longer history of diagenetic growth documented by carbonate and sphalerite stratigraphy (Kuhlemann, 1995). In the Bleiberg deposit, a major mineralizing pulse occurred about 20-25 million years after the early mineralization period. In classic MVT deposits the timing of mineralization may postdate sediment deposition by tens to even hundreds of million years.

In summary, considering geological, mineralogical and geochemical arguments (e.g., trace elements in sphalerite, Fig. 12), APT-deposits appear to represent a subtype of the general MVT type. However, using geographical designations such as MVT, APT, IRT, USCT etc. suggests that similar deposits are restricted to, or at least dominate in a specified region. As this is definitely not the case, it is recommended to use the neutral term carbonate-dominated Pb-Zn deposits, synonymous to clastic-dominated Pb-Zn deposits as the two subtypes of the sediment-hosted Pb-Zn deposits (Leach *et al.*, 2010). Differences within the carbonate-dominated subtype could then be expressed by using additional denominations such as extensional, compressional, manto, pipe-shaped, replacement, skarn and the like.

Conclusions

The data presented allow the following conclusions to be drawn:

(1) More than 500 occurrences of carbonate-hosted, APT Pb-Zn ores divided into 13 Pb-Zn ore Districts are documented in Austroalpine and Southalpine units of the Eastern and Southern Alps.

(2) They are invariably hosted by carbonate rocks of Anisian or Carnian age.

(3) Ore textures are complex and often equivocal. However, biogenic textures and relict bacteria colonies cannot be neglected. Therefore, some mineralization must have occurred at shallow level at low temperature.

(4) Sphalerite is low in Fe, Mn, Co and In, but commonly contains elevated Cd, Ge, As, Tl and Pb.

(5) Sphalerite chemistry indicates low temperatures of formation, ranging from 60 to 140°C. This is lower than suggested by previous fluid inclusion data, but in line with results of thermal modelling.

(6) Metamorphosed sphalerite (>450°C) in the Brenner and Stangalm Mesozoic reveals metal exchange with higher Fe and Mn, and lower Ga, Ge, As and Tl concentrations.

(7) Galena is Ag-poor, although both sphalerite and galena tend to higher Ag concentrations towards the northern areas of the Austroalpine nappe system.

(8) Pyrite- and marcasite rich ores display an As-Tl-(Hg) signature but are low in Co and Ni. Pyrite appears to be stable to higher temperatures, keeping original low-temperature trace element compositions.

(9) Rb-Sr isochron dating of sphalerite reveals two phases of ore deposition: a first one at ≈229Ma and a second at ≈207-201Ma.

(10) Initial $^{87}Sr/^{86}Sr$ of the early (229Ma) sphalerite is consistent with Carnian seawater composition.

(11) The Carnian Rb-Sr isochron age corresponds to U-Pb ages determined for calcite associated with mineralization at the Gorno deposit (Southalpine). The younger (≈205Ma) age is interpreted to reflect fluid flow within the carbonate sequence due to fracturing of the platform caused by initial rifting of the Penninic Ocean.

(12) Sulphur isotopes indicate a dominant bacteriogenic origin for the sulphur, but also point to multiple sulphur sources including thermogenic sources.

(13) Lead isotopes point primarily to a metal source from the Palaeozoic basement and Triassic sedimentary rocks.

Acknowledgements

The authors wish to thank the many contributors to this study. Jens Schneider is specially thanked for sharing his knowledge on Rb-Sr dating of sphalerite. Electron microprobe analyses have been performed under supervision of Federica Zaccarini and Helmut Mühlhans (Chair of Resource Mineralogy, Montanuniversität Leoben). Helmut Mühlhans, Sabine Feuchter and Marie-Luise Harmsen prepared numerous polished sections for analysis. Ralf Schuster (Geosphere Austria) supported us in designing Figure 1. Discussions on stratigraphic and paleogeographic issues with Hans-Jürgen Gawlick and Hugo Ortner are greatly acknowledged. Analytical work was partly financed by projects of the Mineralrohstoffinitiative (MRI) of Geosphere Austria and a PhD programme at Universitätszentrum Angewandte Geowissenschaften (UZAG) Steiermark. We dedicate this work in memory of Prof. Oskar Schulz (Innsbruck; 1923-2017) and Prof. Erich Schroll (Vienna; 1923-2008) who did so much for the understanding of this deposit type.

References

Altamin www.altamin.com/au/gorno, accessed January 27, 2023

Assereto, R., Brigo, L., Brusca, C., Omenetto, P. & Zuffardi, P. (1976) Italian ore mineral deposits related to emersion surfaces – a summary: *Mineralium Deposita,* v. 11, 170-179.

Bechstädt, T. (1975) Lead-zinc ores dependent on cyclic sedimentation: *Mineralium Deposita*, v. 10, 234-248.

Brannon, J.C., Podosek, F.A. & McLimans, R.G. (1992) Alleghenian age of the upper Mississippi Valley zinc-lead deposit determined by Rb-Sr dating of sphalerite: *Nature,* v. 356, 509-511.

Breimann, L. (2001) Random Forests: *Machine Learning*, v.45, 5-32.

Brigo, L. & Cerrato, P. (1994) Trace element distribution of Middle-Upper Triassic carbonate-hosted lead-zinc mineralizations: the example of the Raibl deposit (Eastern Alps, Italy). *In:* Fontboté, L. and Boni, M. (eds.), Sediment-hosted Pb-Zn ores, *Society of Geology Applied to Mineral Deposits, Special Publication,* 10, 179-245.

Brigo, L. & Omenetto, P. (1978) The lead and zinc ores of the Raibl (Cave del Predil, northern Italy) Zone: new metallogenic data. In: Scientific Results of the Austrian Projects of the International Geological Correlation Programme (IGCP) Until 1976. Springer, 103–110.

Brigo, L. & Omenetto, P. (1979) Metallogenese der Italienischen Ostalpen: Verhandlungen der Geologischen Bundesanstalt, 1978, v.3, 249-266 (ISMIDA Leoben, 1977).

Brigo, L., Dulski, P., Möller, P., Schneider, H.-J. & Wolter, R. (1988) Strata-bound mineralizations in the Carnic Alps/Italy. *In:* Boissonas, J. and Omenetto, P. (eds.), Mineral Deposits within the European Community, Springer: 485-498.

Brigo, L., Kostelka, L., Omenetto, P., Schneider, H.-J., Schroll, E., Schulz, O. & Štrucl, I. (1977) Comparative reflections on four Alpine Pb-Zn deposits. In: Klemm, D.D. and Schneider, H.-J. (eds.), Time- and strata-bound ore deposits, Springer, 273-293.

Burisch, M., Markl, G. & Gutzmer, J. (2022) Breakup with benefits - hydrothermal mineral systems related to the disintegration of a supercontinent: *Earth and Planetary Science Letters,* v. 580, 117373.

Büttner, W. & Saager, R. (1983) Factor analyses of stream sediment data from the vicinity of zinc-lead occurrences of S-charl (Unterengadine, Switzerland). In: Schneider, H.-J. (ed.), Mineral deposits of the Alps and of the Alpine Epoch in Europe (Proceedings of the IV. ISMIDA 1981). Special Publication No. 3 of the *Society for Geology Applied to Mineral Deposits,* 231-239.

Canaval, R. (1931) Der Blei- und Galmeibergbau Jauken bei Dellach i.D: Berg- und Hüttenmännisches Jahrbuch, 79, Heft 1, 1-7.

Cerny, I. (1989) Die karbonatgebundenen Blei-Zink-Lagerstätten des alpinen und außeralpinen Mesozoikums. Die Bedeutung ihrer Geologie, Stratigraphie und Faziesgebundenheit für Prospektion und Bewertung: *Archiv für Lagerstättenforschung der Geologischen Bundesanstalt,* v. 11, 5-125.

Cerny, I. & Schroll, E. (1995) Heimische Vorräte an Spezialmetallen (Ga, In, Tl, Ge, Se, Te und Cd) in Blei-Zink- und anderen Erzen: *Archiv für Lagerstättenforschung der Geologischen Bundesanstalt,* v. 18, 5-33.

Christensen, J.N., Halliday, A.N., Vearncombe, J.R. & Kesler, S.E. (1995a) Testing models of large-scale crustal fluid flow using direct dating of sulphides: Rb-Sr evidence for early dewatering and formation of Mississippi Valley-type deposits, Canning Basin, Australia: *Economic Geology,* v. 90, 877-884.

Christensen, J.N., Halliday, A.N., Leigh, K.E., Randel, R.N. & Kesler, S.E. (1995b) Direct dating of sulphides by Rb-Sr: A critical test using the Polaris Mississippi Valley-type Zn-Pb deposit: *Geochimica et Cosmochimica Acta,* v. 59, 5191-5197.

Christensen, J.N., Halliday, A.N. & Kesler, S.E. (1996) Radiometric dating of Mississippi Valley-type Pb-Zn deposits. In: Sangster, D.F. (ed.): Carbonate-Hosted Zinc-Lead Deposits: *Society of Economic Geology Special Publication*, v. 4, 536–545.

Cohen, K.M., Finney, S.C., Gibbard, P.L. & Fan, J.-X. (2013) The ICS International Chronostratigraphic Chart: *Episodes,* v. 36, 199-204.

Cook, N.J., Ciobanu, C.L., Pring, A., Skinner, W., Shimizu, M., Danyushevsky, L., Saini-Eidukat, B. & Melcher, F. (2009) Trace and minor elements in sphalerite: A LA-ICPMS study: *Geochimica et Cosmochimica Acta*, v. 73, 4761-4791.

Cotta, B.v. (1863) Über die Blei- und Zinkerzlagerstätten Kärnthens: *Berg- und Hüttenmännische Zeitung*, v. 22, 9-12 and 33-35 and 41-44 and 53–55.

Drovenik, M., Pezdič, J. & Pungartnik, M. (1988) Sulfur isotope composition of sulfides in the zinc-lead deposit Topla (in Slovene): Razprave Slovenske Akademije Znanosti in Umetnosti, 4 razreda, v. 29, 113–128.

Enzfelder, W. (1972) Geschichte des Blei-Zinkerzbergbaues Bleiberg. In: Bouvier, M. et al. (eds.), Blei und Zink in Österreich, Verlag Naturhistorisches Museum Wien, 3-7.

Escher, E. (1935) Erzlagerstätten und Bergbau im Schams, in Mittelbünden und im Engadin: *Beiträge zur Geologie der Schweiz, Geotechnische Serie,* v. 18., 120 pp.

Fontboté, L. & Boni, M. (1994) Sediment-hosted zinc-lead ores – an introduction. In: Fontboté, L, Boni, M (eds.), Sediment-hosted Zn–Pb ores, Springer, Berlin, 3-12 (*Geological Society Special Publication* 10)

Frenzel, M., Hirsch, T. & Gutzmer, J. (2016) Gallium, germanium, indium, and other trace and minor elements in sphalerite as a function of deposit type? A meta-analysis: *Ore Geology Reviews,* v. 76, 52-78.

Fruth, I. & Maucher, A. (1966) Spurenelemente und Schwefel-Isotope in Zinkblenden der Blei-Zink-Lagerstätte Gorno: *Mineralium Deposita,* v. 1, 238-250.

Gartner, V. (2023) Trace Element Composition of Sphalerite from the Raibl Pb-Zn mine: Master thesis, University of Leoben, 130 p.

Gawlick, H.-J. & Missoni, S. (2019) Middle- to Late Jurassic sedimentary mélange formation related to ophiolite obduction in the Alpine-Carpathian-Dinaridic Mountain Range: *Gondwana Research,* v. 74, 144-172.

Giorno, M., Barale, L., Bertok, C., Frenzel, M., Looser, N., Guillong, M., Bernasconi, S. M. & Martire, L. (2022) Sulphide-associated hydrothermal dolomite and calcite reveal a shallow burial depth for Alpine-type Zn-(Pb) deposits: *Geology*, v. 50, 853-858.

Göbl, W. (1903) Die Blei-Zink-Lagerstätten in Raibl. *In:* Geologisch-bergmännische Karten mit Profilen von Raibl nebst Bildern von den Blei- und Zinklagerstätten in Raibl. K.K.Ackerbauministerium, Wien, 5-71.

Götzinger, M. A. (1985) Mineralisationen in den Gutensteiner Schichten (Anis) in Ostösterreich: *Archiv für Lagerstättenforschung der Geologischen Bundesanstalt,* v. 6, 183-192.

Götzinger, M. A. & Leute, M. (1998) Die Pb-Zn-F-(Cu-Fe)-Mineralisationen der Stangalm-Trias, Nationalpark Nockberge, Kärnten: *Mitteilungen der Österreichischen Mineralogischen Gesellschaft,* v. 143, 281-283.

Götzinger, M.A. & Pak, E. (1983) Zur Schwefelisotopenverteilung in Sulfid- und Sulfatmineralen triadischer Gesteine der Kalkalpen, Österreich: *Mitteilungen der Gesellschaft der Geologie- und Bergbaustudenten Österreich,* v. 29, 191-198.

Gröbner, J. (1998) Die Mineralien des alten Bergbaues bei Flattnitz in Kärnten: *Mineralien-Welt*, v. 9/5, 61-63.

Gstrein, P. & Heissel, G. (1989) Zur Geschichte und Geologie des Bergbaues am Südabhang der Innsbrucker Nordkette: *Veröffentlichungen des Museums Ferdinandeum,* v. 69, 5-58.

Haas, I., Eichinger, S., Haller, D., Fritz, H., Nievoll, J., Mandl, M., Hippler, D. & Hauzenberger, C. (2020) Gondwana fragments in the Eastern Alps: A travel story from U/Pb zircon data: *Gondwana Research,* v. 77, 204–222.

Hagenguth, G. (1984) Geochemische und fazielle Untersuchungen an den Maxerbänken im Pb-Zn-Bergbau von Bleiberg-Kreuth/Kärnten: Mitteilungen der Gesellschaft der Geologie- und Bergbaustudenten Österreich, Sonderheft 1, 110 pp.

Hagenguth, G., Pober, E., Götzinger, M.A. & Lein, R. (1982) Beiträge zur Geologie, Mineralogie und Gechemie der Pb/Zn-Vererzungen Annaberg und Schwarzenberg (Niederösterreich): *Jahrbuch der Geologischen Bundeanstalt,* v. 125, 155-218.

Halverson, G.P., & Théou-Hubert, L. (2014) Seawater Sr Curve. In: Rink, W., Thompson, J. (eds), Encyclopedia of Scientific Dating Methods. Springer, Dordrecht. 733-739.

Hegemann, F. (1949) Die Herkunft des Mo, V, As und Cr in Wulfeniten: *Heidelberger Beiträge zur Mineralogie und Petrographie,* v. 1, 690.

Hegemann, F. (1960) Über extrusiv-sedimentäre Erzlagerstätten der Ostalpen, II. Teil: Blei-Zink-Lagerstätten: *Erzmetall*, v.2, 122–127.

Henjes-Kunst, E. (2010) Petrographical and geochemical investigations on sphalerites from Bleiberg (Austria). Master thesis, University of Freiburg, 86 pp.

Henjes-Kunst, E. (2014) The Pb-Zn deposits in the Drau Range (Eastern Alps, Austria/Slovenia): A multi-analytical research approach for investigation of the ore-forming mechanism. PhD dissertation, Montanuniversität Leoben, 282 pp.

Henjes-Kunst, E., Raith, J.G. & Boyce, A.J. (2017) Micro-scale sulphur isotope and chemical variations in sphalerite from the Bleiberg Pb-Zn deposit, Eastern Alps, Austria: *Ore Geology Reviews*, v. 90, 52-62.

Henjes-Kunst, F., Prochaska, W., Niedermayr, A., Sullivan, N. & Baxter, E. (2014) Sm–Nd dating of hydrothermal carbonate formation: An example from the Breitenau magnesite deposit (Styria, Austria): *Chemical Geology*, v. 387, 184-201.

Herlec, U., Spangenberg, J. & Lavrič, J. (2010) Sulfur isotope variations from orebody to hand-specimen scale at the Mežica lead-zinc deposit, Slovenia: predominantly biogenic pattern: *Mineralium Deposita,* v. 45, 531-547.

Höll, R., Kling, M. & Schroll, E. (2007) Metallogenesis of germanium – A review: *Ore Geology Reviews:* v. 30(3-4), 145-180.

Huang, Q., Neubauer, F., Liu, Y., Genser, Jo., Guan, Q., Chang, R., Yuan, S. & Yu, S. (2022) Permian-Triassic granites of the Schladming complex (Austroalpine basement): Implications for subduction of the Paleo-Tethys Ocean in the Eastern Alps: *Gondwana Research,* v. 109, 205–224.

Isser, M. (1881) Die Blei-Zinkwerke der Gewerkschaft Silberleithen: Österreichische Zeitung für Bergwesen und Hüttenwesen, v. 7/8, 10.

Jerz, H. & Ulrich, R. (1966) Erläuterungen zur Geologischen Karte von Bayern 1:25 000, Blatt Nr. 8533/8633 Mittenwald. Bayerisches Geologisches Landesamt, München

Jicha, H.L. (1951) Alpine lead-zinc ores of Europe: *Economic Geology*, v. 46, 707-730.

Kanaki, F. (1972) Die Minerale Bleibergs (Kärnten): Carinthia II, v.82, Mitteilungen des Naturwissenschaftlichen Vereins für Kärnten, v. 162, 7-84.

Kellerhals, P. (1962) Neue Beobachtungen in den aufgelassenen Pb-Zn-Bergwerken von S-charl (Unterengadin): *Eclogae Geologicae Helvetiae*, v. 55, 467-475.

Knauer, J., (1937) Die Herkunft der Blei- und Zinkerze im Rauschberg- Gebiet bei Inzell: *Abhandlungen des geologischen Landesamts am Bayerischen Oberbergamt*, v. 30, 3-15.

Knoll, T., Huet, B., Schuster, R., Mali, H., Ntaflos, T. & Hauzenberger, C. (2023) Lithium pegmatite of anatectic origin – A case study from the Austroalpine Unit Pegmatite Province (Eastern European Alps): Geological data and geochemical modelling: *Ore Geology Reviews*, v. 154, 105298.

Köppel, V. (1983) Summary of lead isotope data from ore deposits of the Eastern and Southern Alps: some metallogenetic and geotectonic interpretations. In: Schneider, H.-J. (ed.), Mineral deposits of the Alps

and of the Alpine Epoch in Europe (Proceedings of the IV. ISMIDA 1981), *Special Publication No. 3 of the Society for Geology Applied to Mineral Deposits*, 162-168.

Köppel, V. (1997) 3.5. Bleiisotope. In: Weber, L. (ed.), Handbuch der Lagerstätten der Erze, Industrieminerale und Energierohstoffe Österreichs: *Archiv für Lagerstättenforschung Geologische Bundesanstalt,* v. 19, 485-495.

Köppel, V. & Schroll, E. (1978) Lead isotope composition of lead ore deposits from the Mesozoic of the Eastern Alps: *Verhandlungen der Geologischen Bundesanstalt (Wien),* v. 3., 403-409.

Köppel, V.& Schroll, E. (1983) Lead isotopes of Paleozoic, stratabound to stratiform galena-bearing sulfide deposits if the Eastern Alps (Austria): implications for their geotectonic setting: *Schweizerische Mineralogisch-Petrographische Mitteilungen*, v. 63, 347-360.

Köppel, V. &Schroll, E. (1985) Herkunft des Pb der triassischen Pb-Zn-Vererzungen in den Ost- und Südalpen: Resultate bleiisotopengeochemischer Untersuchungen: *Archiv für Lagerstättenforschung der Geologischen Bundesanstalt,* v. 6, 215-222.

Köppel, V. & Schroll, E. (1988) Pb-isotope evidence for the origin of lead in strata-bound Pb-Zn deposits in Triassic carbonates of the Eastern and Southern Alps: *Mineralium Deposita*, v. 23, 96-103.

Korte, C., Kozur, H.W., Bruckschen, P. & Veizer, J. (2003) Strontium isotope evolution of Late Permian and Triassic seawater: *Geochimica et Cosmochimica Acta,* v. 67, 47–62.

Kraus, M. (1913) Das staatliche Blei-Zinkerz-Bergbauterrain bei Raibl in Kärnten. Berg-und Hüttenmännisches Jahrbuch 1 and 2, Special. Vol. LXI, Wien: *Manzsche k.u.k. Hof Verlags und Universitäts Buchhandlung*.

Kucha, H., Schroll, E. & Stumpfl, E.F. (2005) Fossil sulphate-reducing bacteria in the Bleiberg lead-zinc deposit, Austria: *Mineralium Deposita*, v. 40, 123-136.

Kucha, H., Schroll, E., Raith, J.G. & Halas, S. (2010) Microbial sphalerite formation in carbonate-hosted Zn-Pb ores, Bleiberg, Austria: Micro- to nanotextural and sulphur isotope evidence: *Economic Geology*, v.1 05, 1005-1023.

Kuhlemann, J. (1995) Zur Diagenese des Karawanken-Nordstammes (Österreich/Slowenien): Spättriassische, epigenetische Blei-Zink-Vererzungen und mitteltertiäre, hydrothermale Karbonatzementationen: *Archiv für Lagerstättenforschung der Geologischen Bundesanstalt,* v. 18, 57–116

Kuhlemann, J. & Zeeh, S. (1995) Sphalerite stratigraphy and trace element composition in the East Alpine Pb–Zn deposits (Drau Range, Austria/Slovenia): *Economic Geology*, v. 90, 2073–2080.

Kuhlemann, J., Vennemann, T., Herlec, U., Zeeh, S. & Bechstädt, T. (2001) Variations of sulfur isotopes, trace element compositions, and cathodoluminescence of Mississippi Valley-type Pb-Zn ores from the Drau Range, Eastern Alps (Slovenia-Austria): implications for ore deposition on a regional versus microscale: *Economic Geology*, v. 96, 1931-1941.

Kukoč, D., Smirčić, D., Grgasović, T., Horvat, M., Belak, M., Japundžić, D., Kolar-Jurkovšek, T., Šegvić, B., Badurina, L., Vukovski, M. & Slovenec, D. (2023) Biostratigraphy and facies description of Middle Triassic rift-related volcano-sedimentary successions at the junction of the Southern Alps and the Dinarides (NW Croatia): *International Journal of Earth Sciences.*

Lampl, H., Schlagintweit, F. & Gawlick, H.-J. (2008) Die Blei-Zink-Vererzung des Arikogels (Nördliche Kalkalpen, Salzkammergut): *Jahrbuch der Geologischen Bundesanstalt,* v. 148, 107-113.

Läntzsch, M.K. (2015) Die Blei-Zink-Lagerstätten im Wettersteinkalk der Nördlichen Kalkalpen im Raum Bad Reichenhall – Inzell (Bayern): Bergknappe 2015, v.126/127, 39. Jahrgang, 162-171, Tagungsband 18. Internationaler Bergbau- und Montanhistorik-Workshop Andeer, Kanton Graubünden, Schweiz

Leach, D.L., Bechstädt, T.H., Boni, M. & Zeeh, S. (2003) Triassic-hosted MVT Pb-Zn ores of Poland, Slovakia and Italy. *In:* Kelly, J.G., Andrew, C.J., Ashton, J.H., Boland, M.B., Earls, G., Fusciardi, L. and Stanley, G. (eds.), Europe´s major base metal deposits, *Irish Association of Economic Geology, Dublin*. 169-213.

Leach, D.L., Bradley, D.C., Huston, D., Pisarevsky, S.A., Taylor, R.D. & Gardoll, S.J. (2010) Sediment-hosted lead-zinc deposits in Earth history: *Economic Geology,* v. 105, 593-625.

Leach, D.L., Sangster, D.F., Kelley, K.D., Large, R.R., Garven G., Allen C.R., Gutzmer, J. & Walters, S. (2005) Sediment-hosted Pb-Zn deposits: A global perspective: *Economic Geology, 100th Anniversary Volume,* 561-607.

Leitner, C., Neubauer, F., Marschallinger, R., Genser, J.& Bernroider, M. (2013) Origin of deformed halite hopper crystals, pseudomorphic anhydrite cubes and polyhalite in Alpine evaporites (Austria, Germany): *International Journal of Earth Sciences*, v. 102, 813–829.

Leitner, C., Neubauer, F., Genser, J. & Bernroider, M. (2022) Dating of polyhalite: a difficult $^{40}Ar/^{39}Ar$ dating tool of diagenetic to very low-grade metamorphic processes: *International Journal of Earth Sciences*, v. 111, 2037-2051.

Li, Z., Ye, L., Hu, Y., Wei, C., Huang, Z., Yang, Y. & Danyushevsky, L. (2020) Trace elements in sulfides from the Maozu Pb-Zn deposit, Yunnan Province, China: Implications for trace-element incorporation mechanisms and ore genesis: *American Mineralogist,* v. 105, 1734–1751

Liang, X., Li, B., Zhang, X., Qin, H., Li, G. & Zhang, C. (2023) Trace element composition and genesis mechanism of the Fuli Pb-Zn deposit in Yunnan: LA-ICP-MS and in situ S-Pb isotopic constraints: *Frontiers in Earth Sciences*, v. 11, 1104631.

Liu, S., Zhang, Y., Ai, G., Xue, X., Li, H., Shah, S.A., Wang, N. & Chen, X., (2022) LA-ICP-MS trace element geochemistry of sphalerite: Metallogenic constraints on the Qingshuitang Pb–Zn deposit in the Qinhang Ore Belt,South China: *Ore Geology Reviews,* v. 141, 104659.

Melcher, F. (1990) Erzmineralparagenesen und Geochemie an der Basis des Serleskammes, Brennermesozoikum/Tirol. Unpublished Diploma thesis, Leopold-Franzens-Universität Innsbruck, 218 pp.

Melcher, F. & Krois, P. (1992) Syngenetic and diagenetic formation of ore deposits in the metamorphosed sediments of the basal Brenner Mesozoic (Stubai Valley, Austria): *Neues Jahrbuch für Geologie Paläontologie Monatshefte*, 1992 (4), 207-220.

Melcher, F. & Onuk, P. (2019) Potential of critical high-technology metals in Eastern Alpine base metal sulfide ores*: Berg- und Hüttenmännische Monatshefte*, v. 164/2, 71-76.

Melcher, F., Henjes-Kunst, F., Henjes-Kunst, E, Schneider, J. & Thöni, M. (2010a) Datierung der Lagerstätte Bleiberg mit der Rb-Sr Isotopenmethode an Sphalerit und der Sm-Nd-Isotopenmethode an kogenetischem Karbonat und Fluorit. Final report to the Austrian Academy of Sciences (unpublished), 16 pp.

Melcher, F., Henjes-Kunst, F., Henjes-Kunst, E, Schneider, J. & Thöni, M. (2010b) Rb-Sr Isotopendatierung an Sphalerit sowie Sr- und Sm-Nd-Isotopendaten von Karbonat und Fluorit der Zn-Pb Lagerstätte Bleiberg (Kärnten): *Journal of Alpine Geology*, v. 52, 178-180.

Milot, J., Blichert-Toft, J., Ayarzagüena Sanz, M., Fetter, N., Télouk, P. & Albarède, F. (2021) The significance of galena Pb model ages and the formation of large Pb-Zn sedimentary deposits: *Chemical Geology*, v. 583, 120444.

Möller, P., Dulski, P. & Schneider, H.-J. (1983) Interpretation of Ga and Ge content in sphalerite from the Triassic Pb-Zn deposits of the Alps. In: Schneider, H.-J. (ed.), Mineral deposits of the Alps and of the Alpine Epoch in Europe, Proceedings of the IV. ISMIDA 1981. *Special*

Publication No. 3 of the Society for Geology Applied to Mineral Deposits, 213-222.

Mondillo, N., Boni, M., Lupone, F., Granitzio, F. & De Angelis, M. (2018) The Gorno project (Bergamo, Italy): new data on the Pian Bracca exploration area: Abstract, SEG 2018, Keystone.

Mondillo, N., Lupone, F., Boni, M., Joachimski, M., Balassone, G., De Angelis, M., Zanin, S. & Granitzio, F. (2020) From Alpine-type sulphides to nonsulphides in the Gorno Zn project (Bergamo, Italy): *Mineralium Deposita*, v. 55, 953-970.

Muchez, P., Hejlen, W., Banks, D., Blundell, D., Boni, M. & Granida, F. (2005) Extensional tectonics and the timing and formation of basin-hosted deposits in Europe: *Ore Geology Reviews*, v. 27, 241-267.

Nakai, S., Halliday, A.N., Kesler, S.E. & Jones, H.D. (1990) Rb-Sr dating of sphalerites from Tennessee and the genesis of Mississippi Valley type ore deposits: *Nature*, v. 346, 354-357.

Nakai, S., Halliday, A.N., Kesler, S.E., Jones, H.D., Kyle, J.R. & Lane, T.E. (1993) Rb-Sr dating of sphalerites from Mississippi Valley-type (MVT) ore deposits: *Geochimica et Cosmochimica Acta*, v. 57, 417-427.

Nebel, O., Scherer, E. E. & Mezger, K. (2011) Evaluation of the ^{87}Rb decay constant by age comparison against the U-Pb system: *Earth and Planetary Science Letters*, v. 301, 1–8.

Neubauer, F., Liu, Y., Dong, Y., Chang, R., Genser, J., & Yuan, S. (2022). Pre-Alpine tectonic evolution of the Eastern Alps: From Prototethys to Paleotethys: *Earth-Science Reviews*, v. 226, 103923.

Oberthür, T., Melcher, F., Henjes-Kunst, F., Stein, H., Zimmerman, A., Gerdes, A. & El Ghorfi, M. (2009) Hercynian age of the Cobalt-Nickel-Arsenide-(Gold) Ores, Bou Azzer, Anti-Atlas, Morocco: Re-Os, Sm-Nd and U-Pb age determinations: *Economic Geology*, v. 104, 1065-1079.

Ogg, J.G. (2015) The mysterious Mid-Carnian "Wet Intermezzo" global event: *Journal of Earth Sciences*, v. 26, 181–191.

Omenetto, P. (1979) Significant ore fabric relationships in the lead, zinc, fluorite and barite deposits of the Triassic province (Italian Southern Alps): *Annales de la Société géologique de Belgique*, v. 102, 519-529.

Onuk, P. (2018) High-tech metal potential of sphalerite from Eastern Alpine lead-zinc deposits and development of a matrix-matched sphalerite (ZnS) calibration material (MUL-ZnS-1) for calibration of in-situ trace element measurements by laser ablation inductively coupled plasma mass spectrometry (LA-ICP-MS). Dissertation, Montanuniversität Leoben, 196 pp.

Onuk, P., Melcher, F., Mertz-Kraus, R., Gäbler, H.-E. & Goldmann, S. (2017) Development of a matrix-matched sphalerite reference material (MUL-ZnS-1) for calibration of in situ trace element measurements by laser ablation inductively coupled plasma mass spectrometry: *Geostandards and Geoanalytical Research*, v. 41, 263-272.

Ostendorf, J., Henjes-Kunst, F., Mondillo, N., Boni, M., Schneider, J., & Gutzmer, J. (2015) Formation of Mississippi Valley-type deposits linked to hydrocarbon generation in extensional tectonic settings: Evidence from the Jabali Zn-Pb-(Ag) deposit (Yemen): *Geology*, v. 43, 1055–1058.

Ostendorf, J., Henjes-Kunst, F., Schneider, J., Melcher, F. & Gutzmer, J. (2017) Genesis of the carbonate-hosted Tres Marias Zn-Pb-(Ge) deposit, Mexico: Constraints from Rb-Sr sphalerite geochronology and Pb isotopes: *Economic Geology*, v. 112, 1075-1087.

Ostendorf, J., Henjes-Kunst., F., Seifert, T. & Gutzmer, J. (2019) Age and genesis of polymetallic veins in the Freiberg District, Erzgebirge, Germany: constraints from radiogenic isotopes: *Mineralium Deposita*, v. 54, 217-236.

Paar, W. (1995) Gold, Silber und Arsen. In: Grubenhunt & Ofensau: Vom Reichtum der Erde. Landesausstellung Hüttenberg / Kärnten, 29 April - 29 October 1995, v.2: *Beiträge. Kärntner Landesausstellungsbüro*, 51-60.

Paton, C., Hellstrom, J., Paul, B., Woodhead, J.& Hergt, J. (2011) Iolite. Freeware for the visualisation and processing of mass spectrometric data: *Journal of Analytical Atomic Spectrometry*, v. 26 (12), p. 2508.

Pichler, A. (2003) Bergbau in Ostkärnten: Carinthia, II, Sonderheft v. 60, 304 p., Klagenfurt.

Pimminger, M., Grasserbauer, M., Schroll, E. &Cerny, I. (1985) Trace element distribution in sphalerites from Pb-Zn-ore occurrences of the Eastern Alps: *Tschermaks Mineralogisch-Petrographische Mitteilungen*, v. 34, 131-141.

Pohl, W. (2020) Economic Geology. Principles and Practice. Schweizerbart Science Publishers, 2nd edition.

Pošepny, F. (1873) Die Blei- und Galmei-Erzlagerstatten von Raibl in Karnten: Jahrbuch der k.k. *Geologischen Reichsanstalt*, v. 23, 317–424.

Pošepny, F. (1887) Die sogenannten Röhrenerze von Raibl: *Verhandlungen der Geologischen Reichsanstalt*, v. 5, 84–87.

Potočnik Krajnc, B. (2021) Trace element composition of sphalerite from the Mežica Pb-Zn mine. Master thesis, University of Ljubljana, 54 pp.

Prochaska, W. & Henjes-Kunst, F. (2009) Genese der Sideritvererzungen der östlichen Grauwackenzone – aktueller Stand der Forschung: *Arbeitstagung Geologische Bundesanstalt* 2009 – Leoben, Blatt 101 Eisenerz, 153-169.

Rantitsch, G. (1995) Niedrigstgradige Metamorphose im Karbon von Nötsch (Österreich): *Jahrbuch der Geologischen Bundesanstalt*, v. 138/2, 433-440.

Rantitsch, G. (2001) Thermal history of the Drau Range (Eastern Alps): *Schweizerische Mineralogisch-Petrographische Mitteilungen*, v. 81, 181-196.

Rantitsch, G. (2003) A new evaluation of fluid inclusion data based on thermal basin modeling for the Drau Range, Eastern Alps: *Mitteilungen der Österreichischen Geologischen Gesellschaft*, v. 93, 77-85.

Rantitsch, G., Iglseder, C., Schuster, R., Hollinetz, M.S., Huet, B. & Werdenich, M. (2020) Organic metamorphism as a key for reconstructing tectonic processes: a case study from the Austroalpine unit (Eastern Alps): *International Journal of Earth Sciences*, v. 109, 2235–2253.

Rantitsch, G., Jochum, J., Sachsenhofer, R.F., Russegger, B., Schroll, E. & Horsfield, B. (1999) Hydrocarbon-bearing fluid inclusions in the Drau Range (Eastern Alps, Austria): Implications for the genesis of the Bleiberg Pb-Zn deposit: *Mineralogy and Petrology*, v. 65, 141-159.

Rečnik, A., Zavašnik, J. & Fajmut-štrucl, S. (2014) The Mežica mine, Koroška (Slovenia): *The Mineralogical Record*, v. 45, 507-548.

Reiser, M., Rantitsch, G., Scheiber, Th., Frank, W. & Rockenschaub, M. (2019) Tektonisches Modell der östlichen Stubaier Alpen (Oberostalpin; Ötztal- und Steinach-Decken). In: Griesmeier G.E.U. & Iglseder C. (eds.), Arbeitstagung 2019 der Geologischen Bundesanstalt: Geologie des Kartenblattes GK25 Radenthein-Ost, 214-216.

Rotenberg, E., Davis, D.W., Amelin, Y., Ghosh, S.& Bergquist, B.A. (2012) Determination of the decay-constant of ^{87}Rb by laboratory accumulation of ^{87}Sr: *Geochimica et Cosmochimica Acta*, v. 85, 41–57.

Schmid, H. & Weinelt, W. (1978) Lagerstätten in Bayern: *Geologica Bavarica*, v. 77, 160 pp.

Schmid, S. M., Fügenschuh, B., Kissling, E. & Schuster, R. (2004) Tectonic map and overall architecture of the Alpine orogen: *Eclogae Geologicae Helveticae*, v. 97, 93-117.

Schneider, H.-J. (ed.) (1983) Mineral deposits of the Alps and of the Alpine Epoch in Europe: Proceedings of the IV. ISMIDA 1981. *Special Publication No. 3 of the Society for Geology Applied to Mineral Deposits*, Springer.

Schneider, J., Haack, U., Hein, U.F. & Germann, A. (1999) Direct Rb/Sr dating of sandstone-hosted sphalerites from stratabound Pb-Zn deposits in the northern Eifel, NW Rhenish Massif, Germany. *In:* Stanley, C.J. et al. (eds.), Mineral deposits: Processes to processing, Proceedings of the 5th Biennial SGA Meeting and the 10th Quadrennial IAGOD Symposium, London, 22-25 August, 1999, 1287-1290.

Schneider, J., Melcher, F. & Brauns, M. (2007a) Concordant ages for the giant Kipushi base metal deposit from direct Rb-Sr and Re-Os dating of sulphides: *Mineralium Deposita*, v. 42, 791-797.

Schneider, J., von Quadt, A., Wilkinson, J. J. & Boyce, A. J. (2007b) Age of the Silvermines Irish-type Zn-Pb deposit from direct Rb-Sr dating of sphalerite. *In:* Andrew, C.J. et al. (eds.), Digging Deeper, Proceedings of the 9th Biennial SGA Meeting, Dublin/Ireland, 20-23 Aug. 2007, 373-376.

Schroll, E. (1950) Spurenelementparagenese (Mikroparagenese) ostalpiner Zinkblenden: Anzeiger der Österreichischen Akademie der Wissenschaften, *Mathematisch-naturwissenschaftliche Klasse*, 21-25.

Schroll, E. (1951) Spurenelementparagenese (Mikroparagenese) ostalpiner Bleiglanze: Anzeiger der Österreichischen Akademie der Wissenschaften, *Mathematisch-naturwissenschaftliche Klasse*, 6-12.

Schroll, E. (1953a) Über Minerale und Spurenelemente, Vererzung und Entstehung der Blei-Zinklagerstätte Bleiberg-Kreuth/Kärnten in Österreich: Mitteilungen der Österreichischen Mineralogischen Gesellschaft, *Sonderheft* 2, 1-60.

Schroll, E. (1953b) Über Unterschiede im Spurengehalt bei Wurtziten, Schalenblenden und Zinkblenden. Sitzungsbericht der Österreichischen Akademie der Wissenschaften, *Mathematisch-naturwissenschaftliche Klasse*, Abt. I, v. 162, 305-332.

Schroll, E. (1954) Ein Beitrag zur geochemischen Analyse ostalpiner Blei-Zinkerze, Teil I: Mitteilungen der Österreichischen Mineralogischen Gesellschaft, *Sonderheft* 3, 85 pp.

Schroll, E. (1955) Über das Vorkommen einiger Spurenmetalle in Blei-Zink-Erzen der ostalpinen Metallprovinz: *Tschermaks Mineralogisch-petrographische Mitteilungen*, v. 5, 183-208.

Schroll, E. (1979) Beiträge der Geochemie zur Kenntnis der Lagerstätten der Ostalpen: Verhandlungen der Geologischen Bundesanstalt, 1978, 461-470 (3rd ISMIDA 1977).

Schroll, E. (1983) Geochemical characterization of the Bleiberg type and other carbonate hosted lead-zinc mineralization. In: Schneider, H.-J. (ed.), Mineral deposits of the Alps and of the Alpine Epoch in Europe (Proceedings of the IV. ISMIDA 1981), *Special Publication No. 3 of the Society for Geology Applied to Mineral Deposits*, 189-197.

Schroll, E. (1996) The Triassic carbonate-hosted Pb-Zn mineralization in the Alps (Europe): the genetic position of Bleiberg type deposits: *Society of Economic Geology Special Publications*, v. 4, 182-194.

Schroll, E. (1997) V. Geochemische und geochronologische Daten und Erläuterungen. In: Weber, L. (ed.), Handbuch der Lagerstätten der Erze, Industrieminerale und Energierohstoffe Österreichs: Archiv für Lagerstättenforschung Geologische Bundesanstalt, v. 19, 395-538.

Schroll, E. (2006) Neues zur Genese der Blei-Zinklagerstäte Bleiberg: Carithina II, v. 196./116. *Jahrgang*, 483-500.

Schroll, E. (2008) Die Blei-Zink-Lagerstätte Bleiberg. Die Geschichte ihrer Erforschung: Carithina II, v. 62, *Sonderheft*, 287 pp.

Schroll, E. & Pak, E. (1983) Sulphur isotope investigations of ore mineralizations of the Eastern Alps. In: Schneider, H.-J. (ed.), Mineral deposits of the Alps and of the Alpine Epoch in Europe Proceedings of the IV. ISMIDA 1981. *Special Publication No. 3 of the Society for Geology Applied to Mineral Deposits*, 168-175.

Schroll, E. & Prochaska, W. (2004) Contribution to ore fluid chemistry of Bleiberg Pb-Zn deposit (Austria) and affiliated deposits: Goldschmidt 2004 (abstracts), Copenhagen, A 306.

Schroll, E. & Rantitsch, G. (2005) Sulphur isotope patterns from the Bleiberg deposit (Eastern Alps) and their implications for genetically affiliated lead-zinc deposits: *Mineralogy and Petrology*, v. 84, 1-18.

Schroll, E. & Wedepohl, K-H. (1972) Schwefelisotopenuntersuchungen an einigen Sulfid- und Sulfatmineralen der Blei-Zink-Erzlagerstätte Bleiberg-Kreuth: *Tschermaks Mineralogisch-petrographische Mitteilungen*, v. 17, 286-290.

Schroll, E., Schulz, O. & Pak, E. (1983) Sulphur isotope distribution in the Pb-Zn-deposit Bleiberg (Carinthia, Austria): *Mineralium Deposita*, v. 18, 7-25.

Schroll, E., Kürzl, A. & Weinzierl, O. (1994) Geochemometrical studies applied to the Pb-Zn deposit Bleiberg/Austria. In: Fontboté, L., Boni, M. (eds.), Sediment-hosted Pb-Zn ores. *Society of Geology Applied to Mineral Deposits, Special Publication* 10, 228-249.

Schroll, E., Köppel, V. & Cerny, I. (2006) Pb and Sr isotope and geochemical data from the Pb-Zn deposit Bleiberg (Austria): constraints on the age of mineralization: *Mineralogy and Petrology*, v. 86, 129-156.

Schulz, O. (1959) Studien an Zinkblenden im Bereich der erzführenden Raibler Schichten der Grube Max, Kreuth (Kärnten): *Berg- und Hüttenmännische Monatshefte*, v. 104 (9), 187-193.

Schulz, O. (1968) Die diskordanten Erzgänge vom "Typus Bleiberg" syndiagenetische Bildungen. In: ISMIDA (ed.), Atti del Symposium Internazionale sui Giacimenti Minerari delle Alpi, 11 - 18 Settembre 1966, Trento, v.1, 149-162, Saturnia.

Schulz, O. (1981) Die Pb-Zn-Erzlagerstätte Lafatsch-Vomperloch (Karwendelgebirge, Tirol): *Veröffentlichungen des Museums Ferdinandeum*, v. 61, 55-103.

Schulz, O. (1983) Pb-Zn-Erz in der Kiesonkolithbank (Grenze Wettersteinkalk/Raibler Schichten) der Lagerstätte Bleiberg-Kreuth: *Tschermaks Mineralogisch-petrographische Mitteilungen*, v. 32, 135-151.

Schulz, O. (1985) Ausgewählte Gefügebefunde in der kalkalpinen Pb–Zn-Lagerstätte Bleiberg-Kreuth (Gailtaler Alpen, Kärnten): *Archiv für Lagerstättenforschung der Geologischen Bundesanstalt*, v. 6, 91–99.

Schulz, O. (2006) Die Entstehung der Bleiberger Lagerstätte: Res Montanarum, v.39, 4-12.

Schuster, R., Egger, H., Krenmayr, H.-G., Linner, M., Mandl, G.W., Matura, A., Nowotny, A., Pascher, G., Pestal, G., Pistotnik, J., Rockenschaub, M. & Schnabel, W. (2013) Geologische Übersichtskarte der Republik Österreich 1:1 500 000 (ohne Quartär). In: Schuster, R., Daurer, A., Krenmayr, H.-G., Linner, M., Mandl, G.W., Pestal, G. & Reitner, J.M., Rocky Austria – Geologie von Österreich – kurz und bunt. 80 pp., Geosphere Austria, Vienna.

Sidiropoulos, L. (1983) Zn-Pb Vererzungen in Breccienzonen triadischer Karbonatgesteine der Nordtiroler Kalkalpen: *Veröffentlichungen des Museums Ferdinandeum*, v .63, 115-133.

Siegl, W. (1956) Zur Vererzung der Pb-Zn-Lagerstätten von Bleiberg: *Berg- und Hüttenmännische Monatshefte*, v. 101, 108-111.

Spangenberg, J.E. & Herlec, U. (2006) Hydrocarbon biomarkers in the Topla-Mežica zinc-lead deposits, Northern Karavanke/Drau Range, Slovenia: paleoenvironment at the site of ore formation: *Economic Geology*, v. 101, 997-1021.

Stacey, J.S.T. & Kramers, J.D. (1975) Approximation of terrestrial lead isotope evolution by a two-stage model: *Earth and Planetary Science Letters*, v. 26, 207-221.

Štrucl, I. (1960) Geološke značilnosti mežiškega rudišča s posebnim ozirom na kategorizacijo rudnih zalog: *Geologija*, 1960, let. 6, 251–278.

Štrucl, I. (1974) Die Entstehungsbedingungen der Karbonatgesteine und Blei-Zinkvererzungen in den Anisschichten von Topla: *Geologija*, v. 17, 383–399, Ljubljana.

Štrucl, I. (1984) Geological and geochemical characteristics of ore and host rock of lead-zinc ores of the Mežica ore deposit: *Geologija*, v. 27, 215–327, Ljubljana.

Vermeesch, P. (2018) IsoplotR: a free and open toolbox for geochronology: *Geoscience Frontiers*, v. 9, 1479-1493.

Vohryzka, K. (1968) Die Erzlagerstätten von Nordtirol und ihr Verhältnis zur alpinen Tektonik: *Jahrbuch der Geologischen Bundesanstalt*, v. 111, 3-88.

Wang, M., Han, R., Zhou, W., Wu, S., Luo, D. & Song, D. (2023) In situ geochemical and Rb-Sr dating analysis of sphalerite from the Liangyan Pb–Zn deposit in northwestern Guizhou, China: Implication for timing of ore formation: *Ore Geology Reviews*, v. 154, 105340.

Warch, A. (1984) Vererzungen im Alpinen Muschelkalk der nördlichen Gailtaler Alpen: Carinthia II, v. 174./94. Jahrgang, 91-106.

Weber, L. (ed.) (1997) Handbuch der Lagerstätten der Erze, Industrieminerale und Energierohstoffe Österreichs: Archiv für Lagerstättenforschung Geologische Bundesanstalt, v. 19, 1-607.

Wei, C., Ye, L., Hu, Y., Huang, Z., Danyushevsky, L. & Wang, H. (2021) LA-ICPMS analyses of trace elements in base metal sulfides from carbonate-hosted Zn-Pb deposits, South China: A case study of the Maoping deposit: *Ore Geology Reviews,* v. 130, 103945.

Weiß, S. (1982) Bergbau am Riedbodeneck: Lapis, v.7/5, 9-13.

Wetzenstein, W. (1972) Die Mineralparagenesen der Blei-Zinklagerstätte St. Veit (Heiterwand-Gebiet, östliche Lechtaler Alpen, Tirol): Verhandlungen der Geologischen Bundesanstalt, 1972, v. 2, 288-298.

Wilson, S. A., Ridley, W. I. & Koenig, A. E. (2002) Development of sulfide calibration standards for the laser ablation inductively-coupled plasma mass spectrometry technique: *Journal of Analytical Atomic Spectrometry,* v. 17 (4), 406–409.

Wolkersdorfer, C. (1989) Zur Geschichte, Mineralisation und Genese des ehemaligen Bergbaues auf die Blei-Zink-Vorkommen SE des Ehrwalder Talkessels (Tirol) mit einer geologischen Kartierung (M 1:10000) im westlichen Mieminger Gebirge. Diploma thesis, Technical University Clausthal, 92 pp.

Yang, Q., Zhang, X., Ulrich, T., Zhang, J. & Wang, J. (2022) Trace element compositions of sulfides from Pb-Zn deposits in the Northeast Yunnan and northwest Guizhou Provinces, SW China: Insights from LA-ICP-MS analyses of sphalerite and pyrite: *Ore Geology Reviews*, v. 141, 104639.

Ye, L., Li, Z. L., Hu, Y. S., Huang, Z. L., Zhou, J. X., Fan, H. F., & Danyushevsky, L. (2016) Trace elements in sulfide from the Tianbaoshan Pb-Zn deposit, Sichuan province, China: A LA-ICPMS study. *Acta Petrologica Sinica*, v. 32, 3377–3393.

Zeeh, S. & Bechstädt, T. (1994) Carbonate-hosted Pb–Zn mineralisation at Bleiberg-Kreuth (Austria): compilation of data and new aspects. In: Fontboté, L, Boni, M (eds.), Sediment-hosted Zn–Pb ores, Springer, Berlin, 271–296 (Geological Society Special Publication 10).

Zeeh, S., Kuhlemann, J. & Bechstädt, Th. (1998) The classical Pb-Zn deposits of the Eastern Alps (Austria/Slovenia) revisited: MVT deposits resulting from gravity driven fluid flow in the Alpine realm: *Geologija*, v. 41(1), 257–273.